EUROPEAN SOCIETY OF RADIOLOGY

eBook for Undergraduate Education in Radiology

CHAPTER: Central Nervous System

Preface

Undergraduate teaching of radiology in Europe is provided according to national schemes and may vary considerably from one academic institution to another. Sometimes, the field of radiology is considered as a "cross-cutting discipline" or taught within the context of other clinical disciplines, e.g., internal medicine or surgery.

This e-book has been created in order to serve medical students and academic teachers throughout Europe to understand and teach radiology as a whole coherent discipline, respectively. Its contents are based on the *Undergraduate Level of the ESR European Training Curriculum for Radiology* and summarize the so-called ***core elements*** that may be considered as the basics that every medical student should be familiar with. Although specific radiologic diagnostic skills for image interpretation cannot be acquired by all students and rather belong to the learning objectives of the *Postgraduate Levels of the ESR Training Curricula*, the present e-book also contains some ***further insights*** related to modern imaging in the form of examples of key pathologies, as seen by the different imaging modalities. These are intended to give the interested undergraduate student an understanding of modern radiology, reflecting its multidisciplinary character as an organ-based specialty.

We would like to extend our special thanks to the authors and members of the ESR Education Committee who have contributed to this eBook, to Carlo Catalano, Andrea Laghi and András Palkó who initiated this project, and to the ESR Office, in particular Bettina Leimberger and Danijel Lepir, for all their support in realising this project.

We hope that this e-book may fulfil its purpose as a useful tool for undergraduate academic radiology teaching.

Minerva Becker
ESR Education Committee Chair

Vicky Goh
ESR Undergraduate Education Subcommittee Chair

Chapter Outline

Copyright and Terms of Use

How to cite this work:

European Society of Radiology, Laura Oleaga (2022) eBook for Undergraduate Education in Radiology: Central Nervous System. DOI 10.26044/esr-undergraduate-ebook-07

Chapter Outline

Hyperlinks

Core Knowledge

Further Knowledge

Attention

Compare

Questions

References

Chapter Outline

eBook for Undergraduate Education in Radiology

Based on the ESR Curriculum for Undergraduate Radiological Education

Chapter: **Central Nervous System**

Author

Laura Oleaga

Affiliation

Radiology Department, Hospital Clínic Barcelona, Spain

lauraoleaga@gmail.com

Chapter Outline

Chapter Outline

- **Anatomy**
  - Cerebrum
  - Brain Stem
  - Cerebellum
  - Spine
  - Spinal Cord
- **Strengths, Weaknesses and Role of Imaging Modalities**
  - Ultrasound
  - Computed Tomography
  - Magnetic Resonance
  - Digital Subtraction Angiography
- **Main Indications to Brain Imaging by Pathology**
  - Congenital Lesions
  - Trauma
  - Ischemic Disease (Acute Infarct, Chronic Infarct, Haemorrhagic Infarct)
  - CNS Tumours
  - Inflammatory/Infectious Diseases
  - Neurodegenerative Diseases
  - Vascular Lesions
- **Main Indications to Spinal Cord Imaging by Pathology**
  - Trauma
  - Degenerative Disease
  - Tumours
  - Infarct/Inflammatory/Infectious Diseases
- **Take-Home Messages**
- **References and Further Reading**
- **Test Your Knowledge**

Chapter Outline

Anatomy

Strengths, Weaknesses and Role of the Imaging Modalities

Main Indications to Brain Imaging by Pathology

Main Indications to Spinal Cord Imaging by Pathology

Take-Home Messages

References and Further Reading

Test Your Knowledge

Anatomy

The central nervous system (CNS) consists of the brain and spinal cord. It is surrounded and protected by the skull, vertebrae and the three meningeal layers.

The brain can be divided into the cerebrum, brainstem, and cerebellum.

The cerebrum is composed of the right and left hemispheres, with four lobes each: frontal, parietal, temporal and occipital. Its functions include: vision, hearing, speech, reasoning, emotions, learning, and fine control of movement. Both lobes are connected by the connecting fibbers (corpus callosum, anterior commissure, inter-thalamic commissure, posterior commissure).

The brainstem includes the midbrain, the pons, and the medulla. It connects the cerebrum and cerebellum to the spinal cord. It is responsible of different functions such as breathing, heart rate, body temperature, wake and sleep cycles, digestion, sneezing, coughing, vomiting, and swallowing.

The cerebellum is located under the cerebrum. Its function is to coordinate muscle movements, posture and balance.

Chapter Outline

Cerebral Hemispheres

The cerebral hemispheres are divided into six lobes: frontal, parietal, temporal, occipital, insular, and limbic (figure 1)

The frontal lobe is the largest and it is situated anteriorly and superiorly.

The temporal lobe lies below anteriorly and inferiorly.

The parietal lobe is posterior to the frontal lobe and superior to the occipital lobe.

The occipital lobe is the most posteriorly located inferior to the parietal lobe and posterior to the temporal lobe.

The insula lies deep to the Sylvian fissure, covered by the frontal, temporal and parietal opercula.

The limbic system contains the hippocampus and the cingulate gyrus.

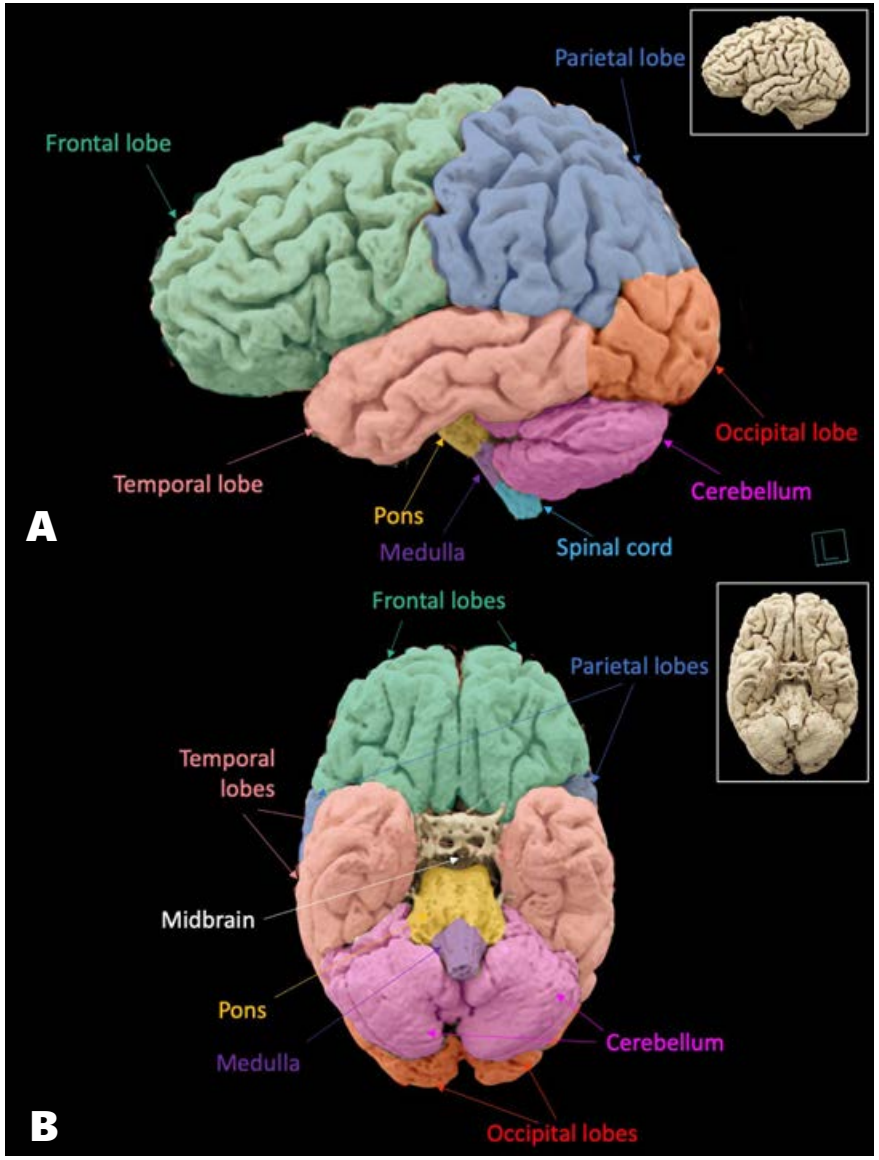

Fig. 1. Annotated human brain surface rendering reconstruction from a 3-dimensional (3D) Magnetic Resonance Imaging (MRI) acquisition. Lateral view (A) and view from below (B). Courtesy Minerva Becker, MD and Jorge Remuinan, Geneva University Hospitals.

Chapter Outline

Cerebral Fissures

The surface of the cerebral hemispheres of the brain has numerous sulci between the gyri and fissures separating the cerebral lobes (figure 2).

The three main fissures are the following:

The Rolandic fissure (central sulcus) separates the frontal and parietal lobes.

The Sylvian fissure (Sylvian sulcus) separates the frontal lobe from the temporal lobe.

The Parieto-occipital fissure (parieto-occipital sulcus) separates the parietal lobe from the occipital lobe.

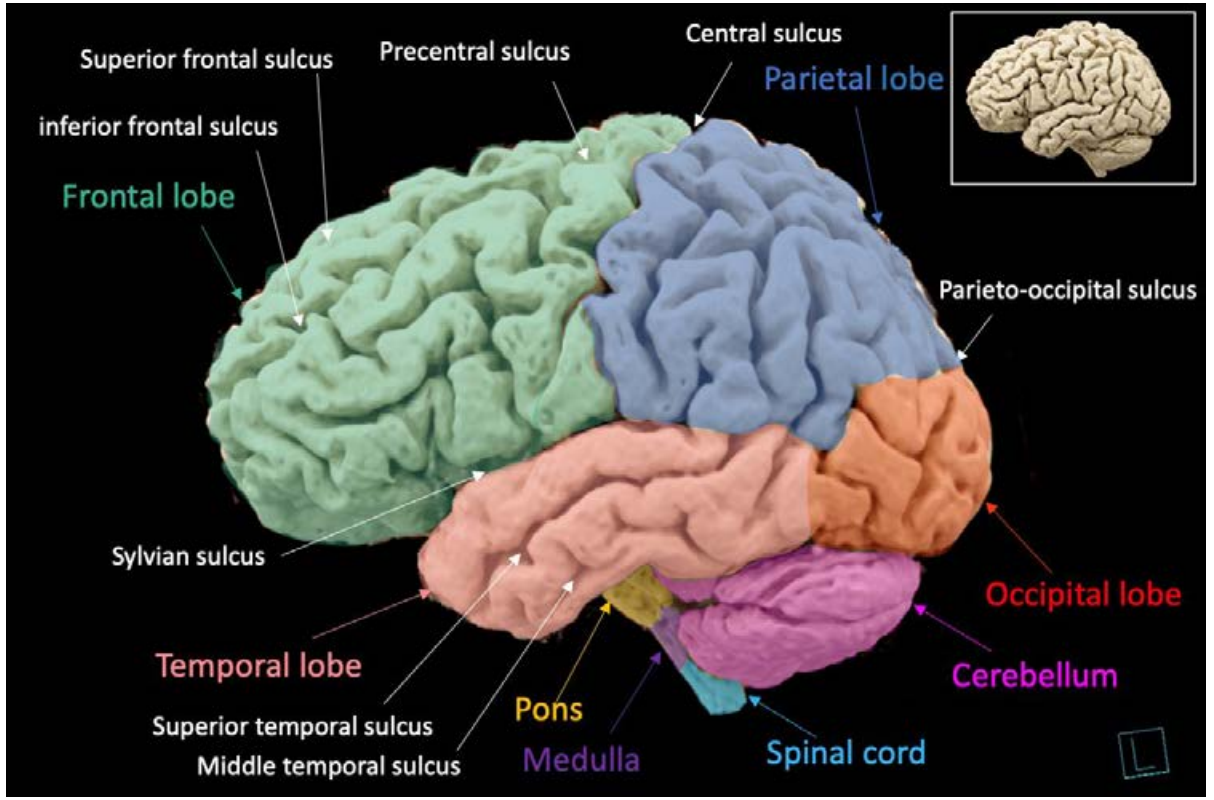

Fig. 2. Annotated human brain surface rendering reconstruction from a 3D MRI acquisition. Lateral view. Courtesy Minerva Becker, MD and Jorge Remuinan, Geneva University Hospitals.

Chapter Outline

Rolandic Fissure (Central Sulcus)

The central sulcus (figure 3) is one of the most important landmarks in the convexity of the brain. It separates motor from sensory areas, and frontal from parietal lobes.

The precentral gyrus is located anterior to the central sulcus and contains the primary motor cortex. The central sulcus resembles an inverted Greek letter Omega. The knob of the omega corresponds to the hand motor cortex.

The postcentral gyrus is located posteriorly and contains the primary somatosensory cortex.

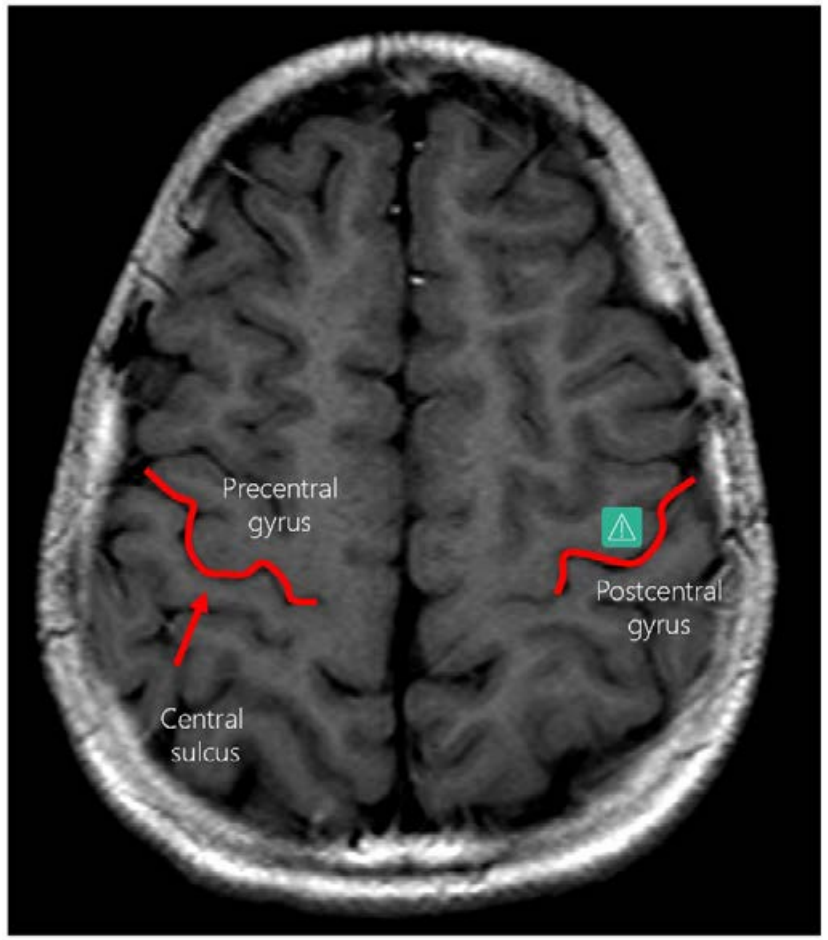

Fig. 3. Axial T1-weighted MRI image showing the normal anatomy of the central sulcus, pre- and postcentral gyri .

Chapter Outline

Rolandic Fissure (Central Sulcus)

- The superior frontal sulcus intersects the precentral sulcus forming an upper case L sign (figure 4).
- On the sagittal view the central sulcus is located immediately anterior to the marginal sulcus that is the continuation of the cingulate sulcus (figure 4).

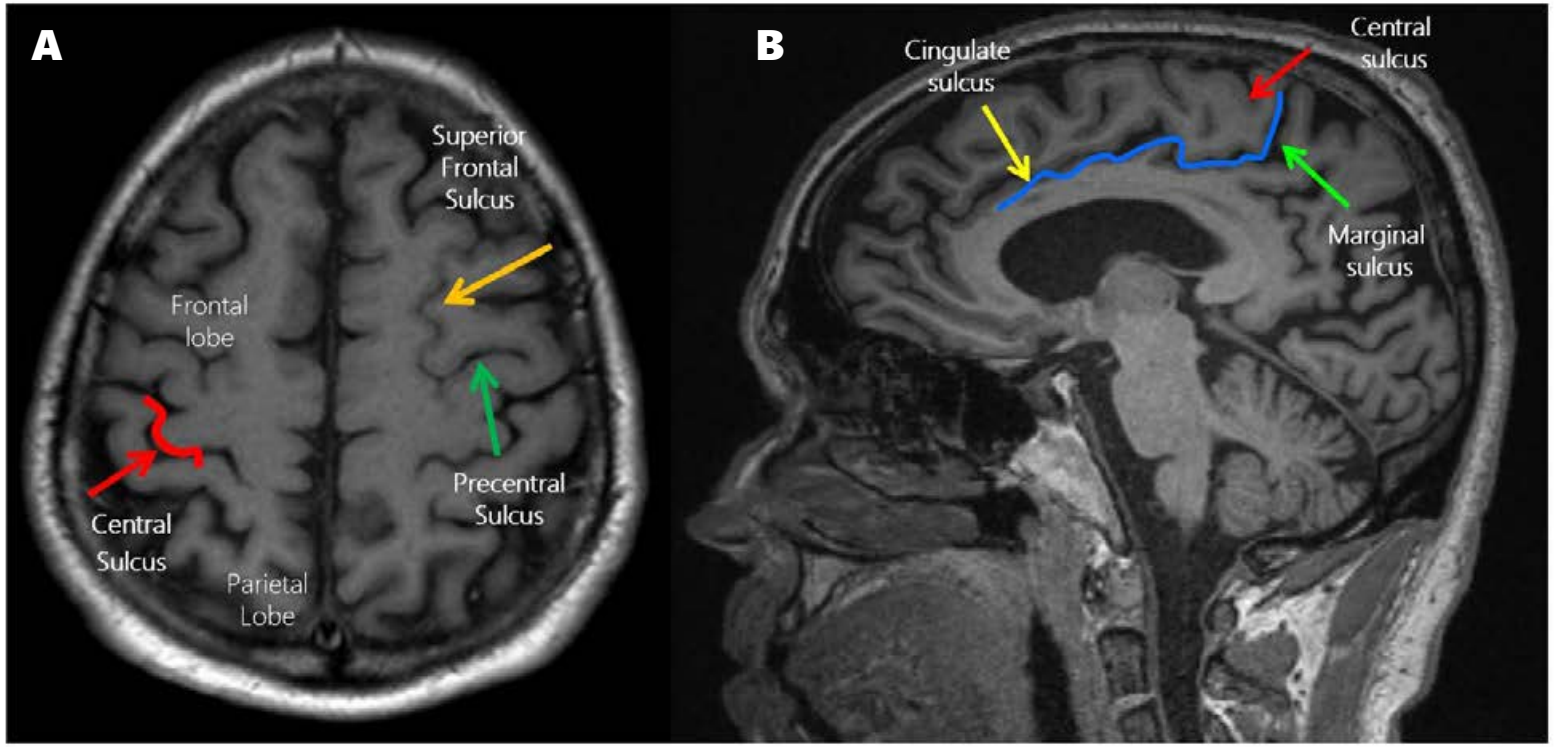

Fig. 4. Axial (A) and sagittal (B) T1-weighted MRI image showing the normal anatomy of the sulci mentioned in the text.

Chapter Outline

Sylvian Fissure

The Sylvian fissure separates the inferior frontal gyrus from the superior temporal gyrus (figure 5).

The inferior frontal gyrus (figure 5) contains three parts: pars orbitalis, pars triangularis, and pars opercularis.

The motor speech area (Broca) is mainly located within pars opercularis.

Wernicke's area is a poorly defined sensory speech area its location may include parts of the supramarginal gyrus, angular gyrus, and the posterior aspects of superior and middle temporal gyrus.

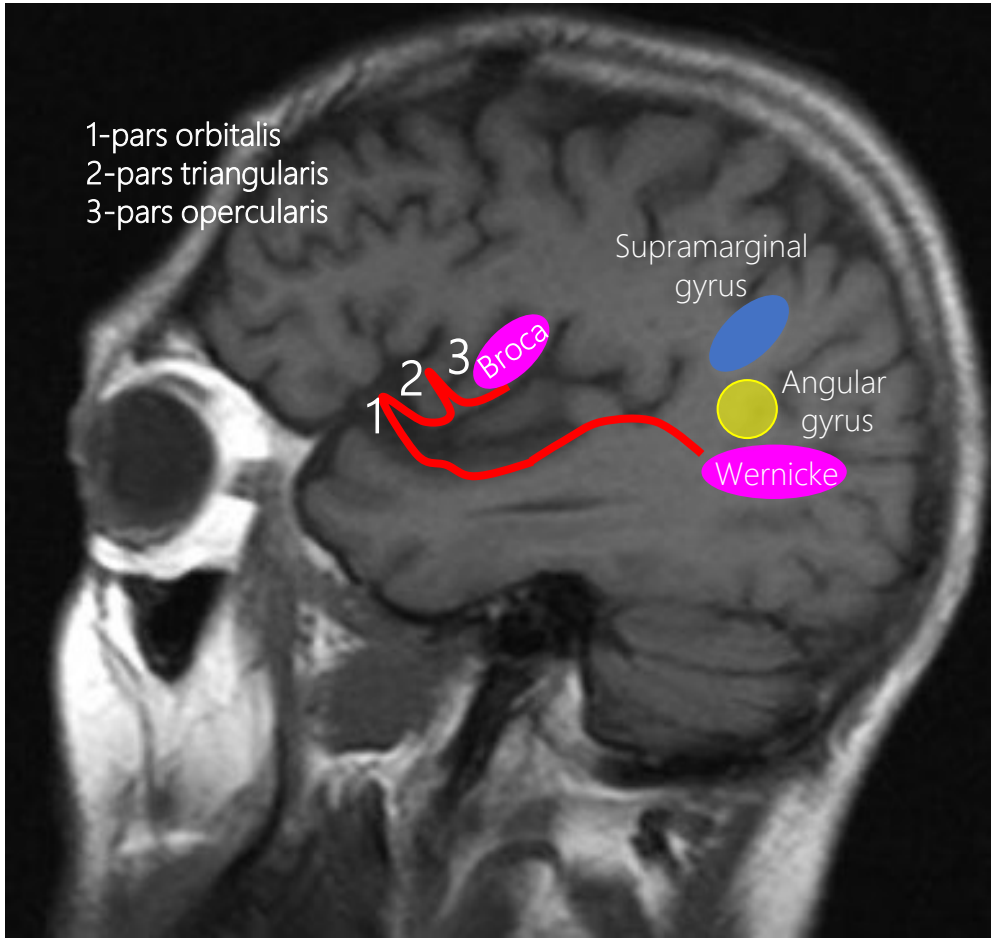

Fig. 5. Parasagittal T1-weighted MRI image showing the Sylvian fissure and adjacent anatomic areas mentioned in the text.

Chapter Outline

Parieto-occipital Fissure

The **Parieto-occipital fissure** (figure 6) separates the parietal lobe from the occipital lobe.

The **Calcarine fissure (figure 6)** located on the medial surface of the occipital lobe separates the visual cortex into two.

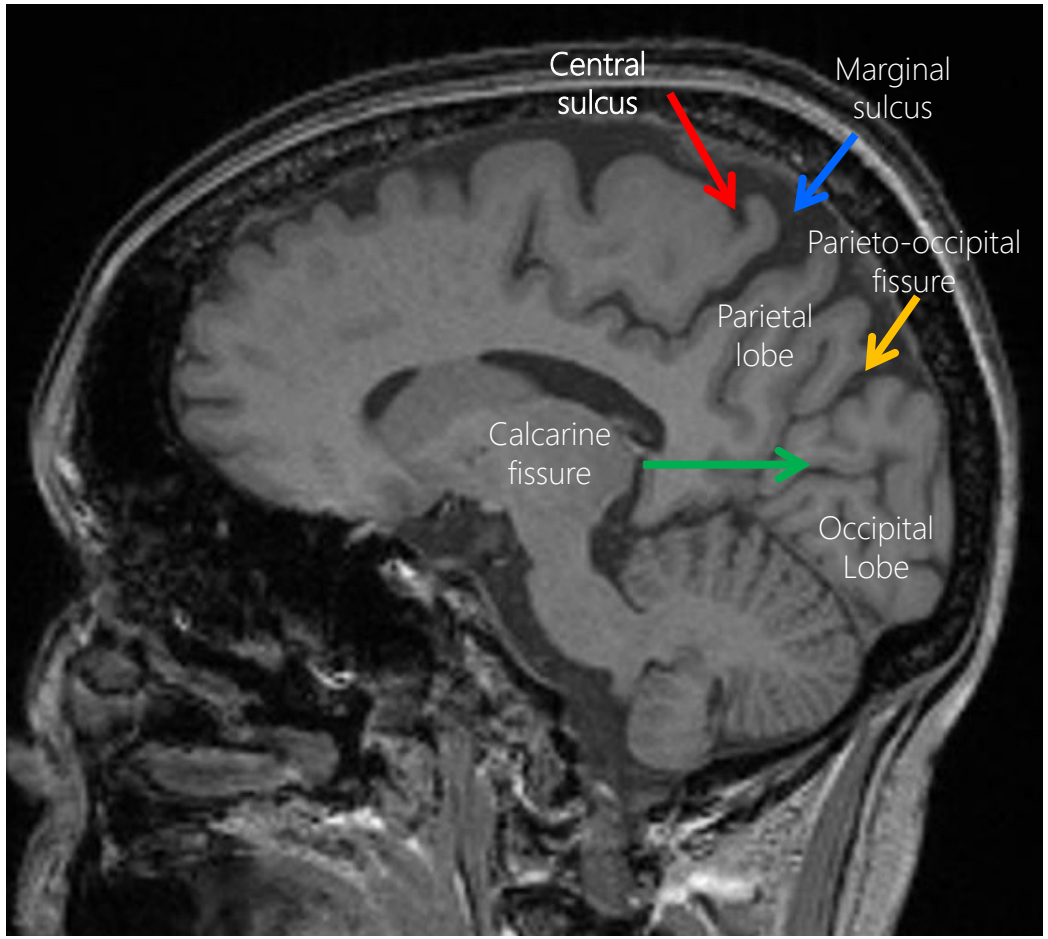

Fig. 6. Parasagittal T1-weighted MRI image showing the parieto-occipital and calcarine fissure.

Chapter Outline

Insula

The insula (figure 7) is located in depth to the Sylvian fissure. It has two lobules anterior and posterior (1).

The anterior insular lobule presents a triangular shape and is divided into anterior (a), middle (m) and posterior (p) insular gyri.

The posterior insular lobule is smaller with a rectangular shape with two gyri anterior and posterior.

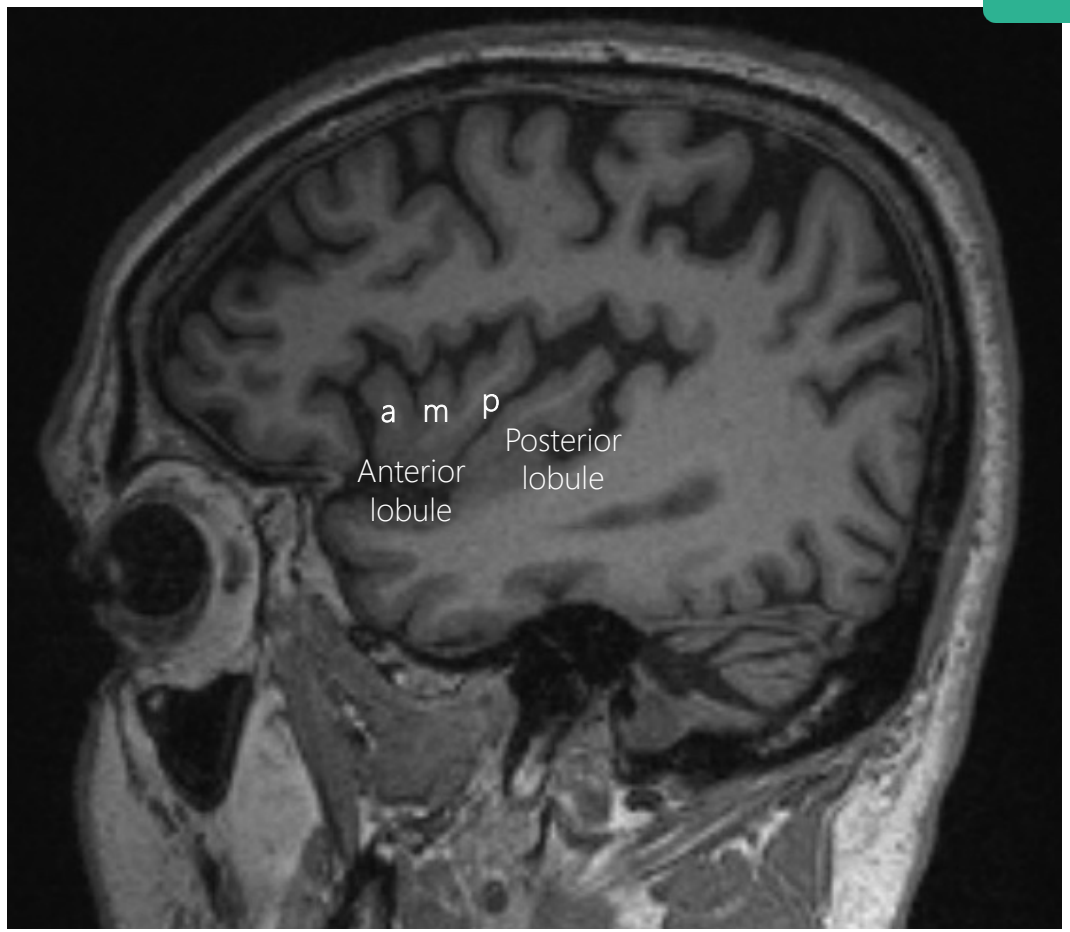

Fig. 7. Parasagittal T1-weighted MRI image showing the anatomy of the insula.

Naidich T.P., Kang E., Fatterpekar G.M., Delman B.N., Gultekin S.H., Wolfe D., Ortiz O., Yousry I., Weismann M., Yousry T.A. The insula: anatomic study and MR imaging display at 1.5 T. AJNR 2004; 25:222-32

Chapter Outline

Limbic Lobe

The **limbic lobe (figure 8)** is located in the medial surface of the cerebral hemispheres.

It includes the **cingulate** and **parahippocampal gyri**, the hippocampus, amygdala and the uncus.

The **hippocampus** is a bilaminar grey matter structure, occupying the medial surface on the floor of the temporal horn of the lateral ventricle. It consists of the dentate gyrus and Ammon's horn together with the subiculum. Ammon's horn contains large pyramidal neurons arranged in three zones called CA1, CA2 and CA3 (2).

The **fornix** is also part of the limbic system, formed by the efferent fibres of the hippocampus, it terminates in the mamillary body of the hypothalamus in the floor of the third ventricle.

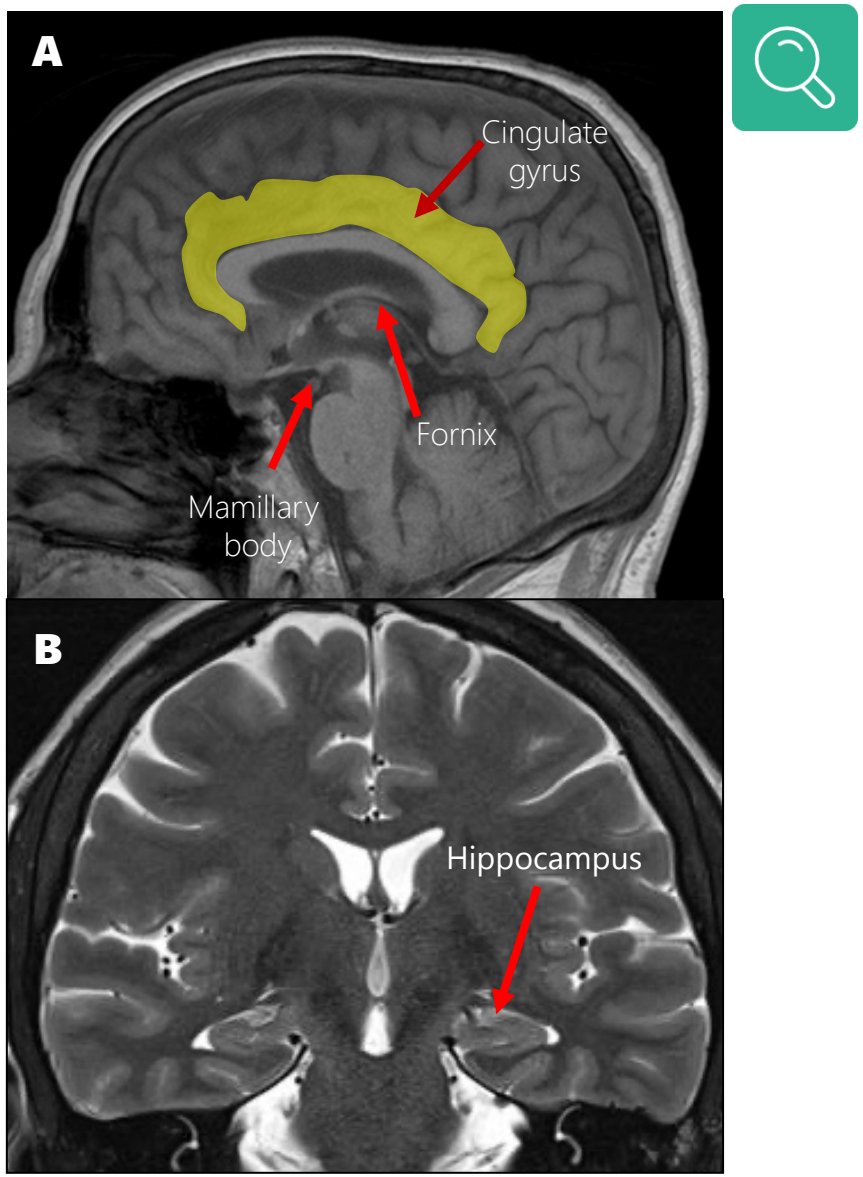

Fig. 8. Midsagittal T1-weighted (A) and coronal T2-weighted (B) MR images showing the anatomy of the limbic lobe

Chapter Outline

Deep Grey Matter Nuclei

The main deep grey matter nuclei (figure 9) are the caudate (c), putamen (p), globus pallidus (gp) and the thalami (th).

The term basal ganglia refers to the caudate nucleus, lentiform nucleus (globus pallidus and putamen), subthalamic nuclei, and the substantia nigra (sn).

The red nucleus (rn) is one of the brainstem nuclei.

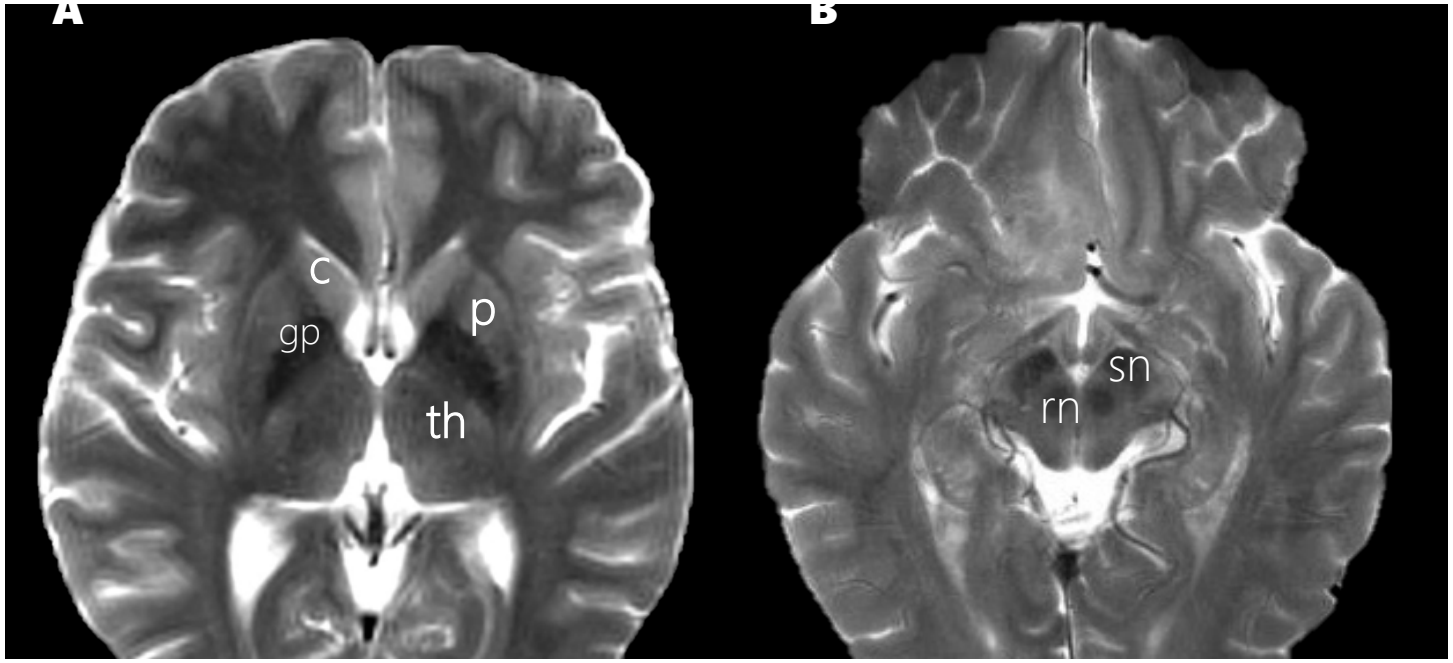

Fig. 9. Deep grey matter nuclei as seen on T2-weighted axial MR images.

Chapter Outline

White Matter

The white matter is formed by the axons surrounded by myelin sheaths. There are three groups of white matter sheaths: the commissural, projections and association fibbers (figure 10) .

The commissural fibres (red) cross the midline to link the two cerebral hemispheres. The three main commissures are the corpus callosum, the anterior commissure (ac), and the posterior commissure (pc). The corpus callosum is the largest of the white matter bundles it is divided in different regions: rostrum (r), genu (g), body (b), isthmus, and splenium (s).

The projection fibres (blue) connect the cortex with the brain stem, cerebellum and spinal cord. The internal capsule with the anterior (al) and posterior limb (pl) is the major projection fibre bundle.

The association fibres (green) connect different regions of the same hemisphere. There are three groups: long association tracts, intralobar association tracts, and U-shaped association tracts.

Chapter Outline

White Matter

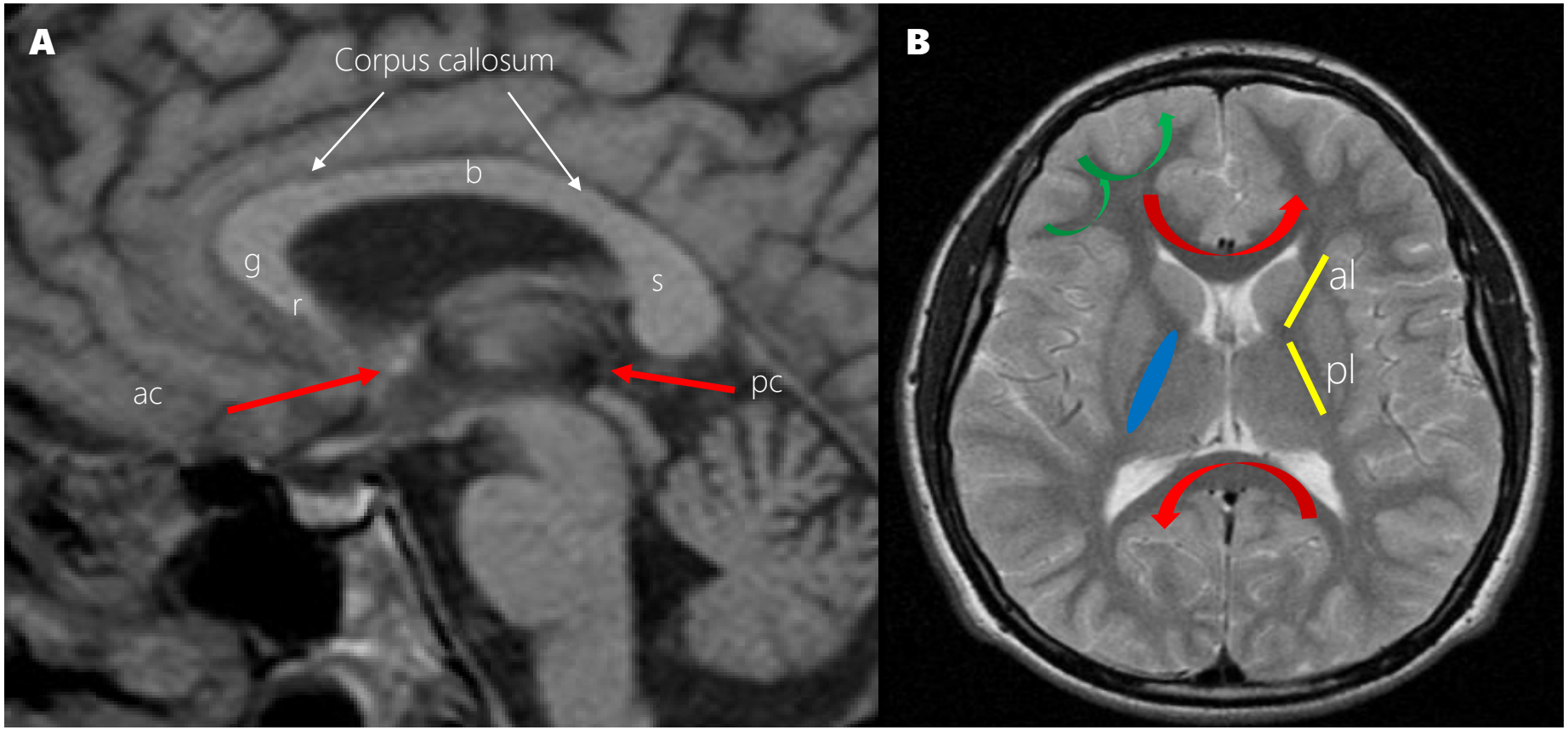

Fig. 10. White matter commissural, projection and association fibres as seen on sagittal T1-weighted (A) and axial T2-weighted (B) images.

Chapter Outline

Brain Stem

The brainstem connects the cerebrum to the cerebellum and the spinal cord (figure 11). There are three distinctive regions the mesencephalon (ms), pons (p) and medulla (md).

The nuclei included in the brainstem are the cranial nerve nuclei, red nucleus and substantia nigra.

Cranial nerve nuclei:

Midbrain: Oculomotor nerve (CN III), trochlear nerve (CN IV).

Pons: Trigeminal nerve (CN V), abducens (CN VI), facial nerve (CN VII), vestibulocochlear nerve (CN VIII)

Medulla: Glossopharyngeal nerve (CN IX), vagus nerve (CN X), accessory nerve (CN XI), hypoglossal nerve (CN XII)

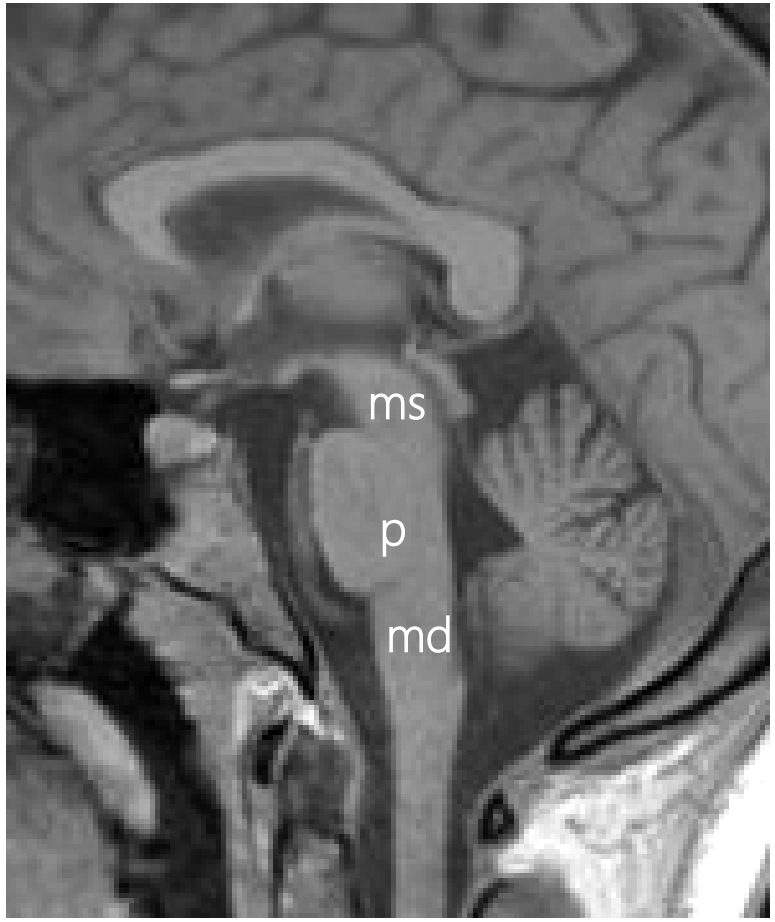

Fig. 11. Basic brain stem anatomy on a sagittal T1-weighted MR image.

Chapter Outline

Cerebellum

The cerebellum (figure 12) has two hemispheres (h) and a midline vermis (v). Each hemisphere is divided into three lobes (anterior, posterior and flocculonodular (f)). There are four groups of cerebellar nuclei; fastigial, globose, emboliform, and dentate nuclei (dn), the dentate nuclei being the largest cerebellar nuclei.

The cerebellum is attached to the brainstem thought the peduncles, the superior (scp), middle and inferior cerebellar peduncles.

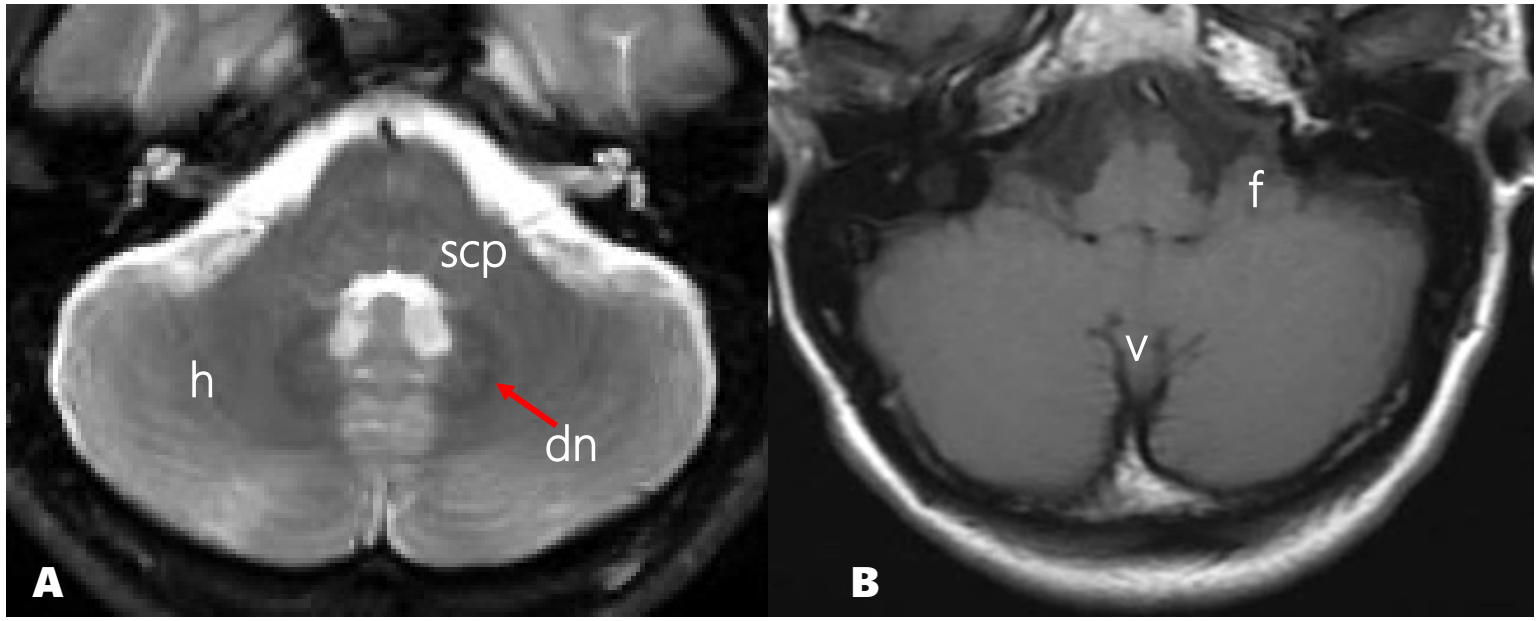

Fig. 12. Anatomy of the cerebellum as seen on axial T2-weighted (A) and l T1-weighted (B) images.

Chapter Outline

Pituitary Gland

The pituitary gland lies in the sella turcica (figure 13), below the hypothalamus and optic chiasm; it is divided into anterior (adenohypophysis) and posterior (neurohypophysis) lobes. The pituitary stalk connects the pituitary gland to the brain. The cavernous sinuses are located lateral to the pituitary gland, they contain the cranial nerves III, IV, V1, V2,VI and the cavernous segment of the internal carotid artery (ICA).

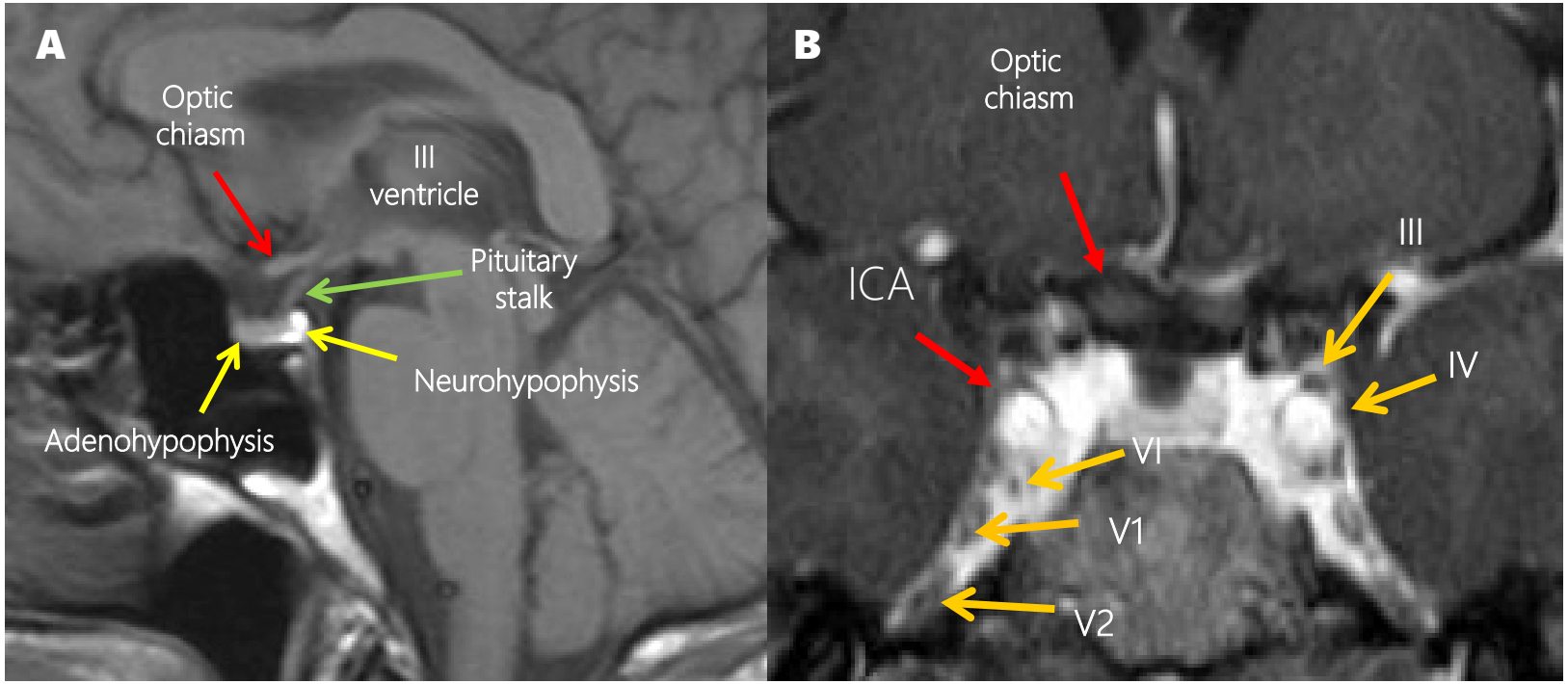

Fig. 13. Anatomy of the pituitary fossa and cavernous sinuses as seen on sagittal T1- weighted (A) and contrast-enhanced coronal T1-weighted (B) images.

Chapter Outline

Meningeal Layers

Three layers of membranous coverings envelop the central nervous system, from inside out, the pia, arachnoid, and dura mater (figure 14).

The pia covers the gyrus and sulcus of the brain surface.

External to the pia lies the arachnoid layer, between the pia and the arachnoid lies the subarachnoid space filled with cerebrospinal fluid (CSF).

The dura is a thick fibrous membrane tightly bound to the inner table of the skull.

Two potential spaces can be differentiated: the subdural space between the arachnoid and the dura and the epidural or extradural space.

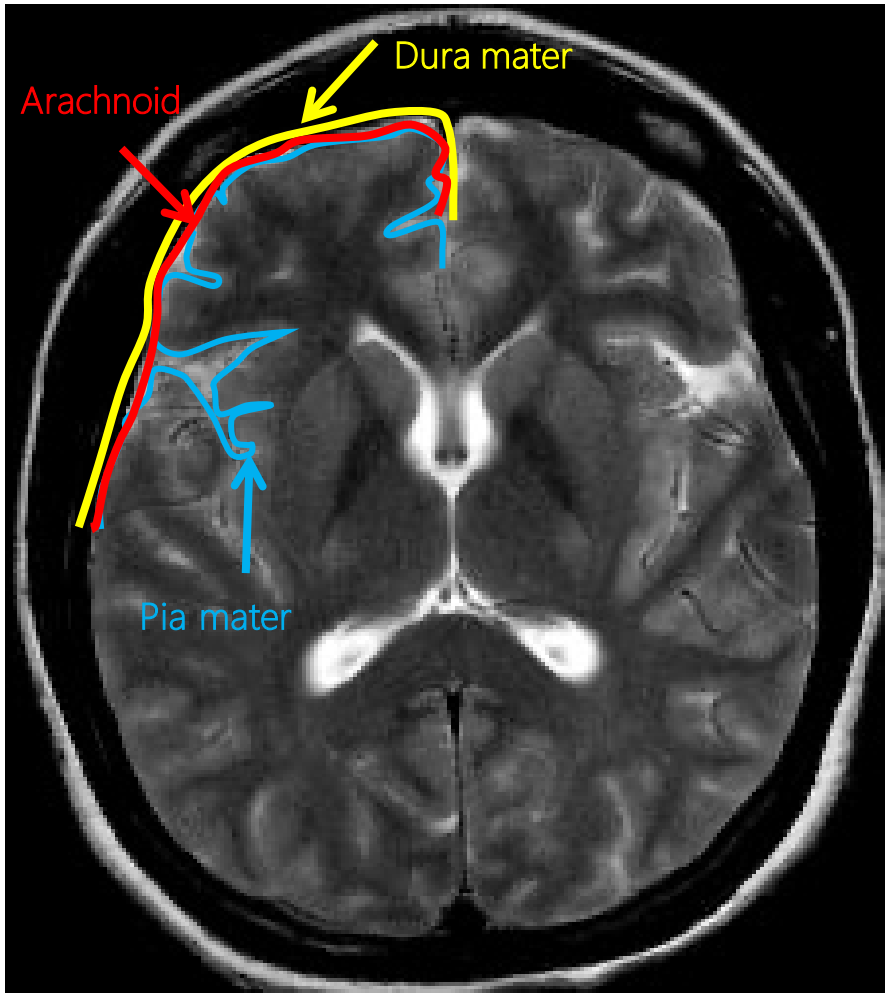

Fig. 14. Schematic illustration of the meningeal layers

Chapter Outline

Ventricles

The lateral ventricles (figures 15 and 16) are paired C-shaped structures comprising a body and atrium (at) along with 3 projections into the frontal (fh), temporal, and occipital lobes termed "horns. The lateral ventricles communicate with the third ventricle through the interventricular foramina of Monro.

The third ventricle communicates with the fourth ventricle through the aqueduct, from here the cerebrospinal fluid (CSF) passes through the Mangendie and Lushka foramina to the foramen magnum (fm) and from here to the cerebral surface.

The choroid plexus is located within the lateral, third, and fourth ventricles and is the primary source of cerebrospinal fluid (CSF).

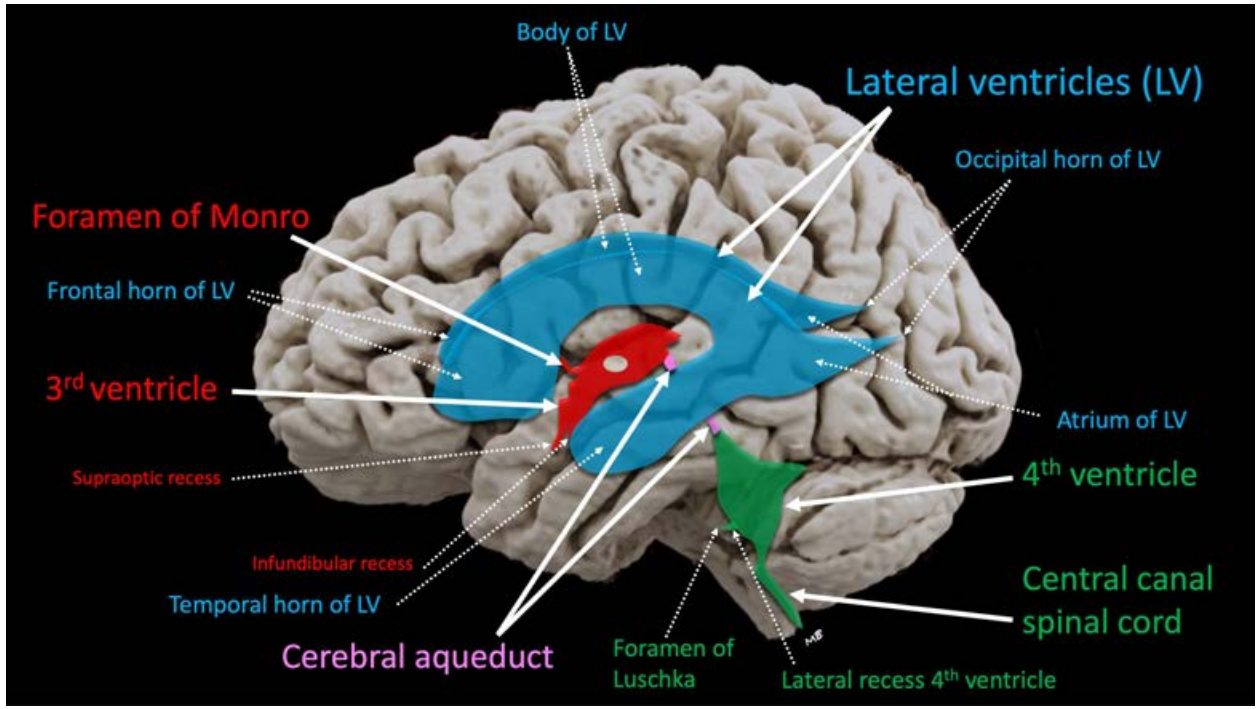

Fig. 15. Schematic illustration of the 3D anatomy of the ventricular system (lateral view). Courtesy Minerva Becker, MD, Geneva University Hospitals.

Chapter Outline

Ventricles

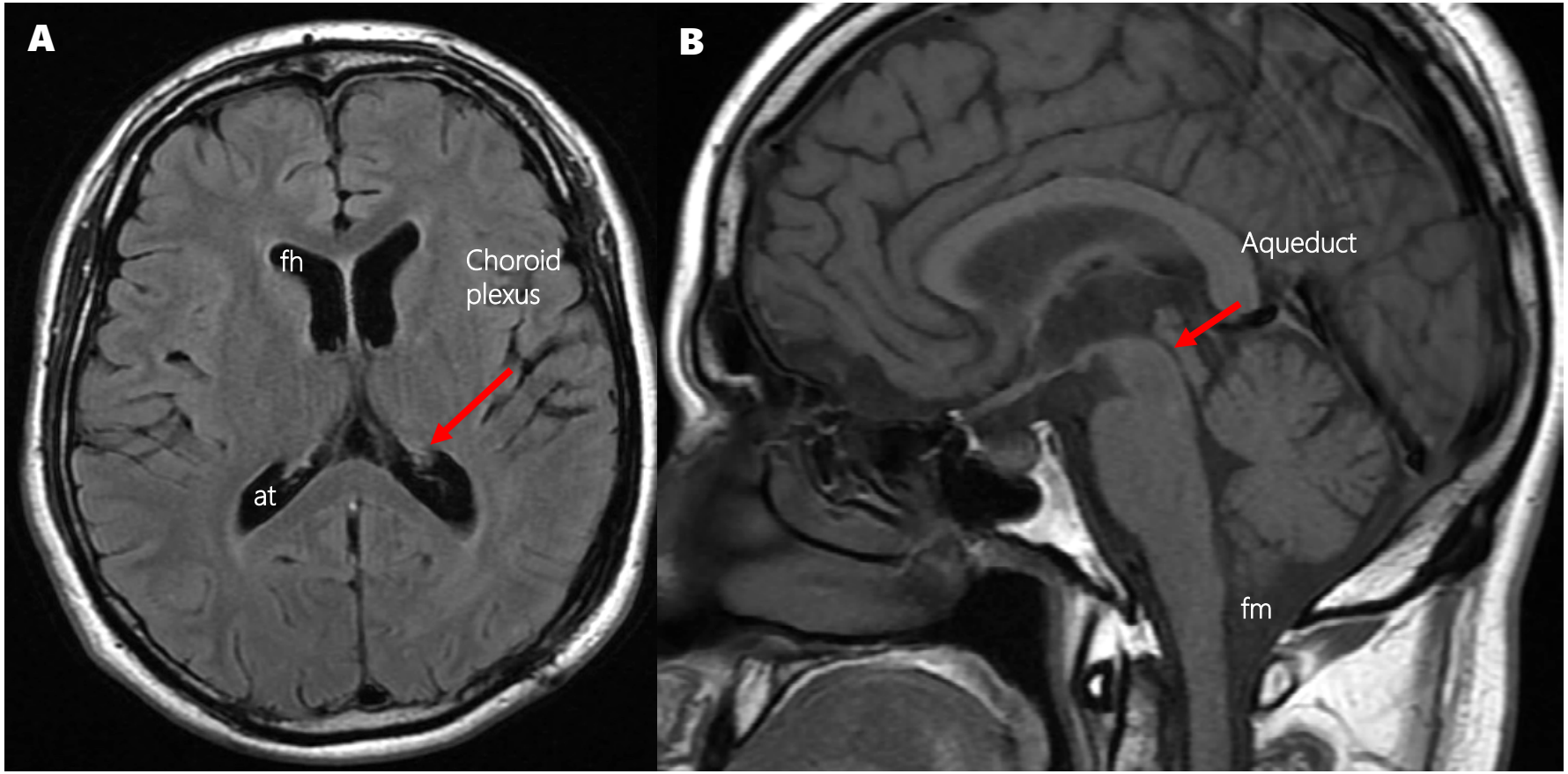

Fig. 16. Anatomy of the ventricular system as seen on axial (A) and sagittal (B) MR images..

Chapter Outline

Cranial Nerves

The human body has 12 pairs of cranial nerves that control motor and sensory functions of the head and neck.

The first two cranial nerves: olfactory nerve (CN I, figure 17) and optic nerve (CN II) are extensions of the CNS.

The cranial nerves III to XII arise from the brainstem and leave the central nervous system through cranial foramina:

- Oculomotor nerve (CN III)
- Trochlear nerve (CN IV)
- Trigeminal nerve (CN V)
- Abducens (CN VI)
- Facial nerve (fn, figure 17)
- Vestibulocochlear nerve (CN VIII, figure 17)
- Glossopharyngeal nerve (CN IX)
- Vagus nerve (CN X)
- Accessory nerve (CN XI)
- Hypoglossal nerve (CN XII)

The cranial nerves can be routinely seen on MRI using dedicated high-resolution sequences.

Romano N., Federici M., Castaldi A. Imaging of cranial nerves: a pictorial overview. Insights Imaging 2019; 10:33

Chapter Outline

Cranial Nerves

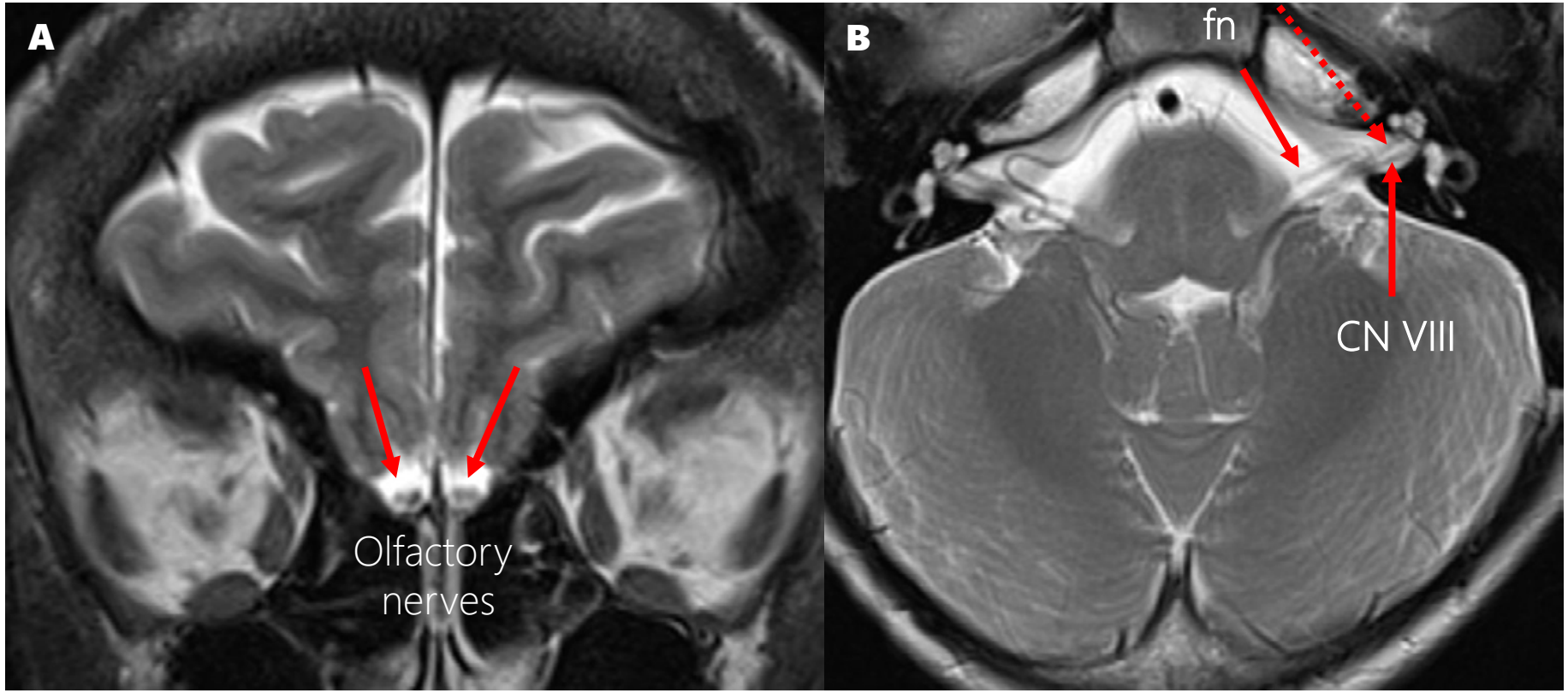

Fig. 17. Anatomy of the cranial nerves. (A) olfactory bulbs as seen on a coronal T2-weighted MR image (arrows). B. Cochleovestibular nerves (CN VIII) as seen on an axial T2-weighted MR image (arrows). The cochlear nerve (dashed arrow) lies anterior to the vestibular nerves (solid arrow).

Chapter Outline

Cerebral Arterial System

The arterial cerebral circulation can be divided into anterior and posterior circulation (figure 18). The anterior circulation comprises all the branches of the internal carotid artery (ICA).

Anterior circulation

Internal Carotid Artery segments
- Cervical
- Lacerum
- Petrous
- Cavernous
- Clinoid
- Ophthalmic

Branches of the internal carotid artery
- Ophthalmic artery
- Posterior communicating artery
- Anterior choroid artery
- Anterior cerebral artery (aca)
- Middle cerebral artery (mca)

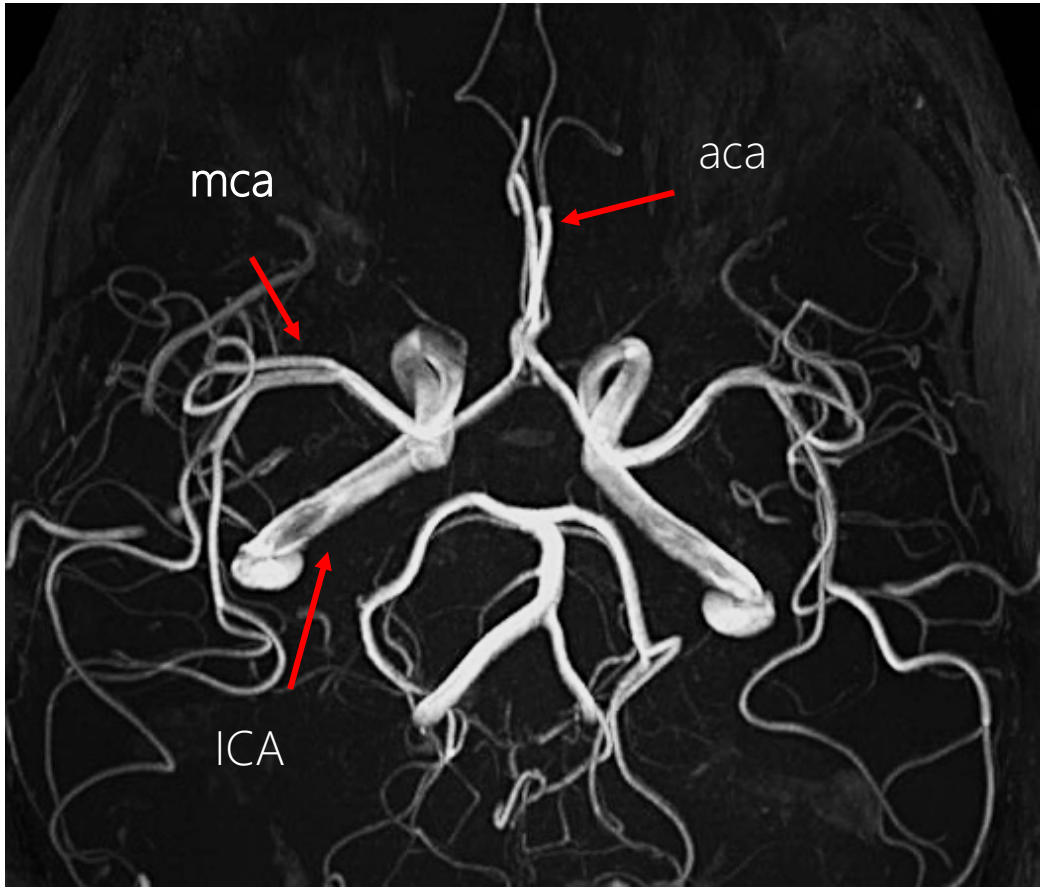

Fig. 18. Anatomy of the circle of Willis as seen on a TOF MRI sequence.

Chapter Outline

Cerebral Arterial System

The posterior circulation (figure 18) comprises all the branches of the vertebral and basilar arteries.

Posterior circulation

Vertebral arteries (va)
Posteroinferior cerebellar artery (pica)

Basilar artery (ba)
Anteroinferior cerebellar artery (aica)
Superior cerebellar artery (sca)
Posterior cerebral artery (pca)

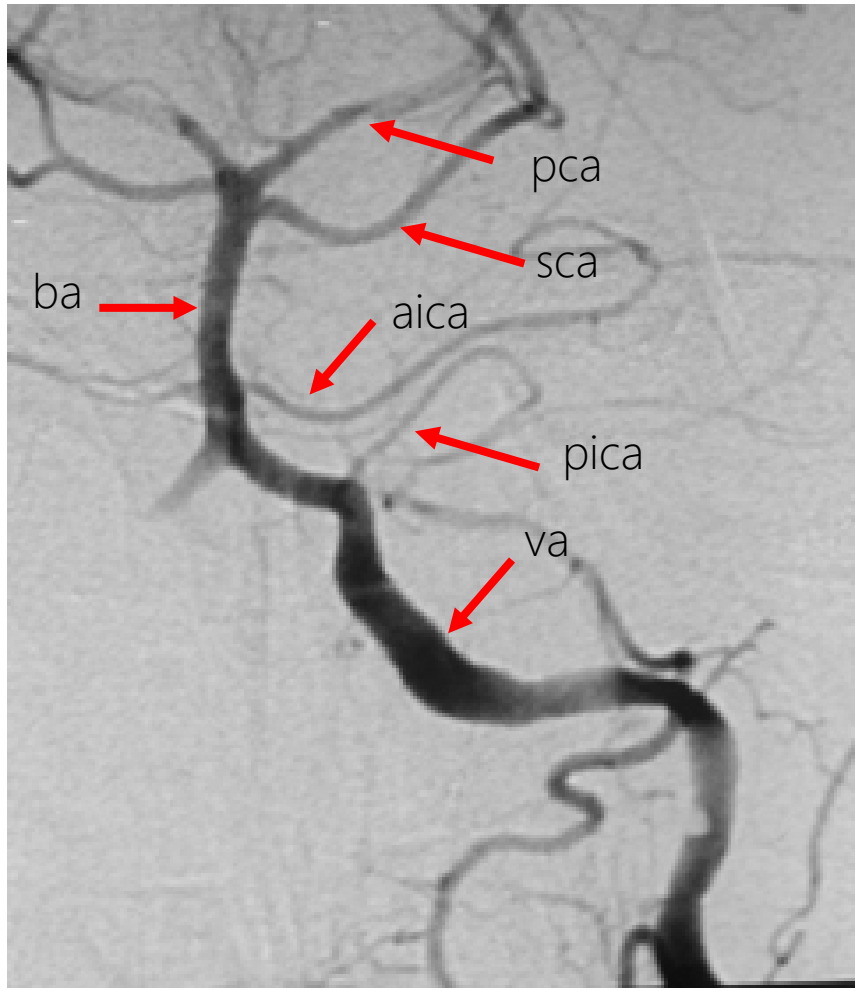

Fig. 19. Anatomy of the posterior circulation as seen on digital subtraction angiography (coronal view).

Chapter Outline

Venous Cerebral System

The cerebral venous system (figure 20) can be divided into a superficial and a deep system.

- The superficial system consists of sagittal sinuses and cortical veins and these drain superficial surfaces of both cerebral hemispheres.
- The deep system consists of the lateral sinus, straight sinus and sigmoid sinus along with draining deeper cortical veins

Superficial system (figure 20)
- Dural sinuses
  - Superior sagittal sinus (SSS)
  - Inferior sagittal sinus
  - Transverse sinus
  - Straight sinus (sts)
  - Sigmoid sinus (sgs)
  - Cavernous sinuses
  - Petrosal sinuses
  - Sphenoparietal sinus
  - Pterygoid sinuses
  - Inferior vermian veins
- Superficial cerebral veins
  - Cortical veins (cv)
  - Superficial middle cerebral vein (Sylvian)
  - Vein of Trolard
  - Vein of Labbé

Deep system (figure 20)
- Internal cerebral veins (iicv)
- Septal veins
- Thalomoestriate veins
- Basal veins of Rosenthal
- Vein of Galen (gv)
- Subependymal veins

Chapter Outline

Venous Cerebral System

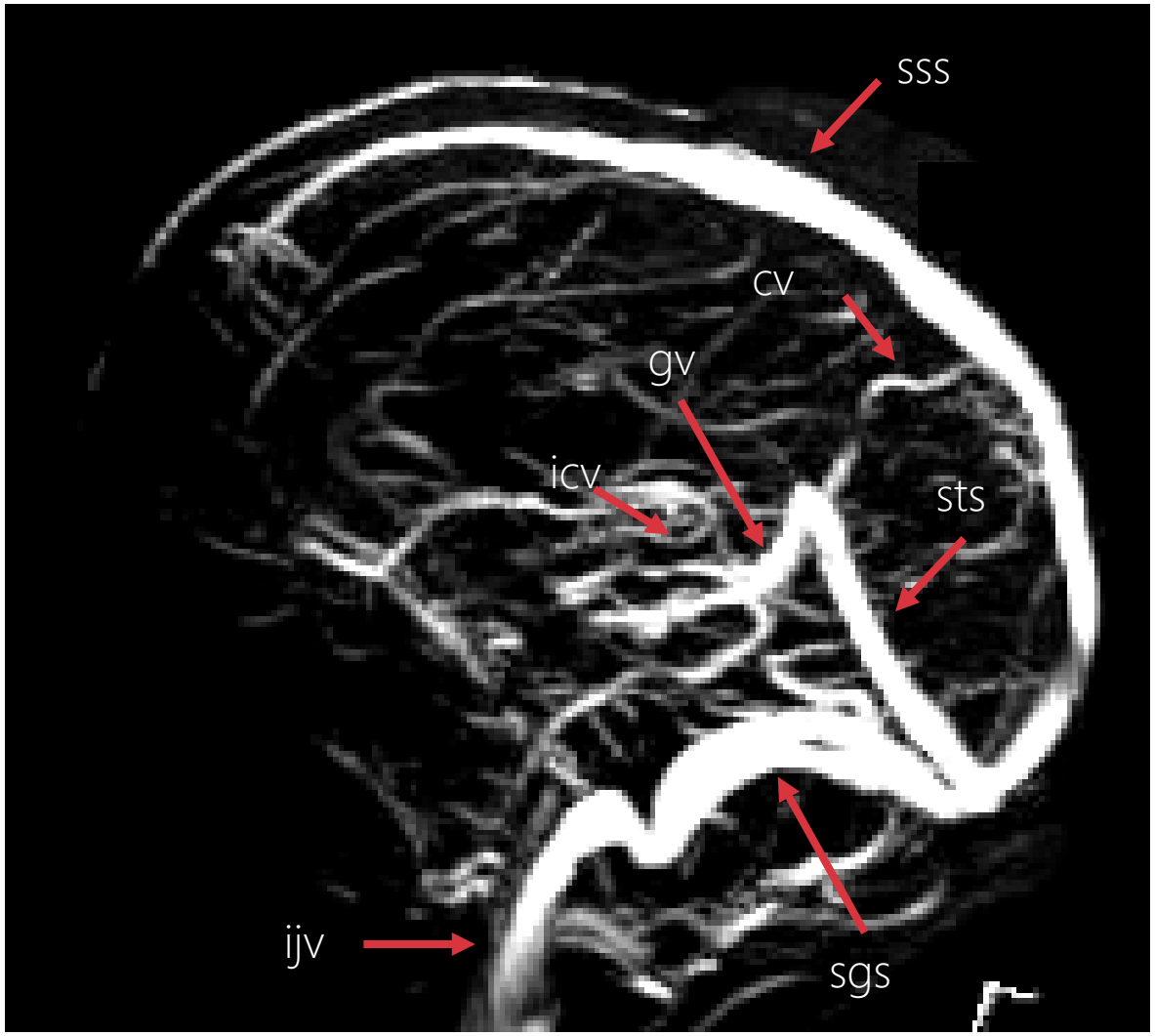

Fig. 20. Anatomy of the cerebral venous system as seen on an MRI phlebogryphy..
cv = cortical veins
Icv = internal cerebral veins
Ijv = internal jugular vein
gv = vein of Galen
SSS = superior sagittal sinus
Sts = straight sinus
Sgs = sigmoid sinus

Chapter Outline

Spine

The adult vertebral column (figure 21) consists of 33 vertebrae (vb) arranged in five regions. Seven cervical vertebrae, twelve thoracic vertebrae, five lumbar vertebrae, five sacral and four coccygeal vertebrae.

The five sacral vertebrae are fused in adults to form the sacrum, and the four coccygeal vertebrae are fused to form the coccyx.

The first two cervical vertebrae the atlas and axis articulate with the head, and the sacrum articulates with the pelvis.

The intervertebral disks (d) separate the vertebral bodies providing flexibility to the vertebral column.

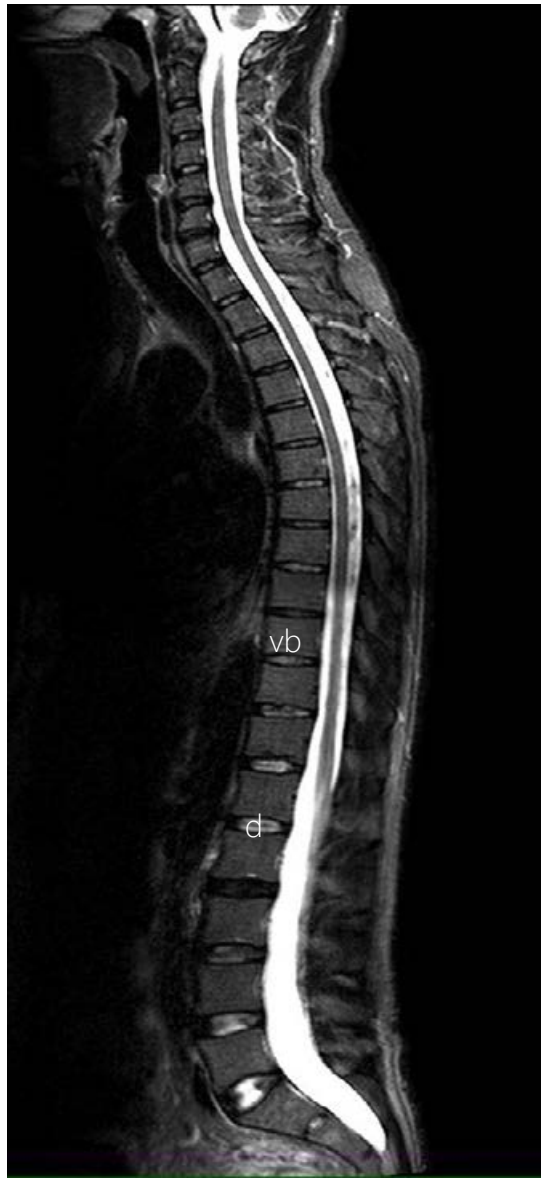

Fig. 21. Anatomy of the spine and spinal cord as seen on a sagittal T2-weighted MR image.

Chapter Outline

Spinal Cord

The spinal cord begins at the end of the brain stem and continues down in the centre of the spinal canal to the level of T12, L1 vertebrae.

Its lower end, the conus medullaris is continuous at its lower end with the threadlike filum terminale that attaches the spinal cord to the osseous canal at S4 level.

A transverse section of the spinal cord (figure 22) shows white matter in the periphery (wm), H-shaped grey matter inside (gm) and a central ependymal canal filled with CSF.

Emerging from the spinal cord are 31 pairs of anterior and posterior nerve roots.

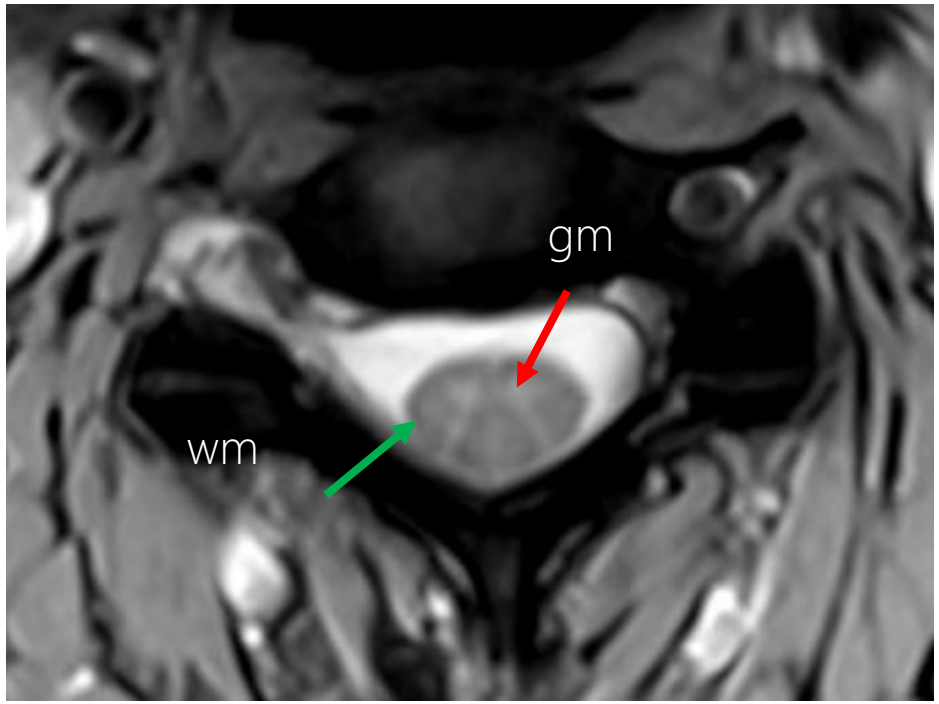

Fig. 22. Anatomy of the spinal cord as seen on an axial T2-weighted MR image.

Chapter Outline

Strengths, Weaknesses and Role of Imaging Modalities

Ultrasonography

Ultrasonography (also called ultrasound examination) uses high-frequency sound waves for imaging. External mechanical waves are applied, that interact with the area of the body to be imaged and a pulse echo technique is used to create an image.

It is a non-invasive, accurate, and cost-effective method of detecting and assessing flow in the carotid and vertebral arteries to diagnose vascular stenosis, dissection, thrombosis, and/or obstruction.

Transcranial ultrasound is indicated in neonates to assess hypoxic-ischemic encephalopathy, haemorrhage, ventricular size and arterial or venous patency.

Chapter Outline

Computed Tomography

Computed Tomography scanners consist of an x-ray tube and an opposing x-ray detector mounted on a ring, rotating around the patient to acquire projections through the patient at various angles.

It is the method of choice for the demonstration of acute intracranial haemorrhage, intracranial calcifications and delineating bony fractures.

CT-Angiography can be used to evaluate the arterial and venous system of the brain.

Perfusion CT is performed by repeated imaging through the brain after intravenous injection of a contrast agent bolus it is used in stroke evaluation.

Dual-energy CT is a recent technique that is used for tissue characterization, bone removal, and metal artifact reduction.

The contrast agent used on CT images is a Iodine-containing contrast medium.

=> See also chapter on contrast media.

Chapter Outline

Magnetic Resonance Imaging

MRI uses a strong static magnetic field and radiofrequency waves to generate the images (4).

MRI has a higher soft-tissue contrast than CT, which means that different types of tissues and can be better distinguished.

The contrast media used on MRI is a Gadolinium chelate. Gadolinium. It is a complex molecule with chemical bonds made between a gadolinium ion and a carrier molecule (a chelating agent) that prevents the toxicity of gadolinium while maintaining its contrast properties.

=> For Gadolinium chelates, see chapter on contrast media

Pooley R.A. Fundamental Physics of MR Imaging.
RadioGraphics 2005; 25:1087–1099

Magnetic Resonance Imaging

Morphological sequences

The basic morphological images obtained on MRI are T1-weighted, T2-weighted) and Fluid attenuated inversion recovery (FLAIR) images. T1-weighted images provide detailed anatomical information, T2-weighted images provide high contrast images with a high spectrum of different signal intensities from the different tissue types. FLAIR images are obtained with an inversion recovery sequence with a long inversion time that removes signal from the cerebrospinal fluid (CSF), the brain tissue contrast is similar to T2-weighted images but CSF appears dark instead of bright.

MR angiography (MRA) is a non-invasive method for imaging of the vasculature, it can be performed with or without a contrast agent injection.

Chapter Outline

Magnetic Resonance Imaging

Functional sequences

Diffusion Weighted Imaging (DWI) is an MRI technique that measures the translational water molecules motion. Apparent diffusion coefficient (ADC) is a quantitative measurement of the magnitude of diffusion of water molecules within tissue, it can be assessed using different b values on the DWI, changing the gradient amplitude. This information is useful for the diagnosis of acute ischemic stroke, infection, and tumour characterization.

Perfusion MRI can be performed with or without a contrast agent injection and depicts the cerebral circulation.

Functional MRI (fMRI) maps the location of the neuronal activity in the cortex and deep grey matter.

MR spectroscopy (MRS) provides chemical information about the cerebral tissue.

Chapter Outline

Digital Subtraction Angiography

Digital Subtraction Angiography (DSA) is used for imaging blood vessels intracranially and in the neck.

A Iodine-containing contrast agent is injected through a catheter introduced percutaneously via the femoral artery. The catheter is advanced into the arteries of interest for selective contrast injection. It is better than CT and MRI for the evaluation of small distal cerebral and spinal arteries due to its superior spatial resolution.

It is used for therapeutic endovascular treatment in stroke patients and patients with vascular lesions (aneurysms, arterio-venous malformations, arterial dissection, venous thrombosis).

Chapter Outline

Imaging Modalities

Modalities	Strengths	Weaknesses	Indications
Ultrasound	Non invasive Non-ionizing radiation	Operator dependent	Carotid and vertebral disease Brain evaluation neonates
Computed Tomography	High resolution Short scanning time	Ionizing radiation Iodine contrast	Stroke Brain hemorrhage Spine fractures Spine degenerative disease
Magnetic Resonance Imaging	Non-ionizing radiation High soft tissue contrast High resolution Functional information	Long scanning time Contraindicated (coclear implants, pace-makers...) Gadolinum contrast	Congenital or developmental lesions Stroke Tumours Neurodegenerative diseases Infectious diseases
Digital Substraction Angiography	Therapeutic procedure High spacial resolution	Invasive Radiation	Stroke (endovascular treatment) Aneurysms Cerebrovascular malformations

Chapter Outline

Brain Main Indications

Congenital Lesions
- Imaging in congenital brain malformations

Trauma
- Brain haemorrhage (epidural, subdural, parenchymal, intraventricular)

Ischemic Disease
- Acute stroke, chronic, haemorrhagic

Brain Tumours
- Intraaxial, extra-axial

Pituitary Gland Tumours
- Adenoma, Rathke's cleft cyst, craniopharyngioma

Inflammatory/Infectious Diseases
- Demyelinating disease, infections (bacterial, viral , fungal, parasitic)

Neurodegenerative Diseases
- Alzheimer, Parkinson

Vascular Lesions
- Aneurysms, cerebro-vascular malformations

Chapter Outline

Congenital Lesions

Congenital brain malformations can be produced by a genetic defect or be secondary to a disruption in the normal anatomical development of the brain structures due to prenatal infection, haemorrhage, and ischemia.

Agenesis of the corpus callosum (figure 23) is caused by disruption of brain cell migration during foetal development. It can occur as an isolated condition or in combination with other brain or facial abnormalities.

Most meningoencephaloceles (figure 24) are of congenital origin. They are neural tube defects with a sac-like structure containing meninges, cerebrospinal fluid (CSF) and/or brain tissue that extends bellow the skull base through a bone defect. Congenital meningoencephaloceles are thought to be caused by TORCH infections (toxoplasma, rubella, cytomegalovirus, herpes simplex virus) during embryogenesis and also by a variety of genetic factors. Encephaloceles can occur as isolated lesions or in combination with other malformations, e.g., Chiari malformation or migration anomalies.

Although MRI is the imaging modality of choice to diagnose congenital brain lesions, in selected cases, additional CT images may be necessary to precisely assess skull base defects for planning of surgery.

=> For further congenital brain anomalies, see chapter on paediatric radiology.

Chapter Outline

Congenital Lesions

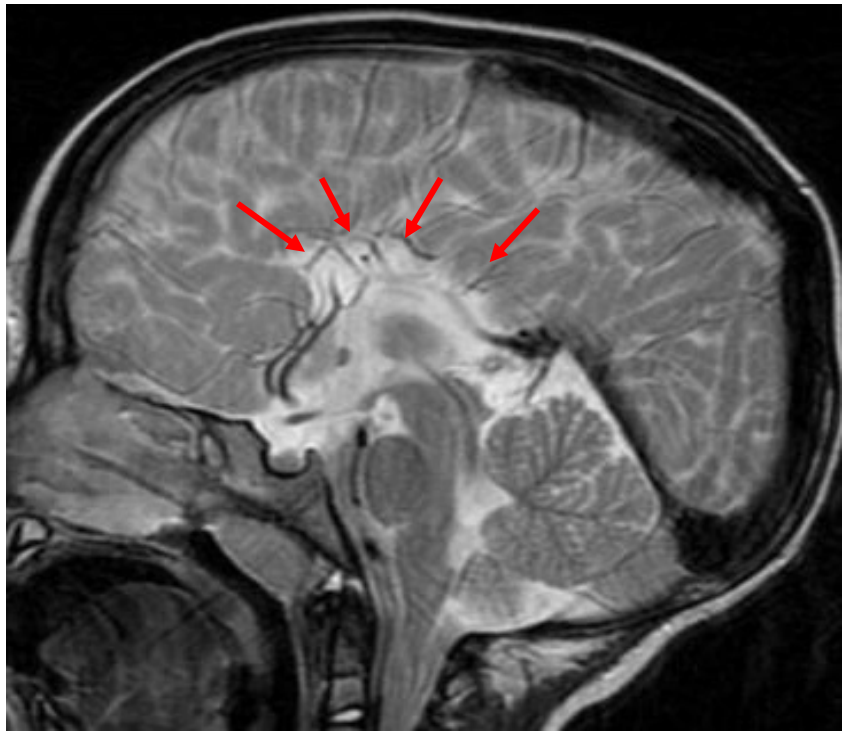

Fig. 23. Agenesis of the corpus callosum. On the sagittal midline T2-weighted image no corpus callosum is demonstrated (arrows). See for comparison Fig. 10 (normal corpus callosum).

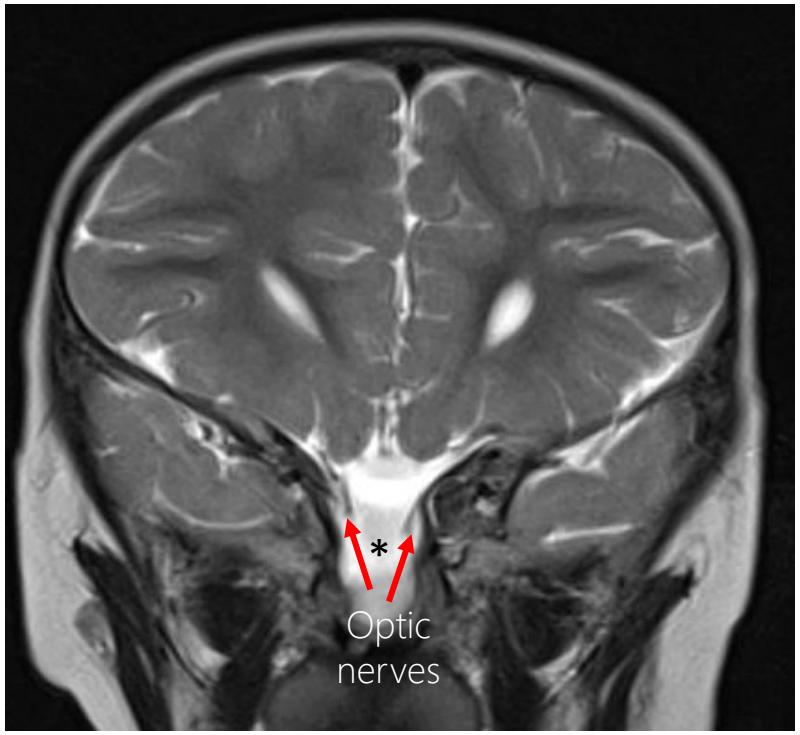

Fig. 24. Anterior encephalocele mostly containing CSF (asterisk) as seen on a coronal T2-weighted image. Anterior skull defect with herniated optic nerves.

Chapter Outline

Trauma

One of the most common causes of brain haemorrhage is trauma. It is important to correctly locate the bleeding site on imaging studies, as treatment and prognosis depend on it. Traumatic haemorrhage can be classified as intra-axial (within brain parenchyma) and extra-axial (external to brain parenchyma):

Intra-axial haemorrhage:

- Cerebral haemorrhage (intraparenchymal bleeding most frequently frontobasal and in the temporal lobes)

Extra-axial haemorrhage (figure 25):

- Subarachnoid (bleeding under the arachnoid, in the subarachnoid space)
- Subdural (bleeding between the inner layer of the dura mater and the arachnoid, cannot cross the midline, can cross suture lines)
- Epidural (bleeding between the dura mater and the skull, associated to bone fracture, can cross the midline, do not cross suture lines)
- Intraventricular (bleeding within the ventricles). It is a distinct entity in the new-born (=> see chapter on paediatric imaging)

CT is the imaging modality of choice to evaluate bleeding after brain trauma.

Chapter Outline

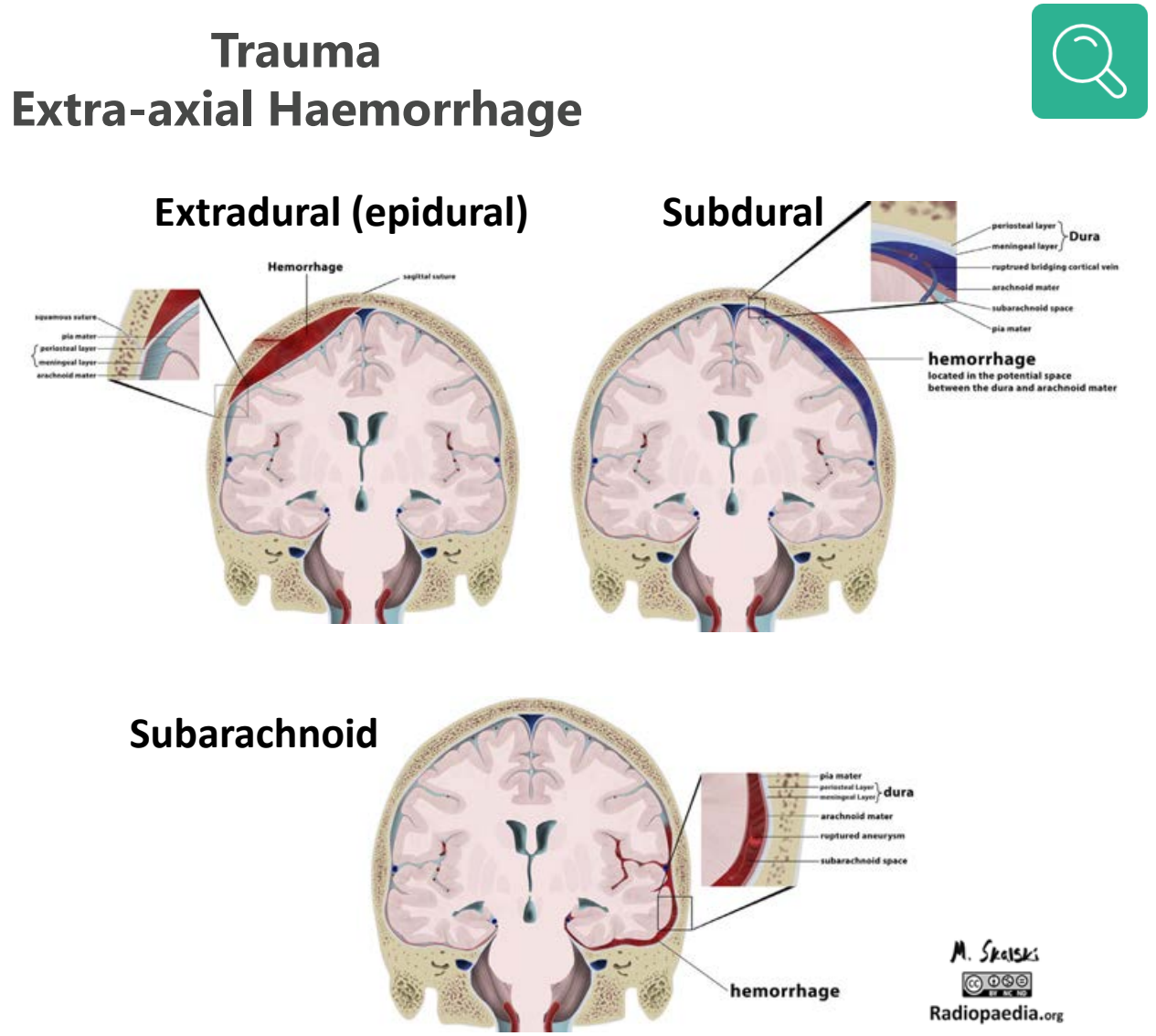

Fig. 25. Schematic representations of the different types of acute extra-axial haemorrhage. Case courtesy of Dr Matt Skalski, Radiopaedia.org. rID: 21542.

Chapter Outline

Trauma

The density of intracranial haemorrhage changes over time (figure 26).

- Prior to clotting, the hyperacute haematoma (during a few minutes) has the same density as normal blood
- As it clots (within hours), the density of acute haematoma increases, which makes it clearly visible on CT
- Over days to weeks, the density of the subacute haematoma decreases, it becomes isodense compared to brain tissue => therefore, it becomes more difficult to detect
- Later, chronic haematoma will have a similar density as cerebrospinal fluid

Multiple factors affect the actual time it takes the haematoma to undergo the above-mentioned changes.

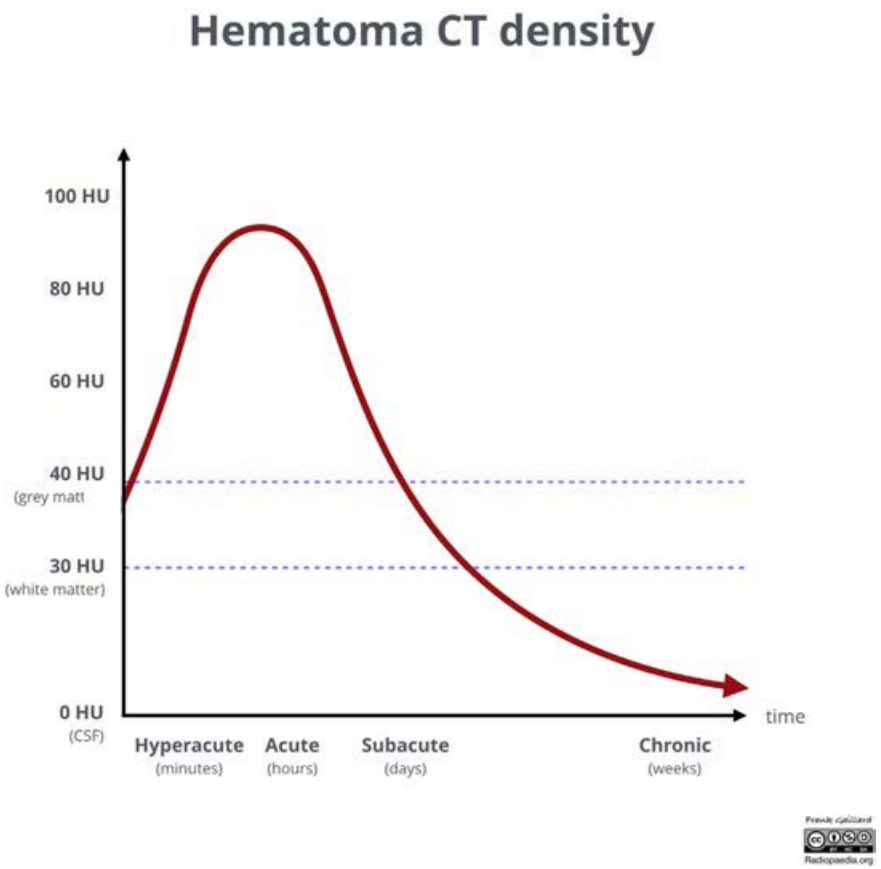

Fig. 26. Graph demonstrating the evolution of the density of intracranial hemorrhage on CT. Case courtesy of Assoc Prof Frank Gaillard, Radiopaedia.org. rID:36064

Chapter Outline

Trauma

Intra-axial Haemorrhage

Intraparenchymal haemorrhage (figure 27) is bleeding into the brain parenchyma proper.

Brain contusions and haemorrhage after trauma characteristically occur in the inferior frontal lobes and anterior-inferior temporal lobes.

Acute intracerebral haemorrhage is seen as areas of high attenuation values on CT images (hyperdense, see also figure 25).

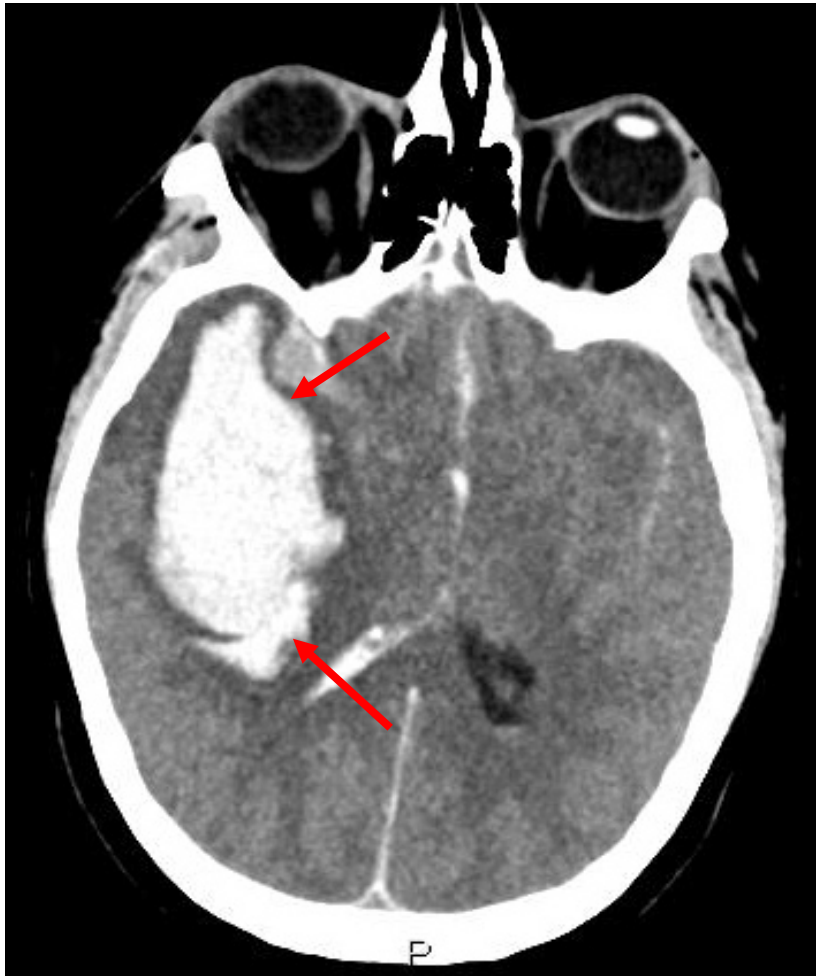

Fig. 27. Acute intraparenchymal haematoma (arrows) seen on a non-contrast enhanced CT image

Chapter Outline

Trauma

Extra-axial Haemorrhage

The different types of acute extra-axial haemorrhage and their distinctive imaging characteristics are illustrated in figure 28.

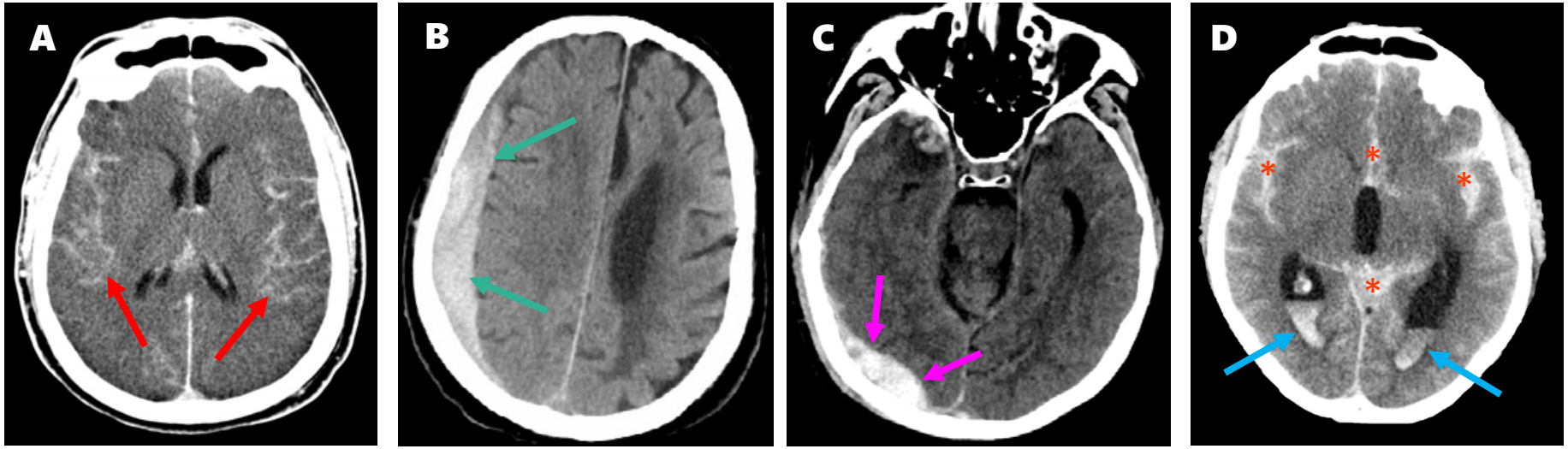

Subarachnoid: hyperdense material fills the subarachnoid space (which is usually hypodense as CSF is hypodense)

Subdural: crescent shape, hyperdense collection

Epidural: biconvex or lenticular shape, sharply demarcated

Intraventricular: hyperdense material within the ventricles. As blood is heavier than CSF, it tends to pool in the occipital horns.

Fig. 28. Illustrative examples of acute extra-axial haemorrhage as seen on axial CT images. Note the presence of additional subarachnoid haemorrhage (asterisks) in D.

Chapter Outline

Ischemic Disease

Acute Infarct

Acute stroke results from a brain blood vessel occlusion. Ischemia accounts for 85% of presentations and primary haemorrhage for 15%.

Primary ischemia results from atherothrombotic occlusion or an embolism.

Knowledge of the vascular territories is crucial to recognize infarctions in arterial territories, in watershed regions or venous infarctions.

Srinivasan A., Goyal M., Al Azri F., Cheemun Lum C. State-of-the-Art Imaging of Acute Stroke. RadioGraphics 2006; 26:S75–S95

Chapter Outline

Ischemic Disease

Acute Arterial Ischemic Infarct

It follows the distribution of the arterial cerebral irrigation territories (figure 29) .

Unenhanced CT can help identify a haemorrhage. This is a contraindication to thrombolytic therapy and it can also detect early-stage acute ischemia.

The CT findings in acute ischemia (figure 30) include: local hypoattenuation in an arterial distribution due to cytotoxic oedema, sulcal effacement and mass effect, the hyperdense vessel sign (middle cerebral artery thrombus), the insular ribbon sign, and obscuration of the lentiform nucleus, caused by a loss of contrast between grey matter and white matter due to cytotoxic oedema.

CT-angiography is useful for evaluating the intracranial and extracranial vessels to demonstrate the location of the arterial occlusion.

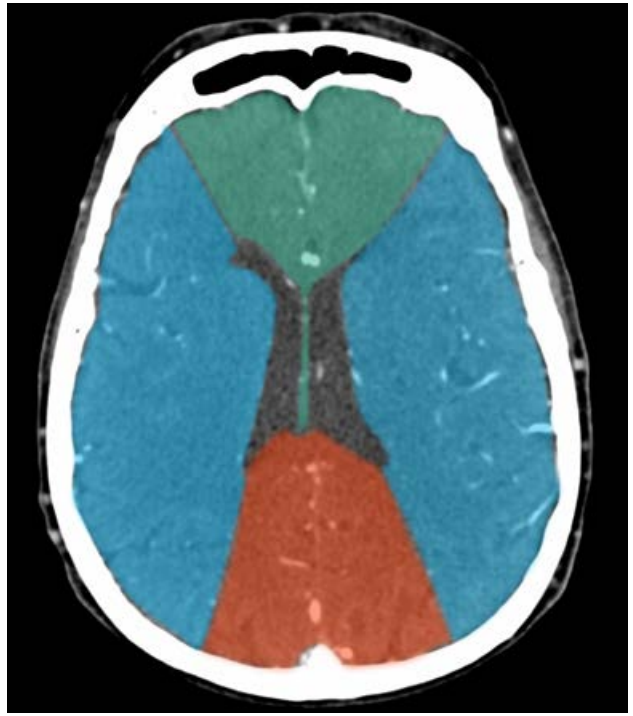

Fig. 29. Cerebral arterial vascular territories. Anterior cerebral artery (green). Middle cerebral artery (blue). Posterior cerebral artery (red).

Chapter Outline

Ischemic Disease

Acute Arterial Infarct

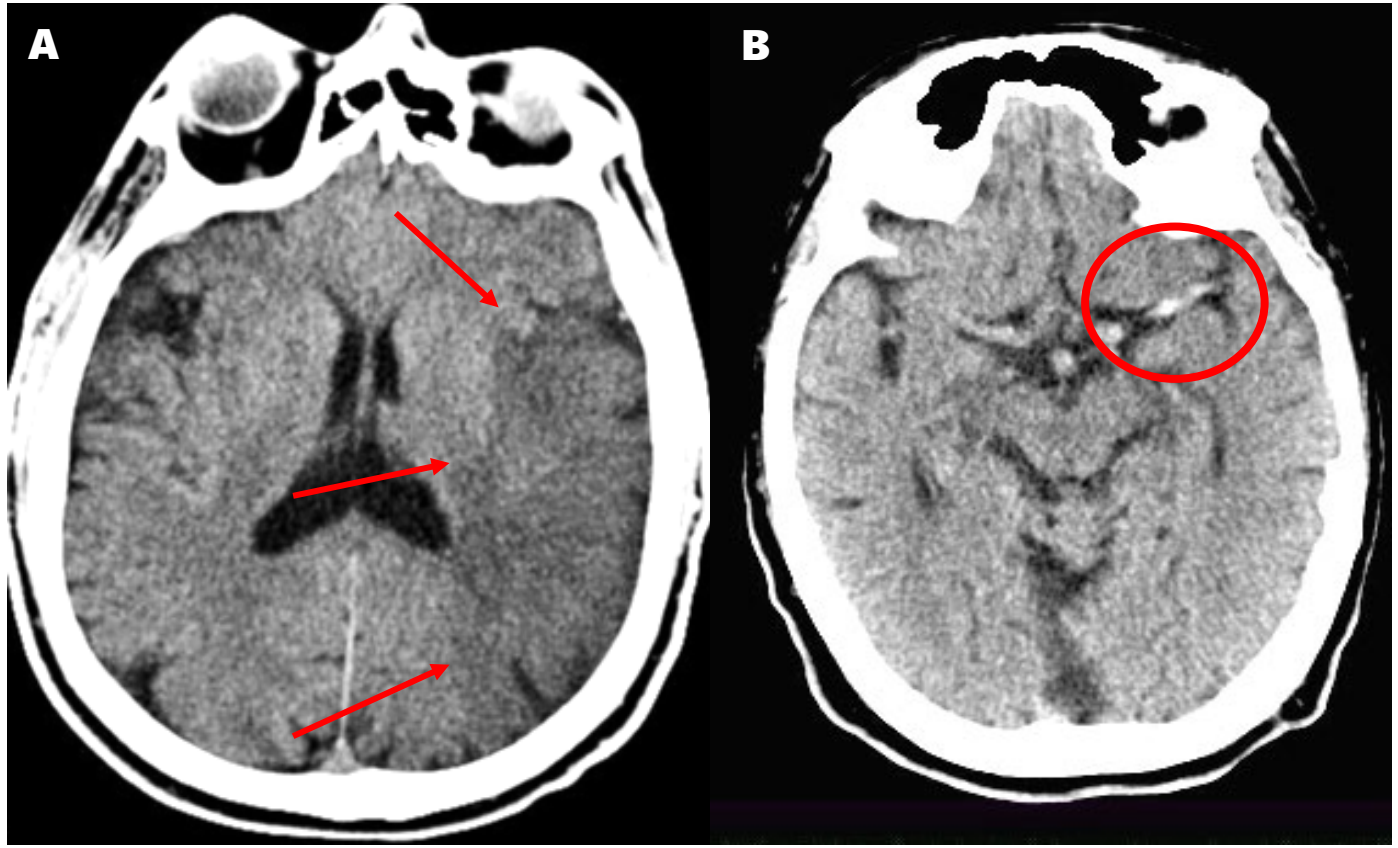

Fig. 30. A. Acute ischemic infarct (arrows) seen as a hypoattenuating area on non-enhanced CT due to cytotoxic oedema in the left middle cerebral artery territory. B. Hyperdense left middle cerebral artery sign (circle) on non-enhanced CT corresponding to an acute thrombus.

Chapter Outline

Ischemic Disease

Acute Arterial Ischemic Infarct

Acute cerebral ischemia may result in a central irreversibly infarcted tissue "core" surrounded by a peripheral region of salvageable tissue, called "penumbra". The ischemia may be reversible if reperfusion is obtained quickly, without early recanalization, the infarction gradually expands to include the penumbra.

The penumbra can be evaluated both on CT images (indicated by a discrepancy in perfusion maps, figure 31) and on MR images (indicated by a mismatch between diffusion and perfusion maps). CT-angiography is used to detect the location of the intravascular occlusion (figure 31).

Chapter Outline

Ischemic Disease

Acute Arterial Infarct

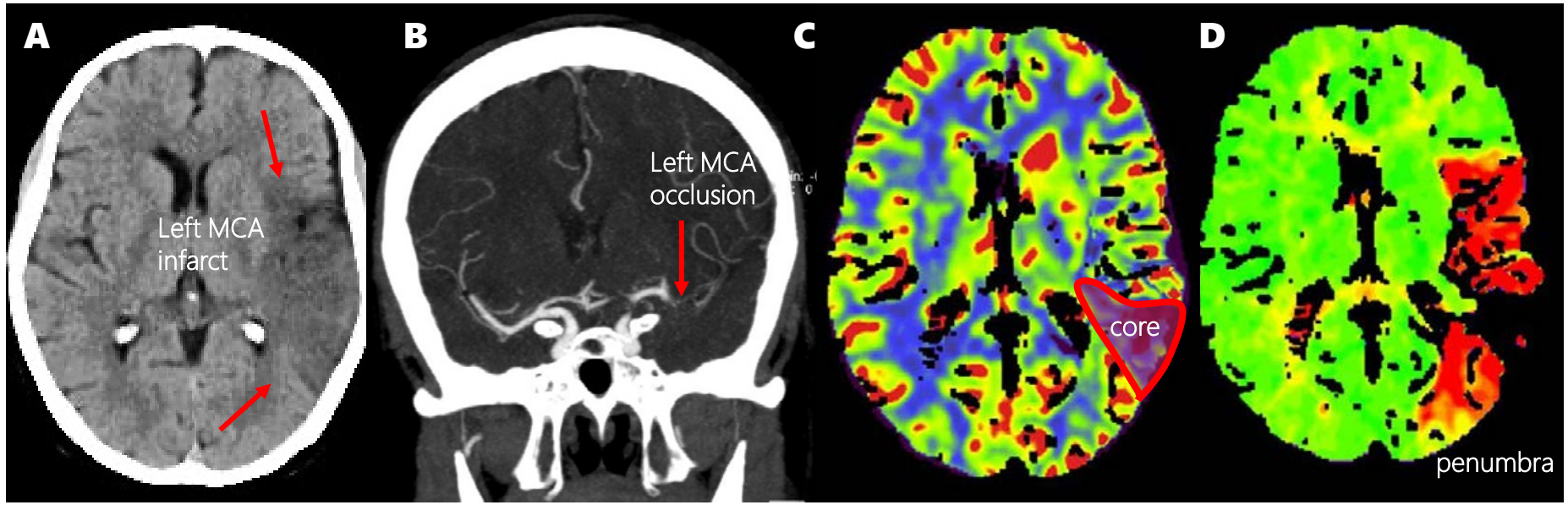

Fig. 31. A. Acute ischemic infarct (arrows) seen as a hypoattenuating area on non-enhanced CT (A) in the left middle cerebral artery territory. B. Coronal reconstruction of an angio-CT series shows occlusion of the left MCA. C. The CBV (cerebral blood volume) perfusion parametric map shows the core whereas the penumbra can be assessed on the TTP (time to peak) perfusion parametric map (D).

Chapter Outline

Ischemic Disease

Acute Arterial Ischemic Infarct

MR imaging findings in patients with acute cerebral ischemia include hypointense signal in white matter on T1-weighted and hyperintense signal on T2-weighted images with loss of grey matter–white matter differentiation, sulcal effacement and mass effect.

Acute stroke causes cytotoxic oedema with intracellular water accumulation and overall decreased rate of water molecular diffusion. Areas of cytotoxic oedema, in which the motion of water molecules is restricted, appear bright on Diffusion Weighted Imaging (DWI) and low on the apparent diffusion coefficient (ADC) map (figure 32).

DWI is the most sensitive sequence for stroke imaging.

MR-angiography is useful for detecting intravascular occlusion.

Chapter Outline

Ischemic Disease

Acute Arterial Infarct

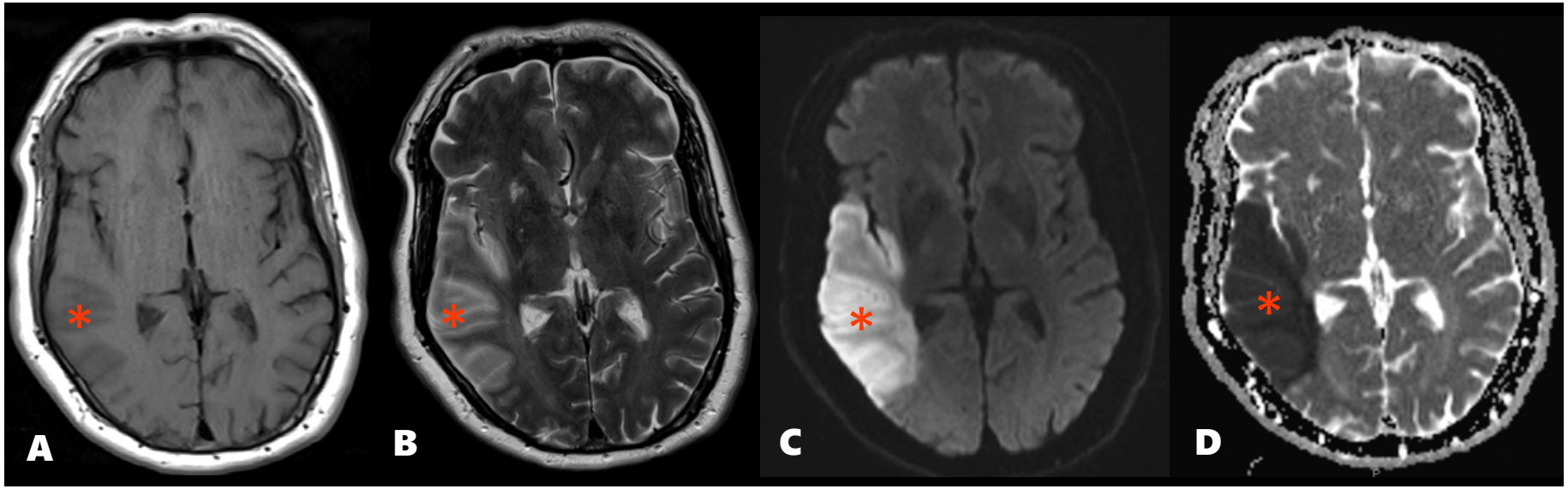

Fig. 32. Acute right middle cerebral artery territory infarct (asterisks). Hypointense on T1-weighted (A) and hyperintense on T2-weighted images (B), sulcal effacement and mass effect. Diffusion restriction, demonstrating high signal on DWI (C) and low signal on the ADC map (D).

Chapter Outline

Ischemic Disease

Chronic Ischemic Infarct

MR imaging may help determine the age of an ischemic stroke.

In chronic infarcts, the T1 signal remains low and the T2 signal is high.

The ADC values are high (figure 33), resulting in high signal. DWI signal is variable, but as time goes on signal progressively decreases.

Ischemic Disease

Chronic Arterial Infarct

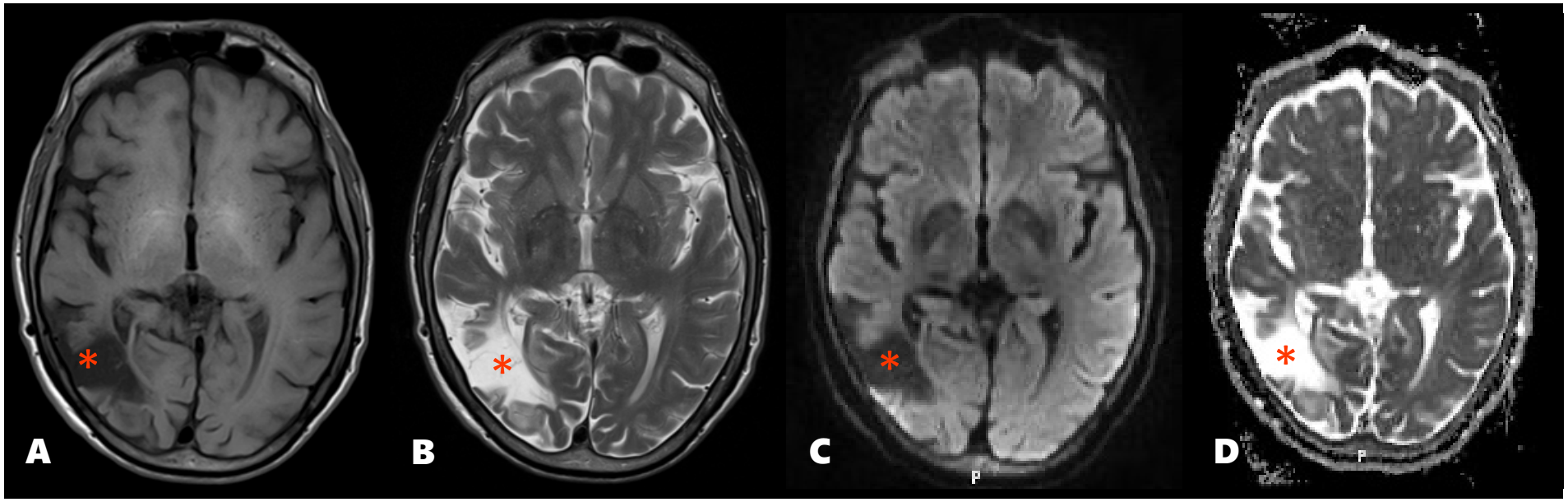

Fig. 33. Chronic right middle cerebral artery territory infarct (asterisks) as seen on MRI. Hypointense on T1-weighted and hyperintense on T2-weighted images. Low signal on DWI and high signal on the ADC map.

Chapter Outline

Ischemic Disease

Cerebral Venous Thrombosis

Cerebral venous thrombosis results from occlusion of a dural venous sinus (figure 34), cortical vein or deep cerebral vein. Very often thrombosis of multiple venous structures coexist.

Risk factors include hormonal factors, oral contraceptive pills, prothrombotic haematogenic diseases, sepsis and tumours.

Clinical presentation and imaging findings are variable and correspond to a venous territory distribution.

A poor venous outflow caused by cerebral venous thrombosis can lead to oedema, cerebral venous infarction (50% of cases) and intracranial haemorrhage.

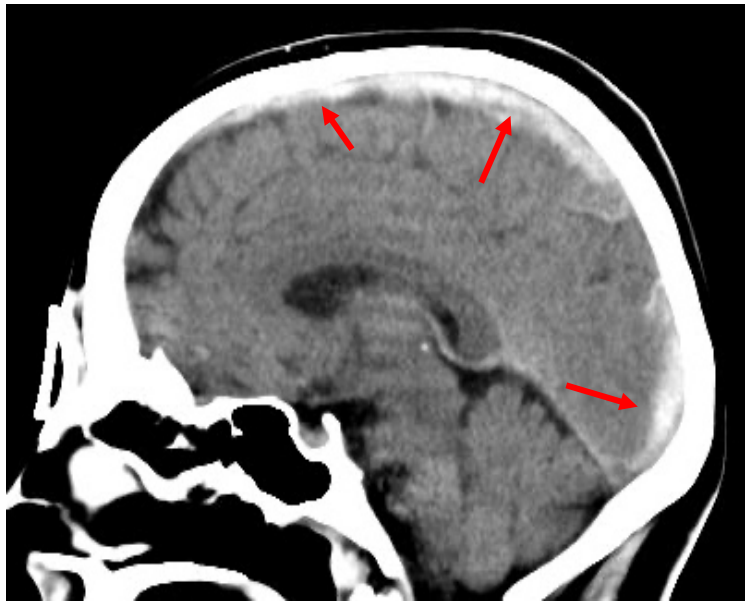

Fig. 34. Extensive superior sagittal sinus thrombosis as seen on non-contrast CT. The acute thrombus appears hyperdense and is indicated by arrows.

Cerebral venous thrombosis **does not respect** the topography of arterial territories. In the absence of a hyperdense sinus or vein, findings can be subtle on non-contrast CT !

Chapter Outline

Ischemic Disease

Haemorrhagic Infarction, Parenchymal Haematoma and Hypertensive Haemorrhage

Haemorrhagic transformation is a complication of ischemic stroke and it includes haemorrhagic infarction (petechial haemorrhage, most often asymptomatic) and parenchymal haematoma (often associated with neurological deterioration). Haemorrhagic transformation is seen more often in patients with anticoagulant treatment or thrombolytic therapy

Intracerebral haemorrhage can be divided into primary haemorrhage (without an underlying lesion) and secondary haemorrhage (with an underlying lesion). The most common cause of primary haemorrhage is hypertension and the most common cause of secondary haemorrhage is cerebral venous thrombosis.

Hypertensive haemorrhage is typically located in the basal ganglia, thalamus, pons, brain lobes or cerebellum. Haemorrhage is most easily detected with CT as an area of high attenuation on non-contrast images (figure 35), but it can also be depicted with gradient echo (GE)MR-sequences, as low signal intensity areas (figure 36).

On CT angiography, active contrast extravasation can be observed within the haematoma. Complications that can be detected by CT include spread of haemorrhage to other brain areas or ventricles, brain oedema, brain herniation and hydrocephalus. Follow-up CT is used to measure haematoma expansion and is useful for clinical decision making and prognosis.

Chapter Outline

Ischemic Disease

Haemorrhagic Infarction

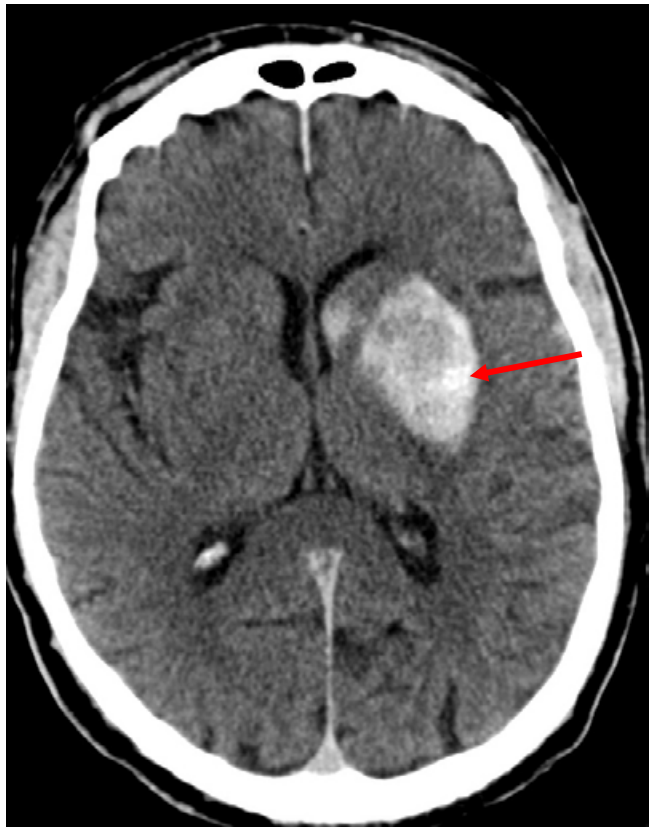

Fig. 35. Haemorrhagic infarct (arrow) as seen on CT.

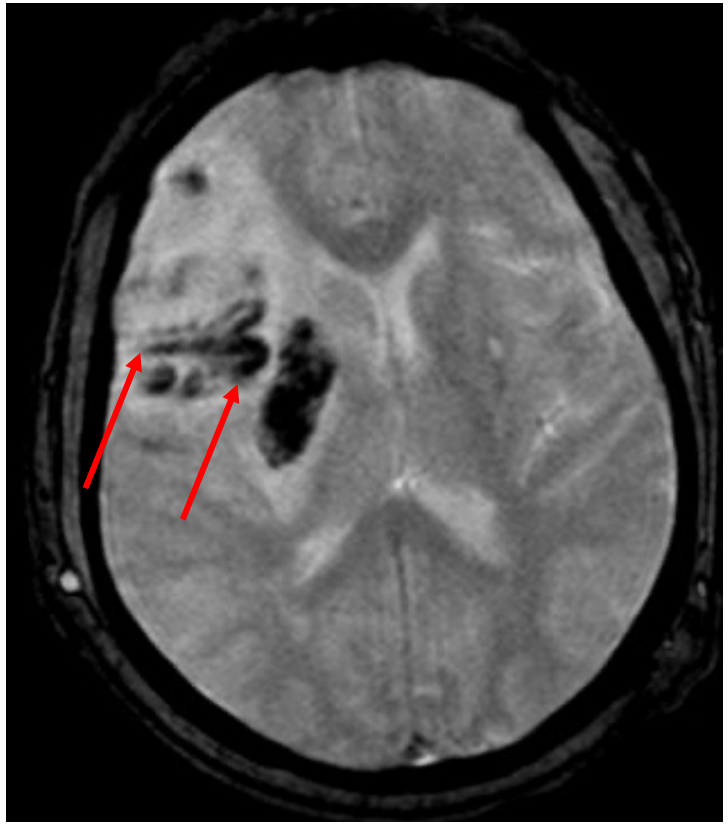

Fig. 36. Haemorrhagic infarct (arrow) on a gradient-echo sequence

Brain Tumours

Intra-axial Brain Tumours

These are tumours located within the brain parenchyma. The characteristic radiological sign of intra-axial tumours is the outward displacement of the grey mater and the CSF of the subarachnoid space (figure 37).

Intra-axial tumours include:

Primary brain tumours:

- Glial tumours (astrocytoma, oligodendroglioma, ependymoma)
- Non-glial tumours (lymphoma)

Brain metastases

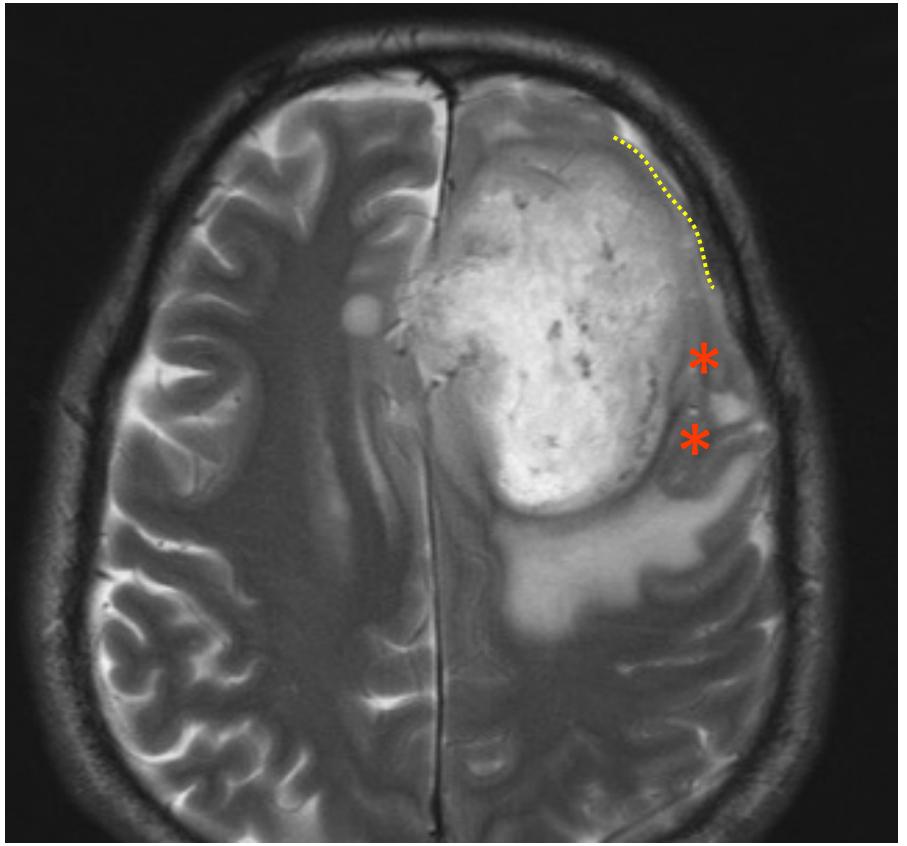

Fig. 37. T2-weighted image demonstrates the characteristic radiological sign of intra-axial tumours (here a glioblastoma): outward displacement of the grey mater (red asterisks) and the CSF (yellow line) of the subarachnoid space.

Chapter Outline

Brain Tumours

Intra-axial Brain Tumours

Glioma

Gliomas are brain tumours that start in glial cells. There are three main types of glial cells: astrocytes (provide nutrients to neurons and structural support), oligodendrocytes (form the myelin sheath of axons in the CNS) and ependymal cells (produce cerebrospinal fluid).

Astrocytoma is the most common glioma; it can be subdivided into low-grade astrocytoma, intermediate anaplastic type and high-grade malignant glioblastoma (GBM). GBM is the most common astrocytoma type; it represents 50% of all astrocytomas (figure 38).

GBM was traditionally subdivided into secondary GBM (progresses from low grade or anaplastic astrocytoma; characteristics: 5%-10% of GBMs, patients <45 years, better prognosis) and primary GBM (develops de novo; characteristics: 90% of GBMs, patients >45 years, dismal prognosis). As primary and secondary GBM are separate tumour entities with distinct genetic alterations, and as isocitrate dehydrogenase (IDH) mutation is the most critical genomic alteration in GBM, the new 2021 WHO classification of CNS tumours, distinguishes between GBM IDH wildtype (which essentially corresponds to what used to be called primary GBM) and astrocytoma IDH mutant grade 4 (which corresponds roughly to what used to be called secondary GBM).

Chapter Outline

Brain Tumours

Intra-axial Brain Tumours

Glioma

Oligodendroglioma is the third most common glioma (5%–18% of all glial neoplasms) typically seen in middle aged adults. Calcification is found in 20%-91% of cases (figure 39). The diagnosis requires the presence of IDH mutation and 1p19q codeletion as molecular markers.

Ependymomas tend to arise within or abutting the ventricular system or from the lining of the central canal of the spinal cord. They most often occur in the posterior fossa (60%) and they account for 33% of paediatric brain tumours seen in children < 3years of age.

=> For paediatric CNS tumours, see chapter on paediatric radiology.

Chapter Outline

Brain Tumours

Intra-axial

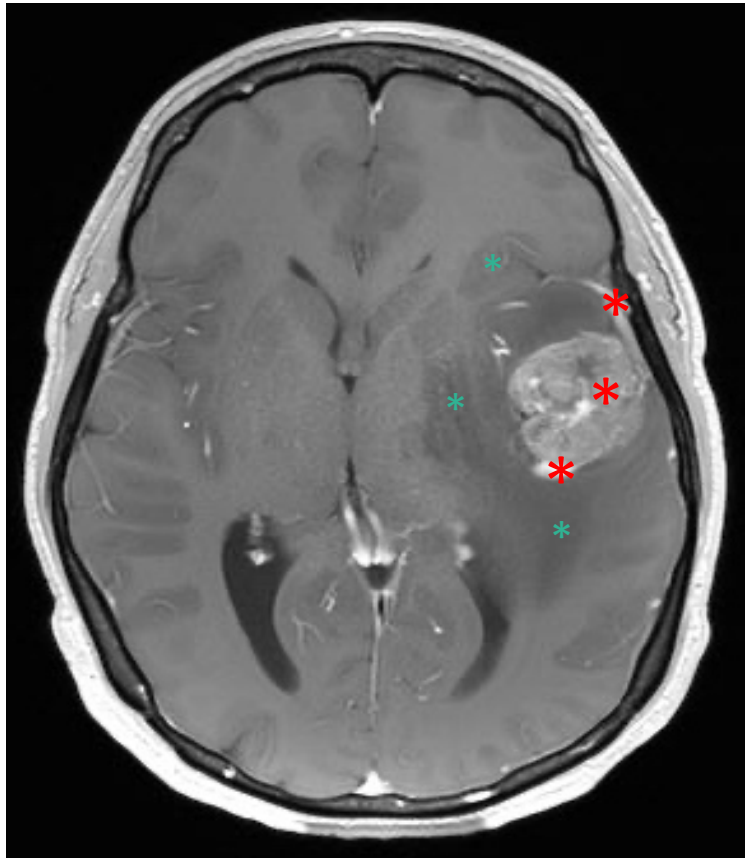

Fig. 38. Contrast-enhanced T1-weighted image shows a glioblastoma with variable enhancement (red asterisks) surrounded by vasogenic oedema (green asterisks).

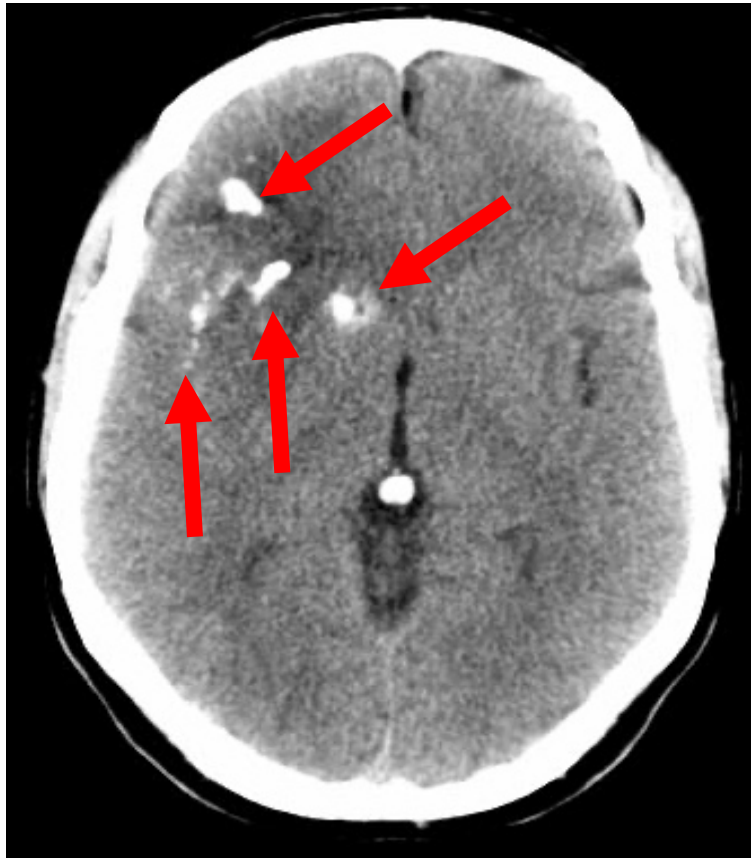

Fig. 39. Non-contrast CT shows an oligodendroglioma with typical calcifications (arrows).

Chapter Outline

Brain Tumours

Intra-axial Brain Tumours

Lymphoma of the CNS has two major subtypes: secondary CNS involvement by systemic lymphoma (most frequent) and primary central nervous system lymphoma (PCNSL) localized in the brain, leptomeninges, spinal cord, or eyes, without evidence of it outside the CNS.

Brain lymphoma classically presents as a well defined homogeneously enhancing supratentorial mass with high attenuation values on non contrast CT images due highly packed abnormal cells.

MRI reveals intermediate to low signal intensity on T1-weighted images and isointense or hypointense signal relative to the grey matter on T2-weighted images, with intense homogeneous enhancement (figure 40). Water diffusion is often restricted due to the high cellularity within the tumour, making it appear strongly hyperintense on DWI and hypointense on ADC maps

Chapter Outline

Brain Tumours

Intra-axial

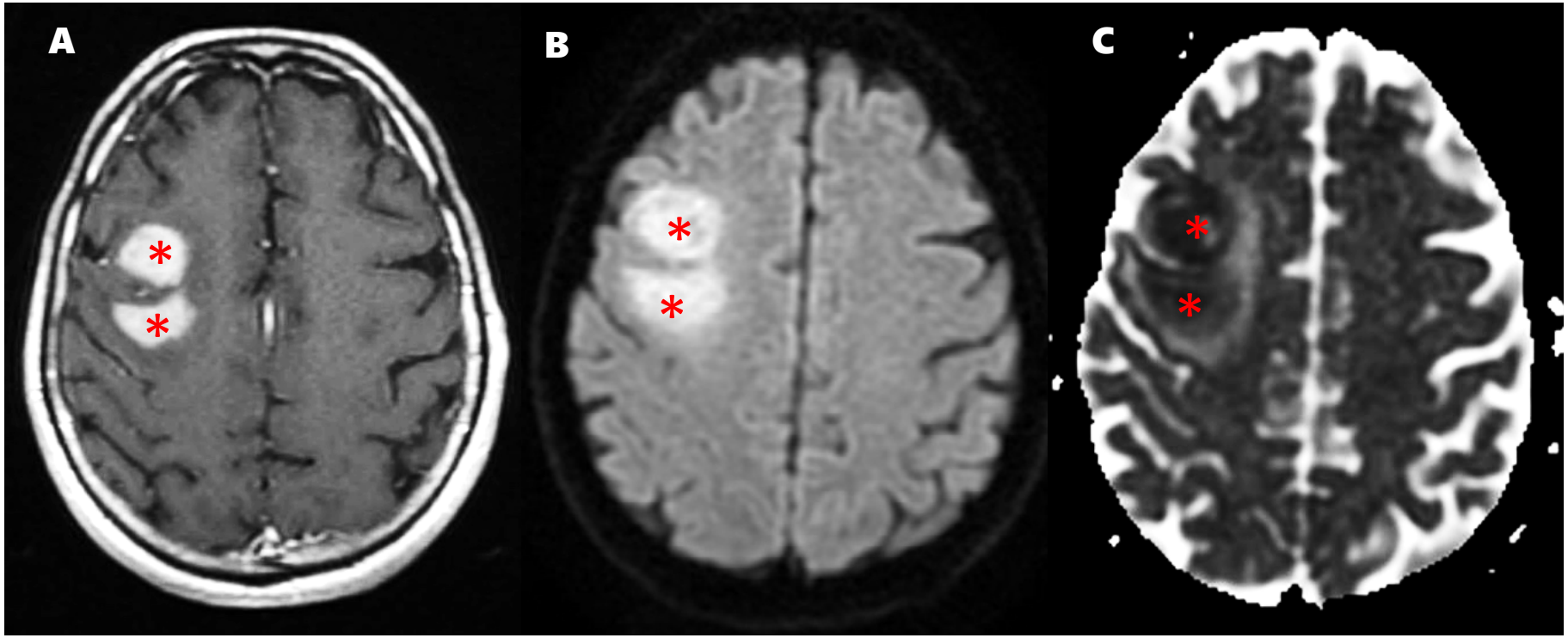

Fig. 40. Lymphoma (asterisks). Frontal intra-axial mass showing enhancement on the T1-weighted gadolinium enhanced image (A) and diffusion restriction, hyperintense on DWI (B) and hypointense on ADC (C).

Chapter Outline

Brain Tumours

Intra-axial Brain Tumours

Brain metastases are characteristically located in the grey matter-white matter junction. They represent the most frequent brain tumours in adults.

Multiple tumours in the brain usually indicate metastatic disease. Multiple nodular enhancing lesions are seen in hematogenous dissemination of metastatic neoplasms (figure 41).

In adults, the most common primary tumours responsible for brain metastases are carcinomas originating in the lung, breast, kidney, colon and melanoma.

MRI is more sensitive than contrast-enhanced CT for the detection of brain metastases.
MRI is the preferred imaging modality to detect brain metastases.

Smirniotopoulos J.G.,. Murphy F.M., Rushing E.J.,Rees J.H.,Schroeder. Patterns of Contrast Enhancement in the Brain and Meninges. RadioGraphics 2007; 27:525–551

Chapter Outline

Brain Tumours

Intra-axial

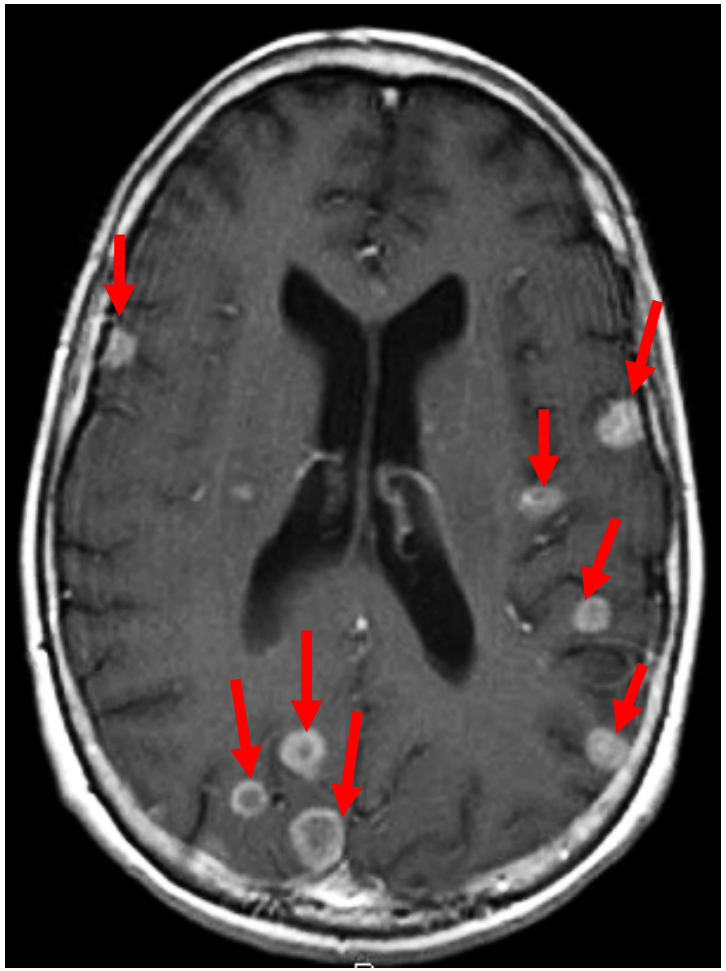

Fig. 41. Multiple ring enhancing intra-axial lesions (arrows) on a T1-weighted contrast-enhanced image. Metastases from lung adenocarcinoma.

Chapter Outline

Brain Tumours

Extra-axial Brain Tumours

These are tumours located outside the brain parenchyma. A CSF cleft and medial displacement of both the subarachnoid vessels and the grey matter are characteristic signs of extra-axial tumours.

The most common extra-axial tumours are the following:
- Meningioma / hemangiopericytoma
- Craniopharyngioma
- Pineal parenchymal tumours
- Cranial nerve schwannomas

Other most common mass-like extra-axial lesions are:
- Epidermoid cysts
- Arachnoid cysts

Chapter Outline

Brain Tumours

Extra-axial

Meningioma is the most common tumour of the meninges (non-glial neoplasm) and the most common extra-axial tumour.

Meningiomas are most often indolent, they are more common in women and are typically seen after 40 years of age. Malignant and atypical meningiomas are slightly more often seen in males.

Clinical symptoms include head ache, paralysis and mental status changes.

As with other CNS tumours, molecular markers contribute to the diagnosis and grading of meningioma subtypes.

The MRI features of meningiomas are characteristic (figures 42 and 43).

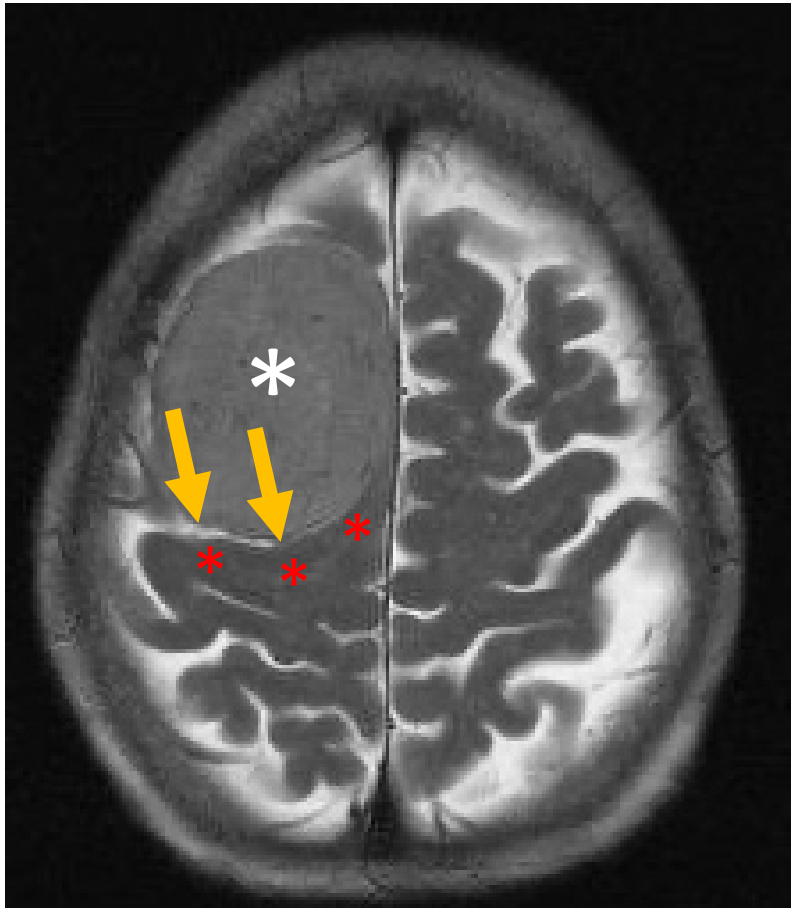

Fig. 42. Meningioma (white asterisk). Medial displacement of the CSF (yellow arrows) and grey matter (red asterisks) typical of an extra-axial tumour.

Chapter Outline

Brain Tumours

Extra-axial

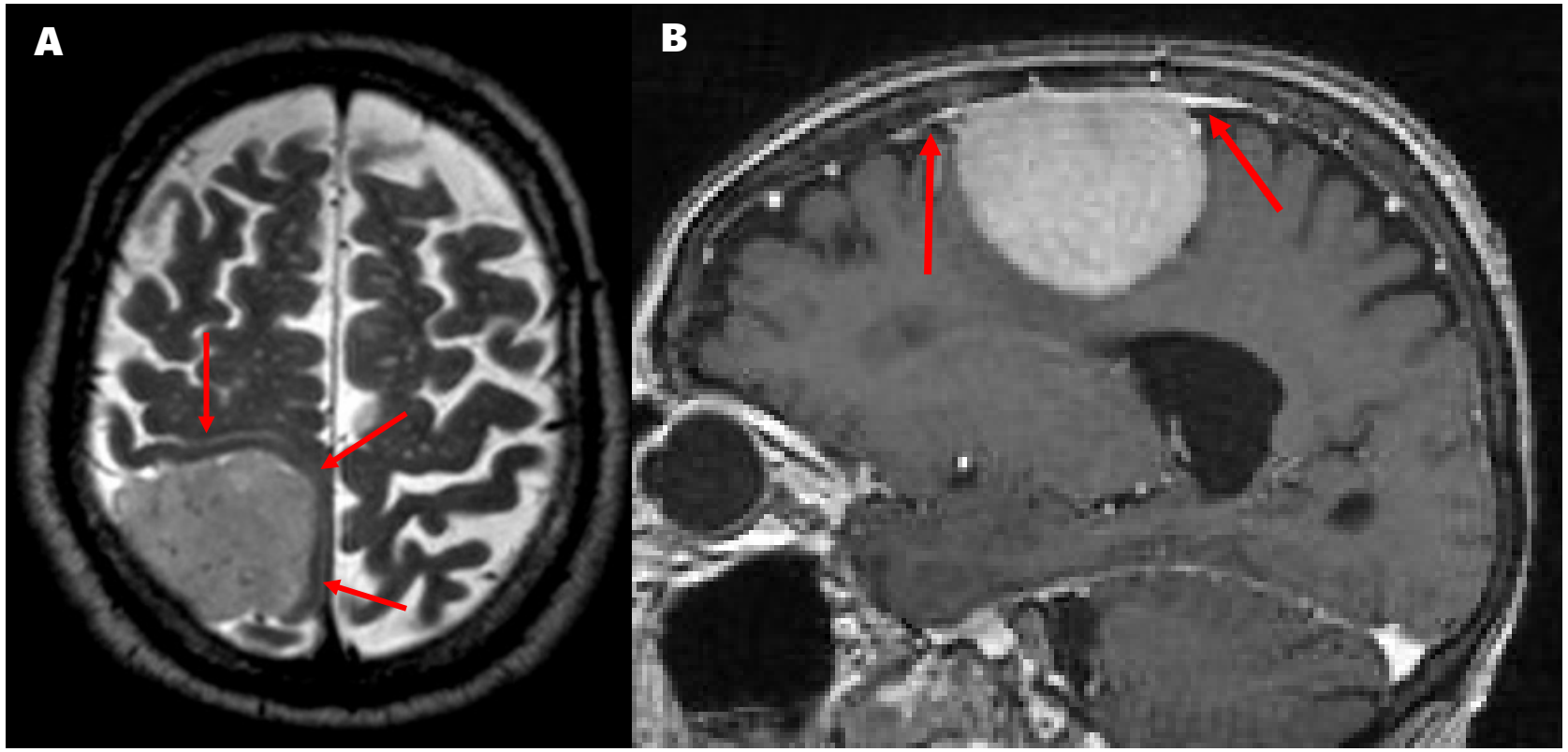

Fig. 43. Characteristic MRI features of meningioma. (A) Axial T2-weighted image shows medial displacement of grey matter (arrows) by the meningioma (asterisk). (B) Contrast-enhanced sagittal T1-weighted image shows homogeneous enhancement and a broad dural base or a dural tail (arrows).

Chapter Outline

Brain Tumours

Extra-axial

Epidermoid is a rare, benign congenital lesion derived from ectoderm and lined by squamous epithelium. Epidermoid has cystic contents including debris, keratin, water, and cholesterol. The lesion typically occurs between 20 and 40 years of age.

On many MRI sequences, epidermoids are indistinguishable from simple arachnoid cysts with the exception of DWI sequences as epidermoids display restricted diffusion as opposed to arachnoid cysts, which do not (figure 45).

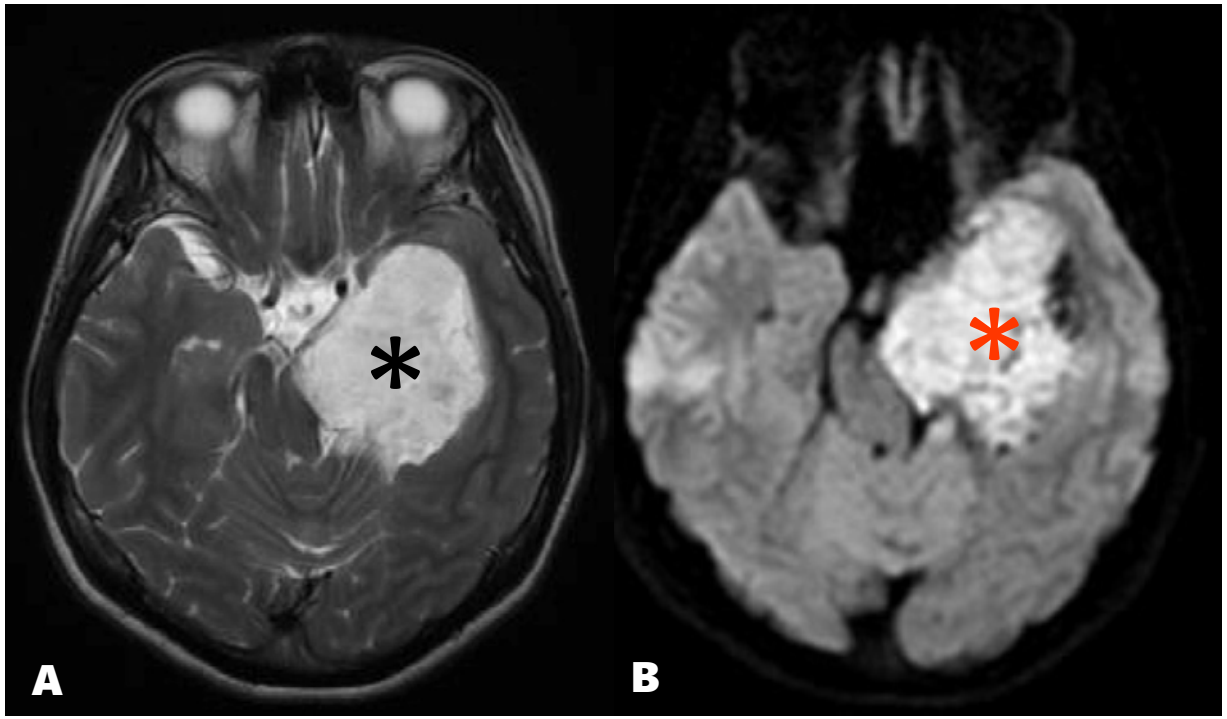

Fig. 44. On T2-weighted MR images (A) the epidermoid (asterisk) has a high signal similar to CSF. On the DWI image (B), the epidermoid (asterisk) has a high signal because of restricted diffusivity allowing its differentiation from an arachnoid cyst. Arachnoid cysts have a low signal on DWI because diffusivity is not restricted as they contain CSF.

Chapter Outline

Pituitary Gland Tumours

The most frequent pituitary gland tumours are adenomas (figure 45): microadenomas <10mm size and macroadenomas >10mm size. Macroadenomas can extend superiorly compressing the optic chiasm and laterally they can extend into the cavernous sinus.

Pituitary adenomas either present with hormonal imbalance (about half of them are secretory) or mass effect on the optic chiasm and cavernous sinus. Very large tumours can lead to hydrocephalus or they can invade the paranasal sinuses.

Other common lesions that can be found in the pituitary gland region are Rathke's cleft cyst and craniopharyngiomas (figure 46). There are two distinct types of craniopharyngiomas (adamantinomatous and papillary) that can be differentiated one from another on the basis of molecular testing. Both craniopharyngioma types arise in the sellar/ suprasellar region and are relatively benign.

Chapter Outline

Pituitary Gland Tumours

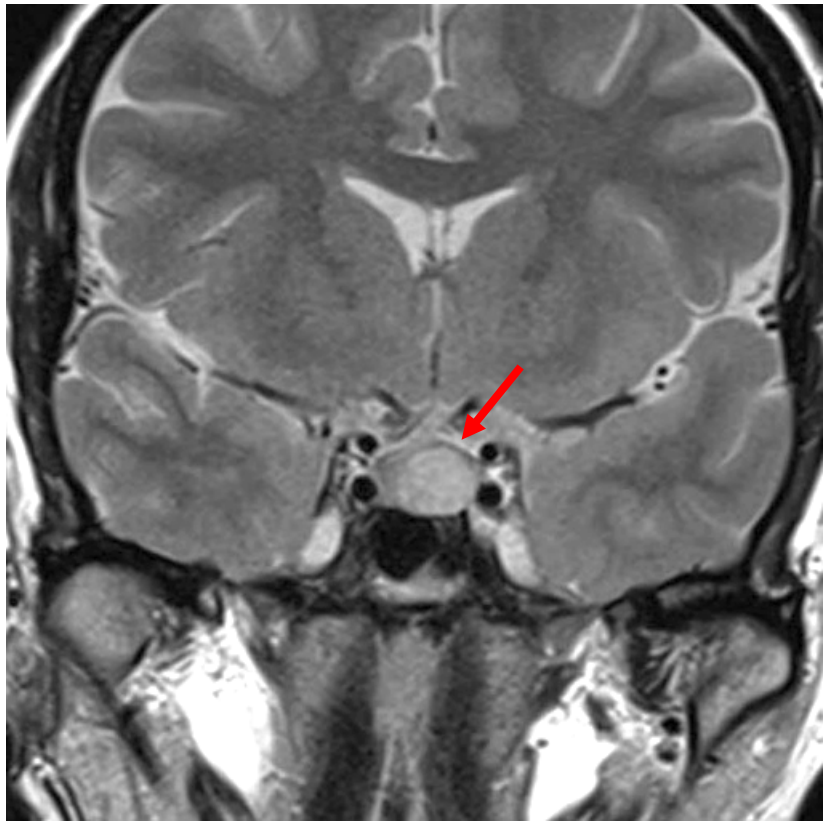

Fig. 45. Typical macroadenoma (arrow) on a coronal T2-weighted image

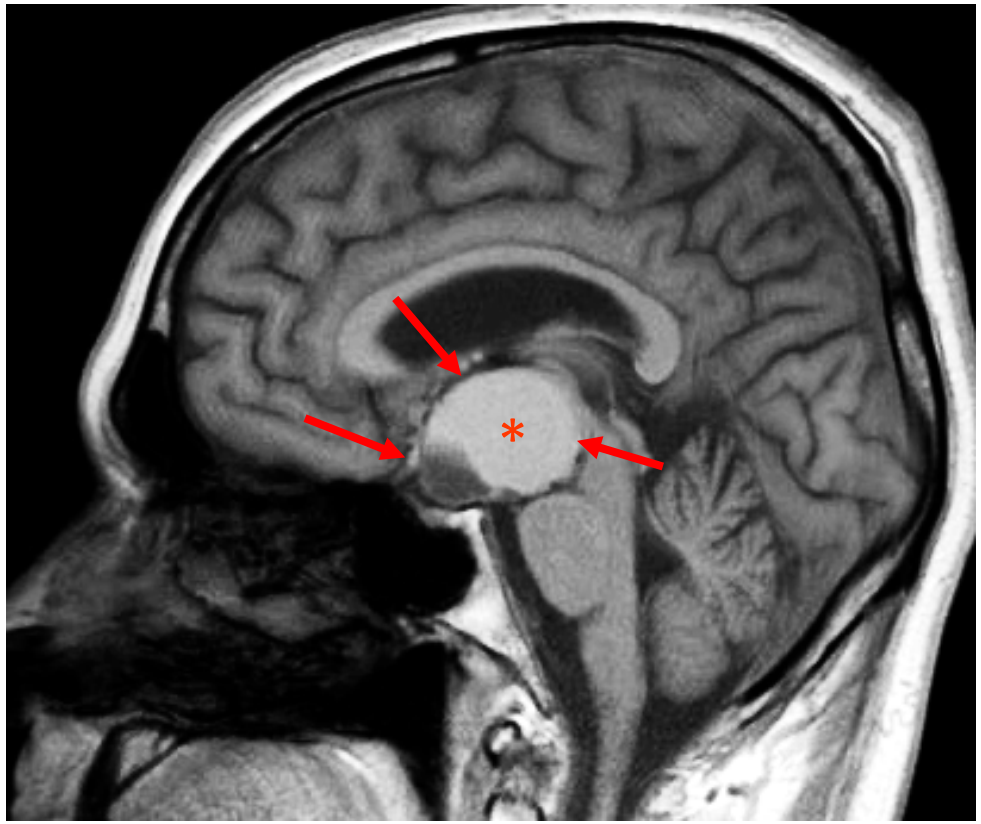

Fig. 46. Craniopharyngioma (arrows) on a sagittal T1-weighted image. Note the large cystic hyperintense component (asterisk).

Chapter Outline

Inflammatory/Infectious Disease

Demyelinating Disease

Multiple sclerosis (MS) is the most common inflammatory demyelinating disease of the central nervous system in young and middle-age adults.

White matter lesions in MS characteristically involve the periventricular white matter, corpus callosum, U-fibers, temporal lobes, brainstem, cerebellum and spinal cord (figure 47).

Dawson fingers (ovoid lesions perpendicular to the ventricles) are typical for MS and are the result of inflammation around penetrating venules.

Chapter Outline

Inflammatory Infectious Diseases

Demyelinating Disease

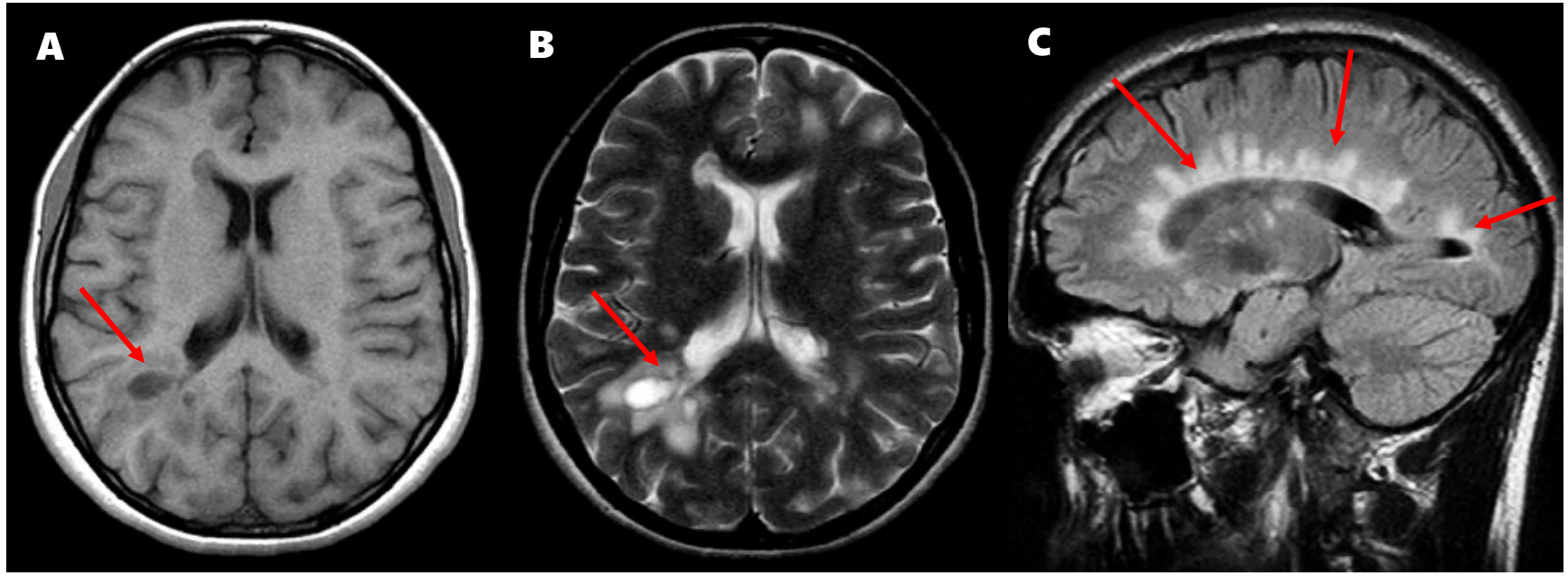

Fig. 47. Multiple sclerosis with characteristic periventricular white matter ovoid lesions perpendicular to the ventricles (arrows). The lesions are isointense on T1-weighted (A), hyperintense on T2-weighted (B) and on FLAIR (C) images.

Chapter Outline

Inflammatory/Infectious Disease

Infections

Infections of the CNS can be produced by different agents; bacterial, viral, fungal or parasitic. The spectrum of abnormalities seen include: meningitis, cerebritis, abscesses, subdural or epidural empyema and ventriculitis.

Immunocompromised patients have an increased risk for infectious complications. Infections can be viral, bacterial, fungal, or parasitic in origin.

Bacterial brain abscesses (figure 48) present as focal masses with a high signal intensity centre on T2-weighted images with marked perifocal oedema, and ring-like enhancement on gadolinium enhanced T1-weighted images. Restricted diffusion is seen on DWI due to the viscosity of pus, resulting in a high signal intensity on DWI and low ADC.

Progressive multifocal leukoencephalopathy (PML) is a demyelinating disorder which occurs in immunocompromised patients as a results of the reactivation of the John Cunningham (JC) virus. Classically it is seen in HIV patients, in post-transplant or leukemia patients. In addition, PML is also seen in patients with recovering immune system. PML involves the white matter. Lesions have low signal intensity on T1-weighted and high signal intensity on T2-weighted images and neither show restriction on DWI nor enhancement with gadolinium (figure 49).

Chapter Outline

Inflammatory Infectious Diseases

Bacterial Abscess

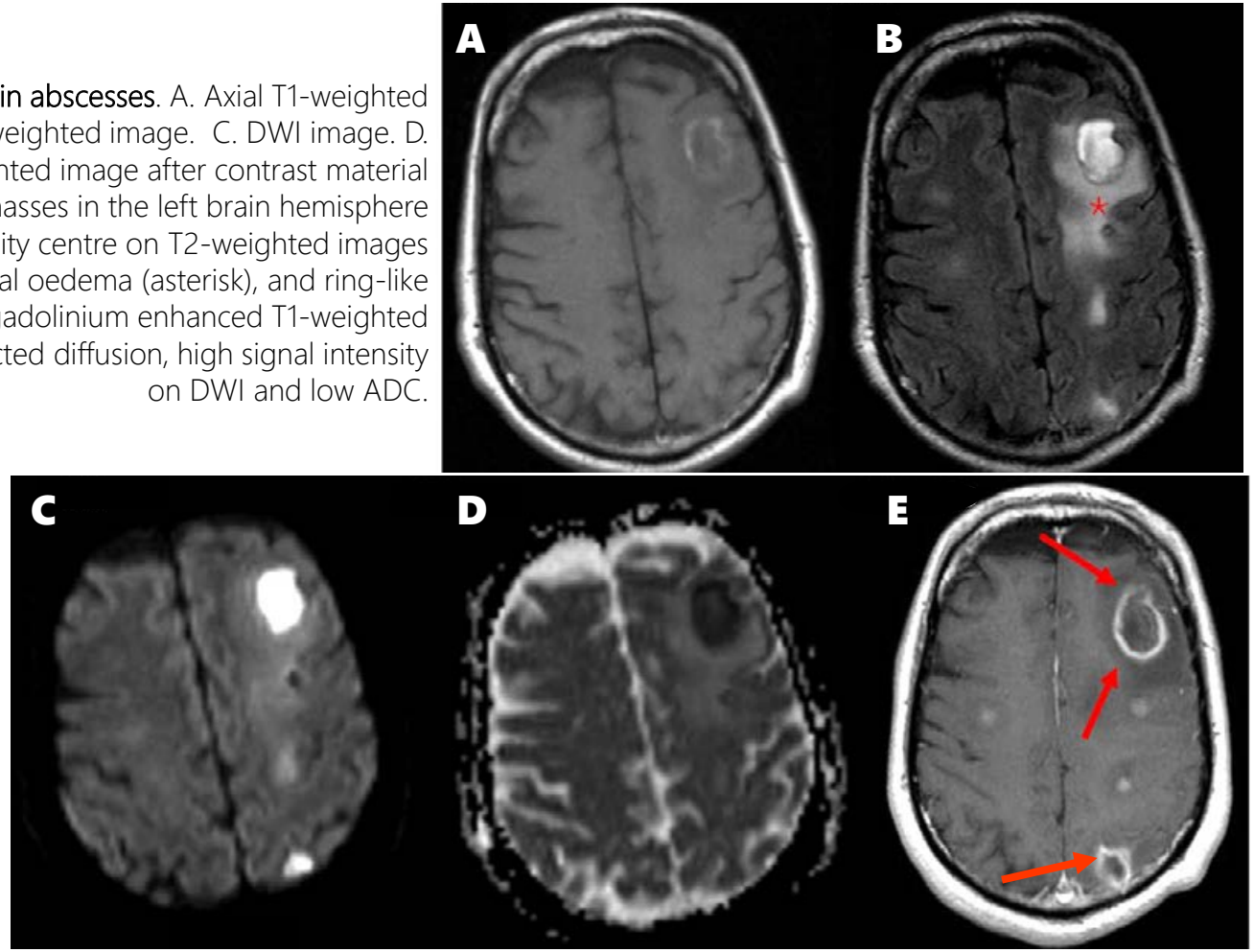

Fig. 48. Bacterial brain abscesses. A. Axial T1-weighted image. B. Axial T2-weighted image. C. DWI image. D. ADC map. E. T1-weighted image after contrast material injection. Multiple masses in the left brain hemisphere with a high signal intensity centre on T2-weighted images with marked perifocal oedema (asterisk), and ring-like enhancement on gadolinium enhanced T1-weighted images (arrows). Restricted diffusion, high signal intensity on DWI and low ADC.

Chapter Outline

Inflammatory Infectious Diseases

Progressive Multifocal Leukoencephalopathy

Progressive multifocal leukoencephalopathy (PML) is a demyelinating disorder which occurs in immunocompromised patients as a results of the reactivation of the John Cunningham (JC) virus. Classically it is seen in HIV patients, in post-transplant or leukemia patients. In addition, PML is also seen in patients with recovering immune system. PML involves the white matter (figure 49).

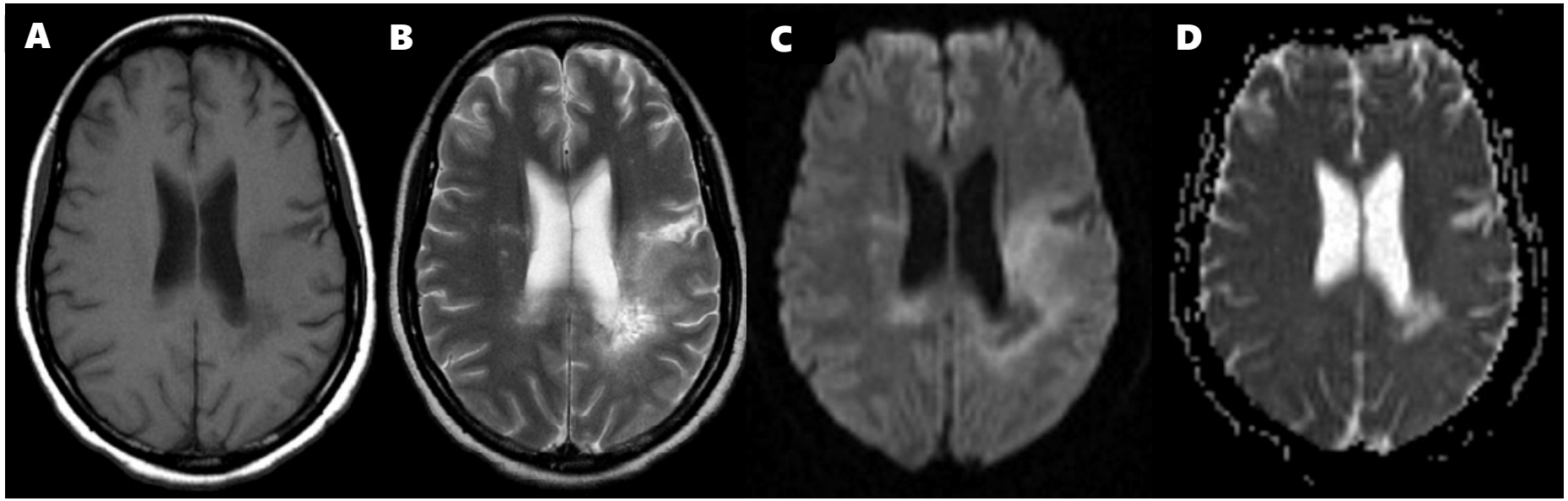

Fig. 49. Characteristic PML findings. Lesions have low signal intensity on T1-weighted (A) and high signal intensity on T2-weighted (B) images and neither show restriction on DWI (C and D). They are bilateral, asymmetric, supratentorial and confluent. No enhancement with gadolinium is seen (not shown).

Chapter Outline

Neurodegenerative Disorders

Neurodegenerative disorders include a wide spectrum of diseases including diseases that produce dementia and movement disorders.

- Alzheimer disease (figure 50): most common form of dementia. Accumulation of cerebral amyloid-β (Aβ) within the brain leads to inflammation, neurotoxicity and finally atrophy in typical brain locations, i.e., mesial temporal lobe, especially the hippocampus, and temporo-parietal cortex.
- Vascular dementia: second most common cause of dementia. The accumulation of white matter lesions and cerebral haemorrhage is caused by chronic hypertension and atherosclerosis.
- Parkinson: nigrostriatal dopaminergic degeneration.
- Multiple system atrophy (MSA, figure 51): anomalies in alpha synuclein metabolism
- Cerebral amyloid angiopathy: accumulation of cerebral amyloid-β (Aβ) in cortical vessels leading to lobar intracerebral haemorrhage
- Creutzfeldt-Jakob disease (CJD, figure 52): transmissible encephalopathy caused by a prion protein (causes bovine spongiform encephalopathy in cows)

MRI is the imaging modality of choice for the assessment of volume changes in typical brain locations and can distinguish between different types of dementia.

Nuclear medicine studies are also very useful to assess dementias as they can detect brain abnormalities prior to symptom onset.

Chapter Outline

Neurodegenerative Disorders

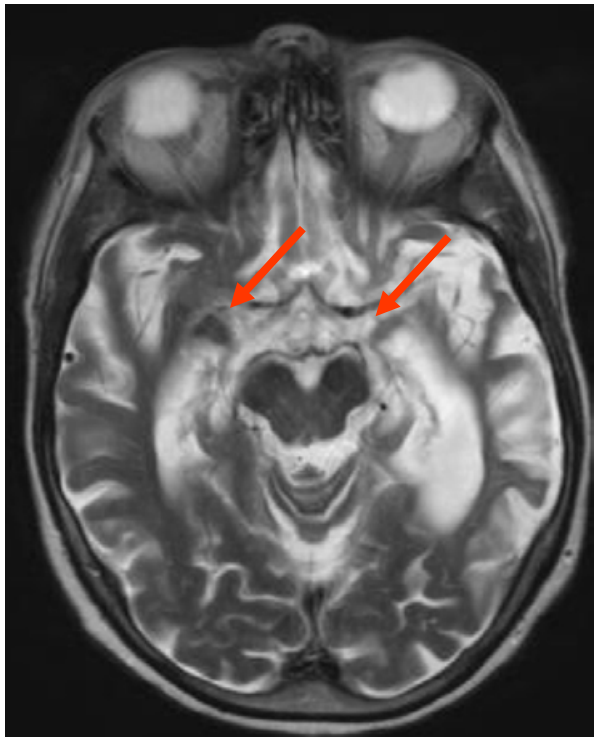

Fig. 50. Alzheimer global cortical atrophy and hippocampal atrophy (arrows) on T2-weighted image. Compare image with Fig. 9 (normal brain without atrophy).

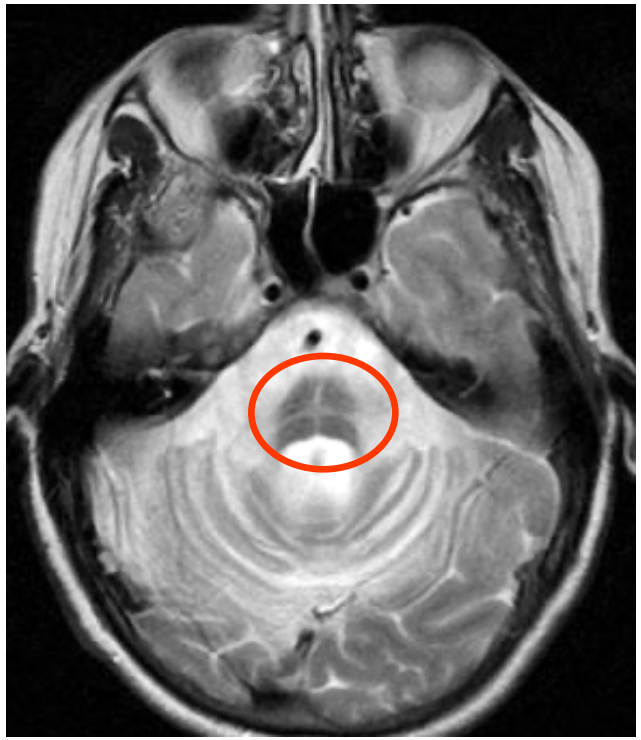

Fig. 51. MSA pontine atrophy with hot cross bun sign on T2-weighted images (hyperintense signal of the pons, red circle).

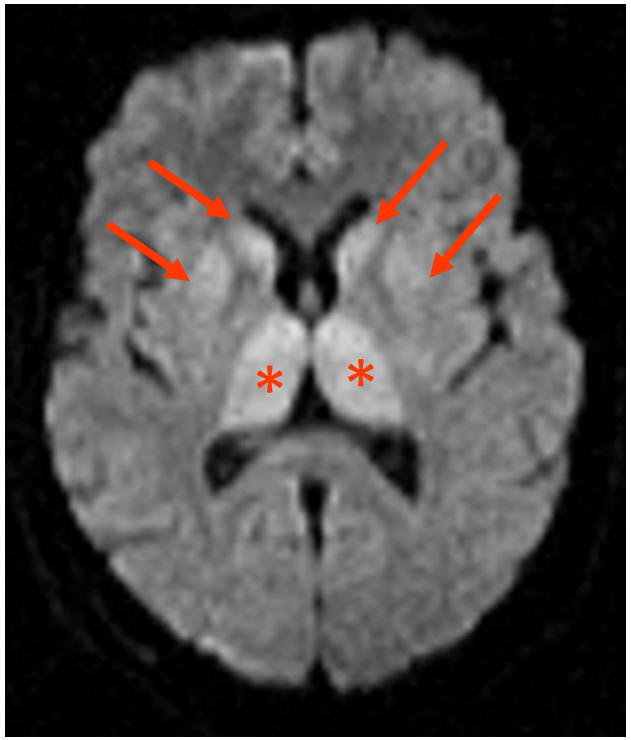

Fig. 52. CJD characteristic imaging findings on DWI include restricted diffusion in the cerebral cortex, in the striatum (arrows) and in the thalamus (asterisks).

Chapter Outline

Vascular Lesions

Intracranial aneurysms are localized pathological dilatations of cerebral arteries (figure 53). Rupture risk is estimated using a score which includes several parameters, such as age, population characteristics, hypertension, site and size of the aneurysm and previous subarachnoid haemorrhage.

Intracranial vascular malformations (figure 54) include: brain capillary telangiectasia, development venous anomaly, cerebral cavernous malformation, arteriovenous and dural arteriovenous malformations.

CT-angiography and MR-angiography are the imaging methods of choice for the diagnosis of vascular lesions.

Digital subtraction angiography is used to assess the flow dynamics and for endovascular treatment.

Vascular Lesions

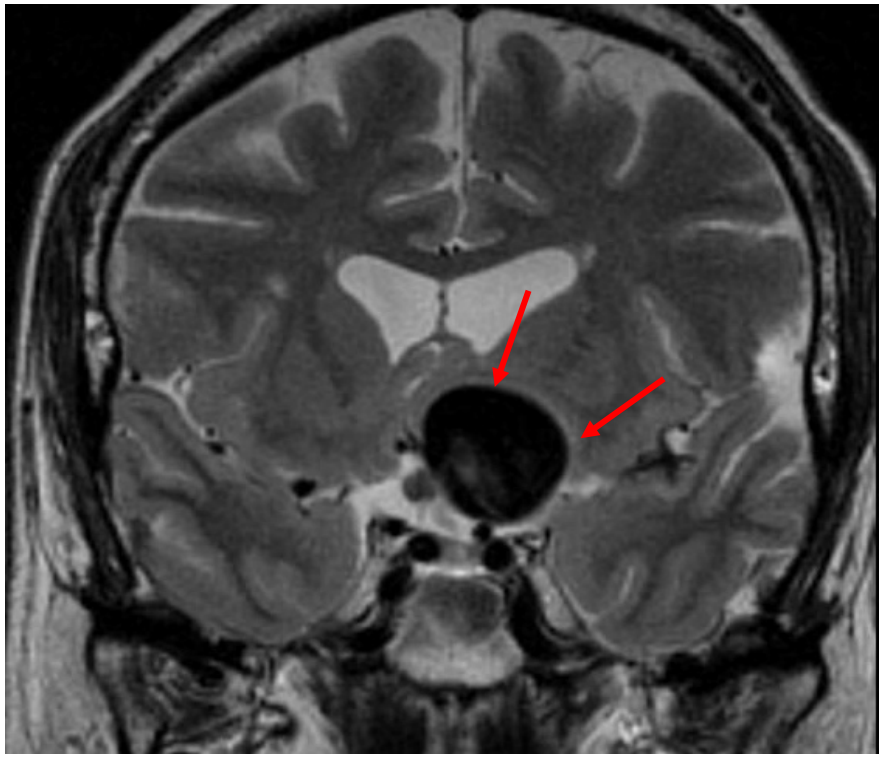

Fig. 53. Left internal carotid artery aneurysm (arrows)

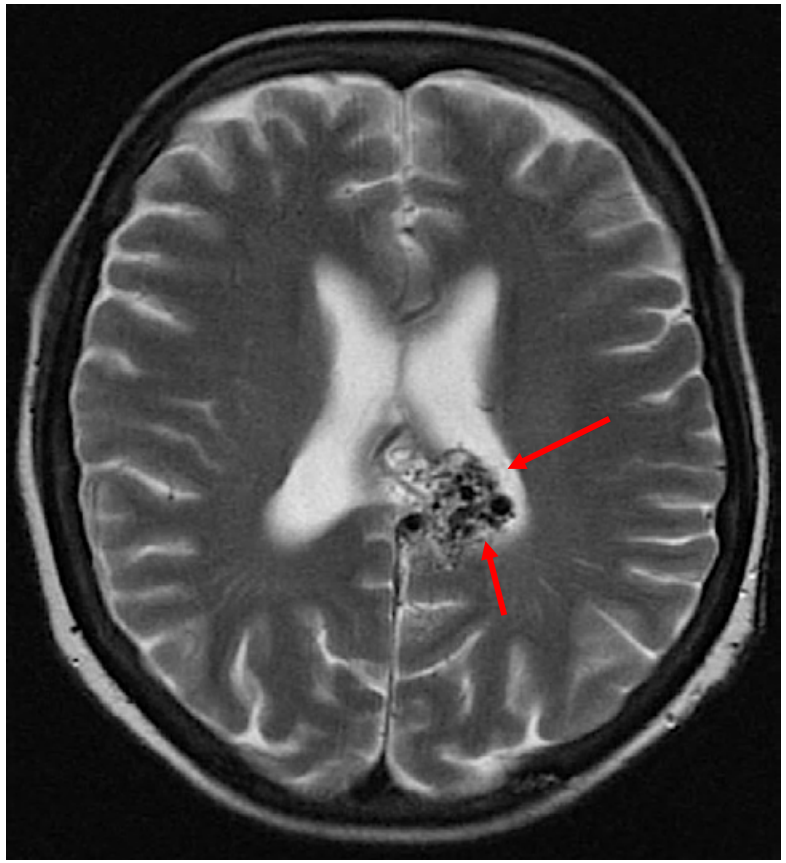

Fig. 54. Arteriovenous malformation seen as curvilinear, dilated structures with flow voids (arrows)

Chapter Outline

Spinal Cord: Main Indications

Trauma
Vertebral fractures, spinal cord injury

Degenerative disease

Spinal tumours
Intramedullary, intradural, extradural

Infarcts/Inflammatory/infectious diseases

Vascular lesions
- Infarct, Arterio-venous malformations

Chapter Outline

Trauma

Vertebral Fractures

=> See also chapter on musculoskeletal radiology

Compression fractures are the most common form of spinal injury seen in 90% of cases. There is either loss of height of the anterior part of the vertebral body or disruption of the vertebral endplate, the posterior cortex of the vertebral body is intact (figure 55).

In burst fractures, there is loss of height of the vertebral body and retropulsion of a posterior vertebral body fragment (figure 56).

In translation – rotation fractures, there is displacement in the horizontal plane.

In distraction fractures, there is separation of two adjacent vertebrae.

CT and MRI are complementary imaging techniques in spinal trauma:

- CT is the first line imaging technique in the emergency setting. It is accurate, fast and cost-effective and allows precise evaluation of bone structures.
- Disc herniation and haemorrhage should be evaluated with MRI. In addition, MRI should be used whenever spinal cord injury is suspected and to determine the cause of spinal cord compression.

Chapter Outline

Trauma

Vertebral Fractures

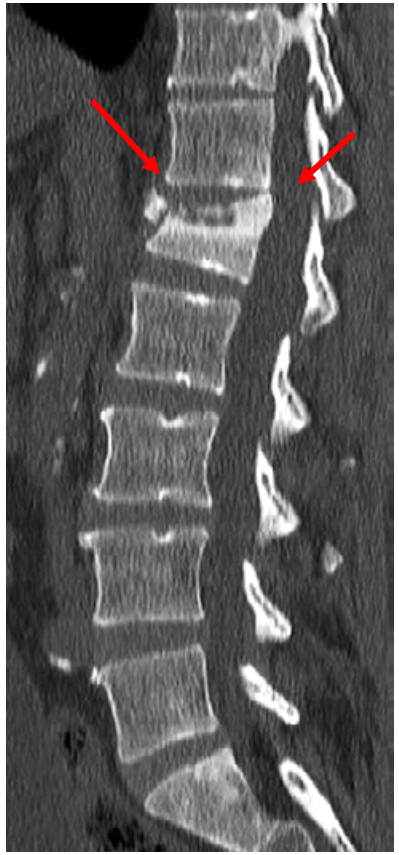

Fig. 55. Compression fracture

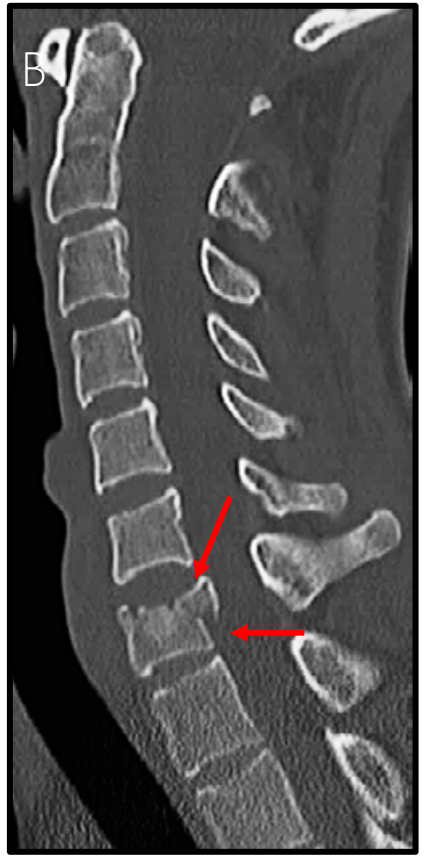

Fig. 56. Burst fracture

Trauma

Spinal Cord Injury

Spinal cord injuries after trauma are better depicted on MRI images.

The spectrum of cord injuries after trauma include; intraspinal haemorrhage, cord oedema and contusion.

Cord oedema and contusion depict high signal intensity on T2-weighted MRI images (figure 57).

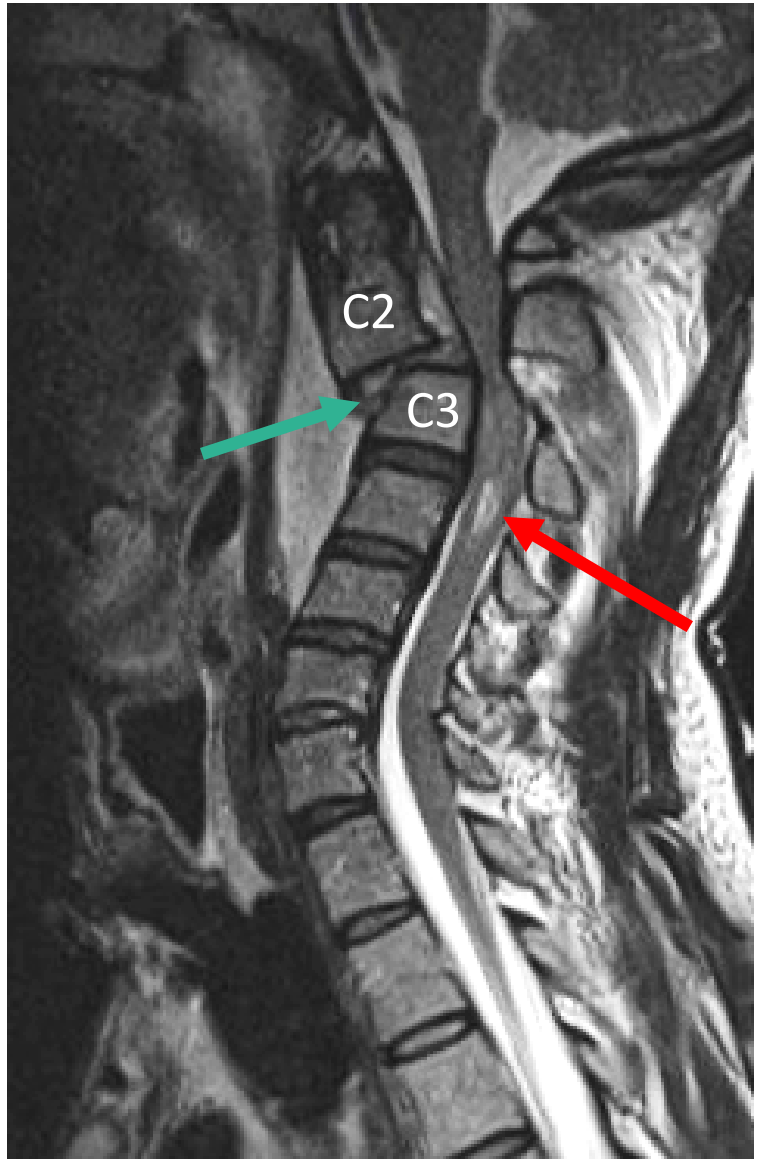

Fig. 57. Sagittal T2-weighted image depicting disc fracture (green arrow), C2-C3 vertebral luxation and cord contusion (red arrow)

Chapter Outline

Degenerative Disease

Degenerative disease of the spine includes degeneration of bony structures and the intervertebral disc.

Osteochondrosis comprise; disc height loss, intradiscal gas collections (vacuum), endplate erosion and sclerosis.

Spondylosis occurs as a consequence of degeneration of the vertebral bodies with osteophytes or bony spurs formation.

Disc herniation is defined as localized displacement of disc material beyond the normal margins of the intervertebral disc space (figures 58 and 59).

Disc herniation is classified as protrusion or extrusion (figure 60).

=> See also chapter on musculoskeletal radiology

Kushchayev S.V., Glushko T., Jarraya M., Schuleri K.H., Preul M.C., Brooks M.L., Teytelboym O.M. ABCs of the degenerative spine. Insights into Imaging 2018; 9:253–274

Chapter Outline

Degenerative Disease

Disc Herniation

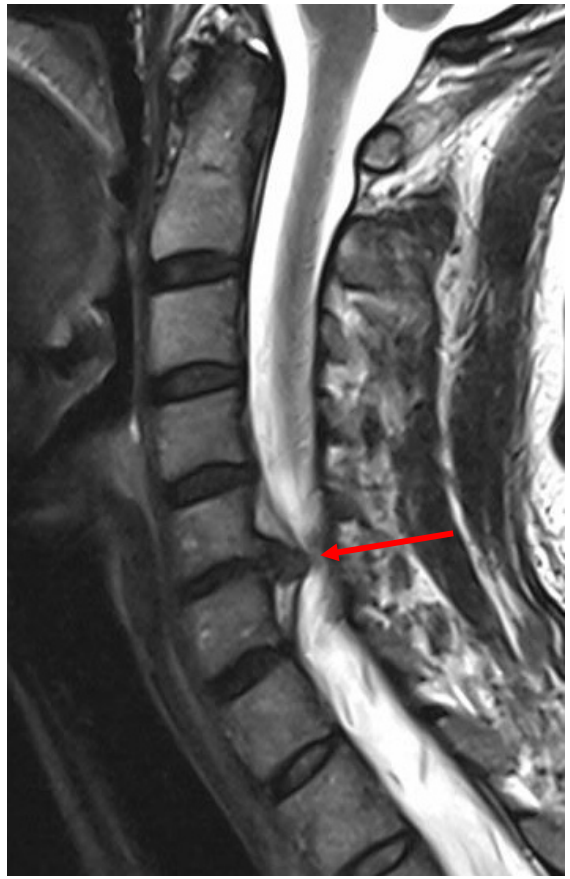

Fig. 58. Cervical disc herniation (T2-weighted image, arrows)

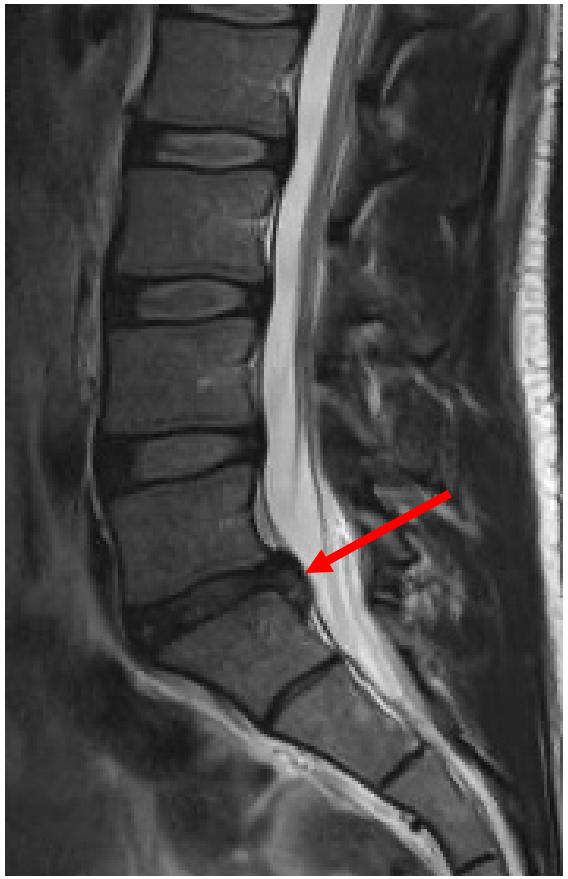

Fig. 59. Lumbar disc herniation (T2-weighted image, arrow)

Degenerative Disease

Disc Herniation

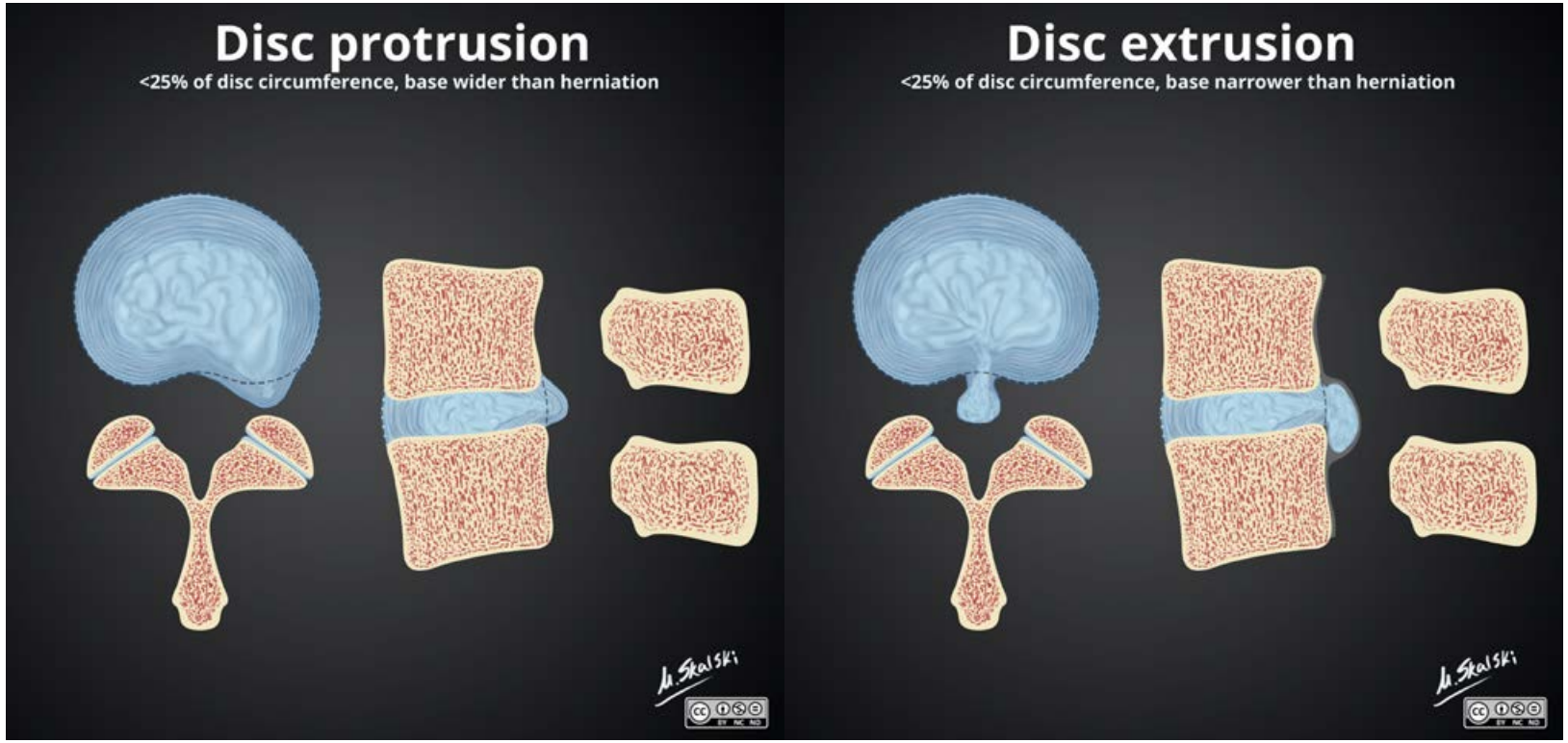

Fig. 60. Difference between disk protrusion and disk extrusion.
Case courtesy of Dr Matt Skalski, Radiopaedia.org, rID: 32040.

Chapter Outline

Degenerative Disease

The abnormalities that can be demonstrated by CT in spinal degenerative disease include osteophyte formation (spondylosis); hypertrophy of articular processes; articular cartilage thinning; vacuum phenomenon in joints and discs; synovial and subchondral cysts (osteochondrosis) and calcification of the joint capsule, vertebral end plates, and ligaments (figure 61).

Magnetic resonance imaging better depicts internal disc dehydration and degeneration demonstrating low signal on T2 Weighted images secondary to decrease in the water content (figure 61).

Degenerative Disease

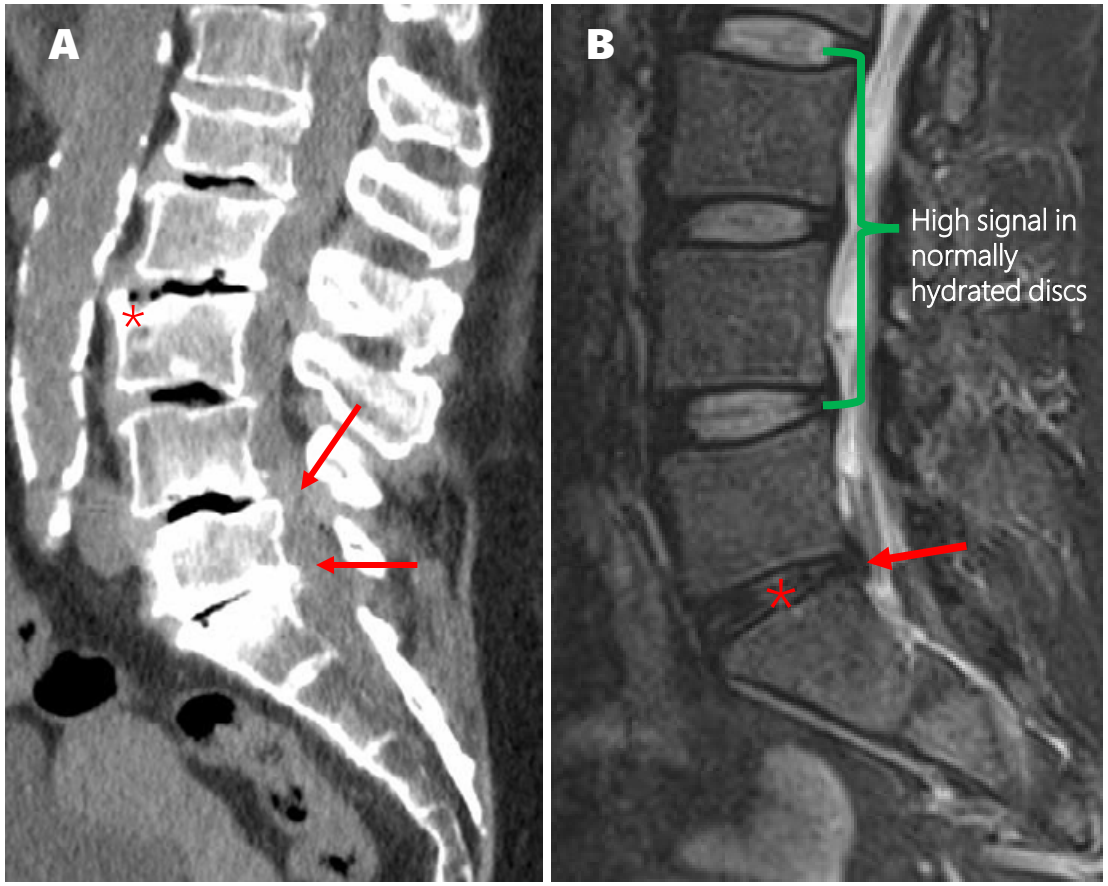

Fig. 61. Spondylosis and osteochondrosis. A. Sagittal CT image showing degenerative changes : spondylosis (arrows) and osteochondrosis (asterisks). B. T2-weighted MRI image showing the normal high signal on hydrated discs and the low signal on L5-S1 disc due to degeneration (asterisk). Disc protrusion (arrow).

Chapter Outline

Spinal Tumours

MRI is the modality of choice to help evaluate spinal cord tumours.

A key issue on imaging is location of the mass in the different compartments:

- Intramedullary

- Intradural-extramedullary

- Extradural

Shih R.Y., Koeller K.K. Intramedullary Masses of the Spinal Cord: Radiologic-Pathologic Correlation. RadioGraphics 2020; 40:1125–1145

Chapter Outline

Intramedullary Spinal Cord Tumours

Intramedullary masses of the spinal cord are located inside the substance of the cord and expand the cord parenchyma.

Ependymoma is the most common intramedullary spinal cord tumour in adults other spinal cord followed by astrocytoma and hemangioblastoma. Ependymomas are centrally located, well defined enhancing masses, hypointense to isointense on T1-weighted and hypointense to isointense on T2-weighted MR images and they can present cystic or haemorrhagic components (figure 62).

Astrocytoma are well-defined enhancing masses eccentrically located in the spinal cord.

Hemangioblastoma is the third most common intramedullary tumour, it is a mesenchymal hypervascular enhancing tumour cantered in the pial surface.

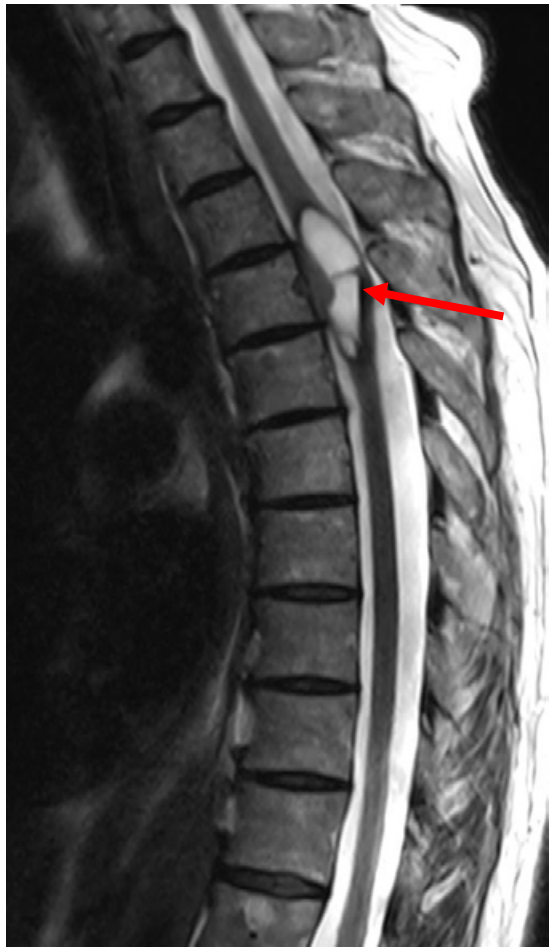

Fig. 62. Ependymoma with cystic components (arrow) on sagittal T2-weighted image.

Chapter Outline

Intradural-extramedullary Spinal Tumours

Schwannomas and meningiomas are the most common intradural-extramedullary masses.

Meningiomas are characteristically iso to hypointense on T1-weighted images and slightly hyperintense on T2-weighted MR images with strong enhancement on postcontrast images imaging and a sharp-edged enhancing border (dural tail sign) as seen in figure 63.

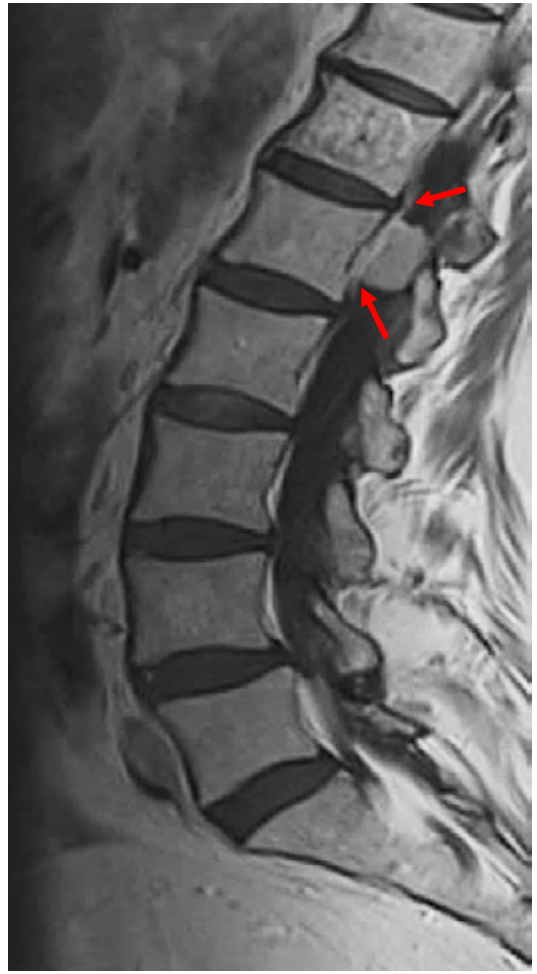

Fig. 63. Sagittal T1-weighted gadolinium enhanced image demonstrating the dural tail sign (arrows) in a spinal meningioma.

Chapter Outline

Extradural Spinal Tumours

The spine is the third most common site for metastatic disease, following the lung and liver.

Spinal metastases are the most common spinal tumors 20 times more common than primary spinal neoplasms. Metastatic disease to the spine can involve the bone, epidural space, leptomeninges, and the spinal cord.

The most common primary malignant tumours involving the spine are breast, lung and prostate tumours (figure 64).

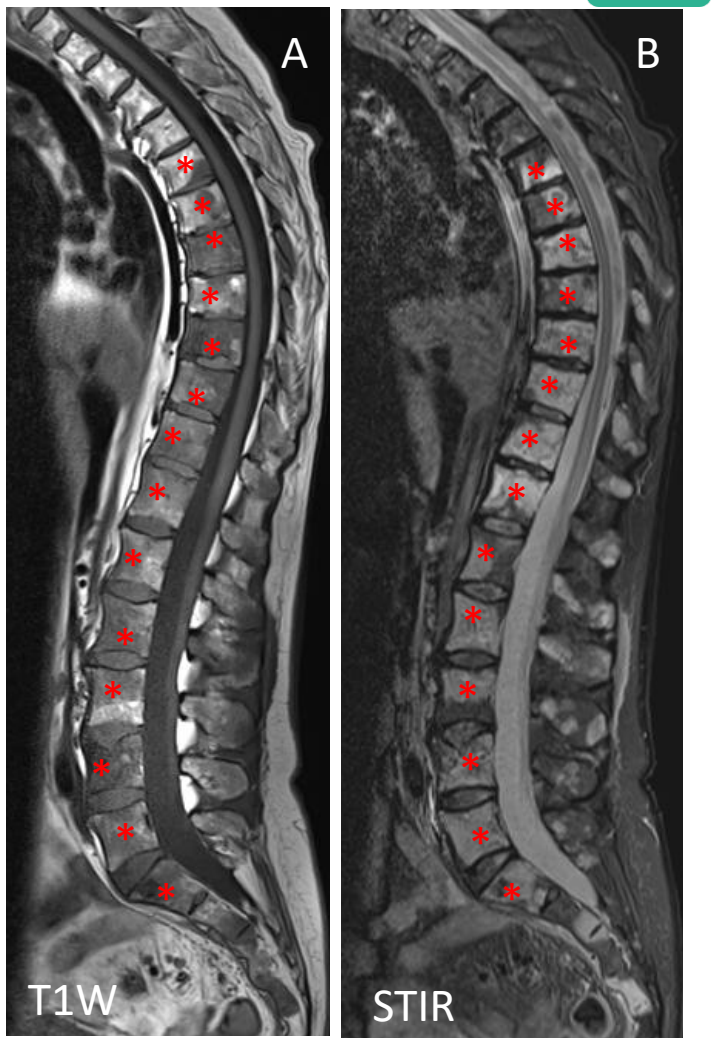

Fig. 64. . Sagittal T1-weighted (A) and STIR (B) images demonstrating multiple vertebral bone marrow metastases from a breast carcinoma: low signal on T1W sequence, high signal on STIR sequence (asterisks).

Chapter Outline

Inflammatory/Infectious Diseases

Inflammatory/infectious diseases include, demyelinating, infectious, granulomatous, metabolic, toxic and paraneoplastic disorders.

MRI is the modality of choice in the evaluation of inflammatory/infectious conditions of the spine.

Multiple sclerosis (MS) spinal cord lesions are more frequently located in the cervical spine (figure 65); they show high signal intensity on T2-weighted MRI images and are usually about the length of a vertebral body on sagittal images.

Postinfectious myelitis (figure 66) depicts high signal on T2-weighted MR images and usually extends over three to four vertebral segments.

Moghaddam S.M., Bhatt A.A. Location, length, and enhancement: systematic approach to differentiating intramedullary spinal cord lesions. Insights into Imaging 2018; 9:511–526

Chapter Outline

Inflammatory/Infectious Disease

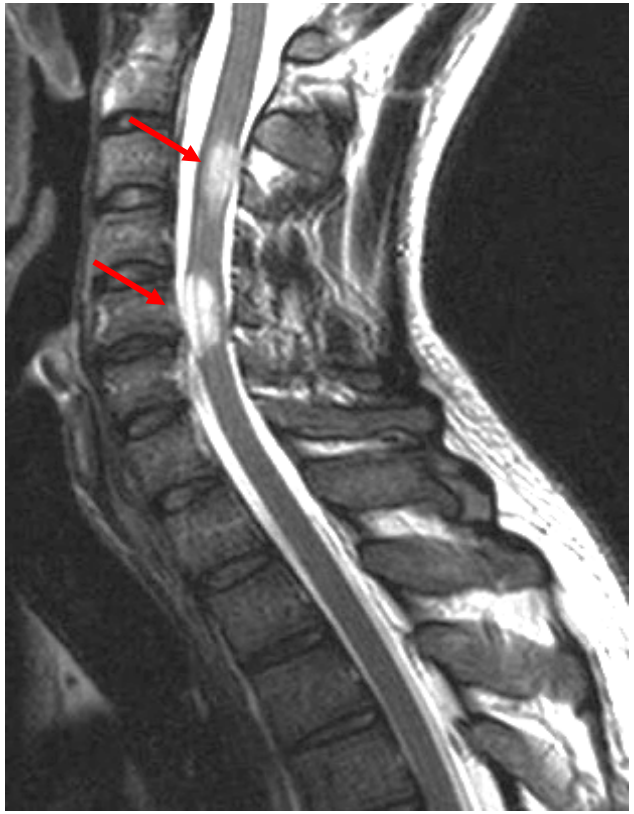

Fig. 65. Sagittal T2-weighted image demonstrating two short segment high signal intensity lesions in the cervical spinal cord in MS

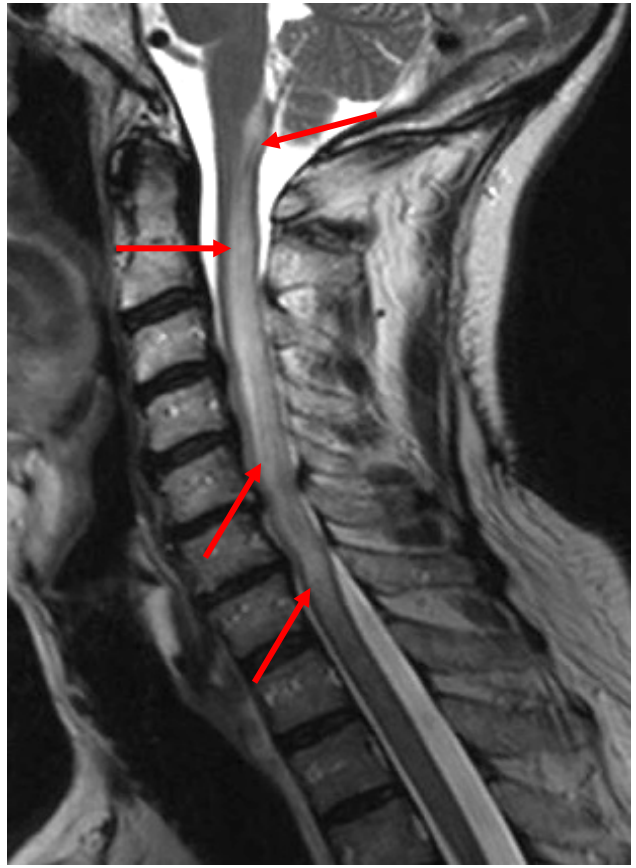

Fig. 66. Sagittal T2-weighted image demonstrating a long segment high signal intensity lesion in the cervical spinal cord in postinfectious myelitis.

Chapter Outline

Vascular Lesions

Vascular disorders of the spinal cord can be caused by venous or arterial ischemia and vascular malformations.

Acute arterial ischemia is typically seen as a complication of aortic aneurysm surgery or catheterization. Spinal cord infarctions show a swollen cord and hyperintensity on T2-weighted images (figure 67).

Vascular malformations depict abnormal, dilated, serpiginous vascular structures within the spinal cord or subarachnoid space (figure 68).

Chapter Outline

Vascular Lesions

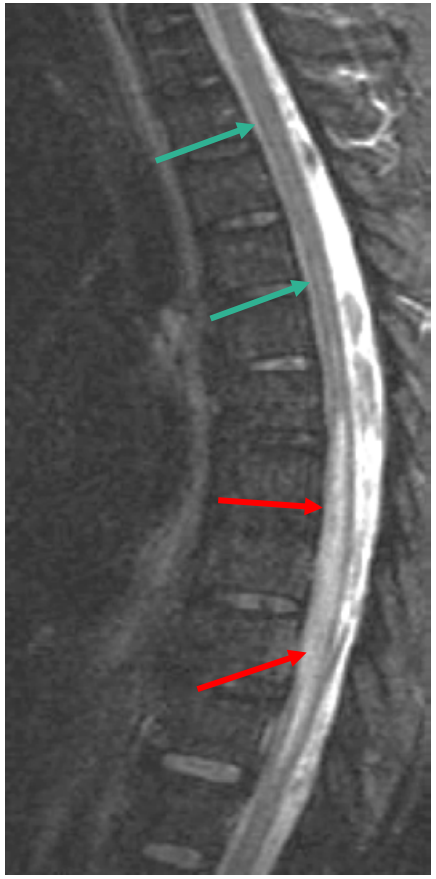

Fig. 67. Spinal cord infarction demonstrating cord swelling and increased signal (red arrows) on a sagittal T2-weighted image. Areas without spinal cord infarction (green arrows)

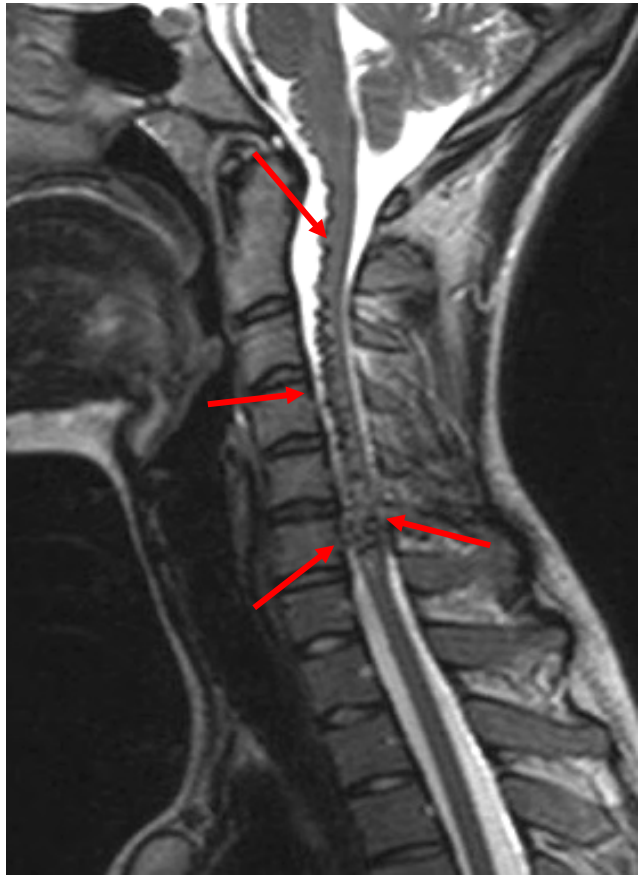

Fig. 68. Vascular malformation. Sagittal T2-weighted image showing dilated serpiginous vessels (arrows).

Take-Home Messages

- Detailed knowledge of the anatomy is essential for image interpretation
- Magnetic resonance imaging is the imaging modality of choice for the evaluation of CNS pathology
- Computed tomography is an important diagnostic modality used for urgent evaluation of patients with head or spinal trauma, to assess the presence of haemorrhage or bone fractures
- Digital subtraction angiography is used for cerebrovascular interventions including mechanical thrombectomy, carotid angioplasty and stenting
- Ultrasound is a safe and non-invasive imaging technique for the visualization of intra and extracranial vessels and the measurement of blood velocity using Doppler imaging

Take-Home Messages

- Knowledge of the vascular territories is important to recognize infarctions in arterial territories
- The first thing to determine when evaluating a brain tumour is if it is located outside the brain (extra-axial) or within the brain (intra-axial)
- Functional MRI Diffusion Weighted images are very useful for the diagnosis of acute ischemic stroke, infection, and tumour characterization
- MRI is the best imaging method to visualize the spinal cord and nerves
- Computed tomography allows an excellent delineation of vertebral fractures

References

1- Naidich T.P., Kang E., Fatterpekar G.M., Delman B.N., Gultekin S.H., Wolfe D., Ortiz O., Yousry I., Weismann M., Yousry T.A. The insula: anatomic study and MR imaging display at 1.5 T. AJNR 2004; 25:222-32

2- Dekeyzer, S., De Kock, I., Nikoubashman, O. et al. "Unforgettable" a pictorial essay on anatomy and pathology of the hippocampus. Insights Imaging 2017; 8:199–212

3- Romano N., Federici M., Castaldi A. Imaging of cranial nerves: a pictorial overview. Insights Imaging 2019; 10:33

4- Pooley R.A. Fundamental Physics of MR Imaging. RadioGraphics 2005; 25:1087–1099

5- https://radiologyassistant.nl/neuroradiology/brain-ischemia/vascular-territories

6- Srinivasan A., Goyal M., Al Azri F., Cheemun Lum C. State-of-the-Art Imaging of Acute Stroke. RadioGraphics 2006; 26:S75–S95

7- Smirniotopoulos J.G.,. Murphy F.M., Rushing E.J.,Rees J.H.,Schroeder. Patterns of Contrast Enhancement in the Brain and Meninges. RadioGraphics 2007; 27:525–551

8- Kushchayev S.V., Glushko T., Jarraya M., Schuleri K.H., Preul M.C., Brooks M.L., Teytelboym O.M. ABCs of the degenerative spine. Insights into Imaging 2018; 9:253–274

9- Shih R.Y., Koeller K.K. Intramedullary Masses of the Spinal Cord: Radiologic-Pathologic Correlation. RadioGraphics 2020; 40:1125–1145

10- Moghaddam S.M., Bhatt A.A. Location, length, and enhancement: systematic approach to differentiating intramedullary spinal cord lesions. Insights into Imaging 2018; 9:511–526

Chapter Outline

Further Reading

11- Offiah, C.E., Day, E. The craniocervical junction: embryology, anatomy, biomechanics and imaging in blunt trauma. Insights Imaging 2017; 8:29–47

12- Leah J.:, Fortuna R.B., Jones B. V., Gaskill-Shipley M.F. Imaging of cerebral venous thrombosis: current techniques, spectrum of findigns and diagnostic pitfalls. Radiographics 2006;26:S19-S43

13- Nuñez S. Mantilla M.T., Bermúdez S. Midline congénital malformations of the brain and skull. Neuroimag Clin N Am 2011; 4:429-482

14- Cody D.D AAPM/RSNA physics tutorial for residents: topics in CT. Radiographics 2002; 22:1255-1268

15- Tanya J. Rath T.J., Hughes M., Arabi M., Shah G.V. Imaging of Cerebritis, Encephalitis, and Brain Abscess. Neuroimaging Clin N Am 2012; 22:585–607

Chapter Outline

Test your knowledge

1 - Through which foramina do the lateral ventricles communicate with the third ventricle?

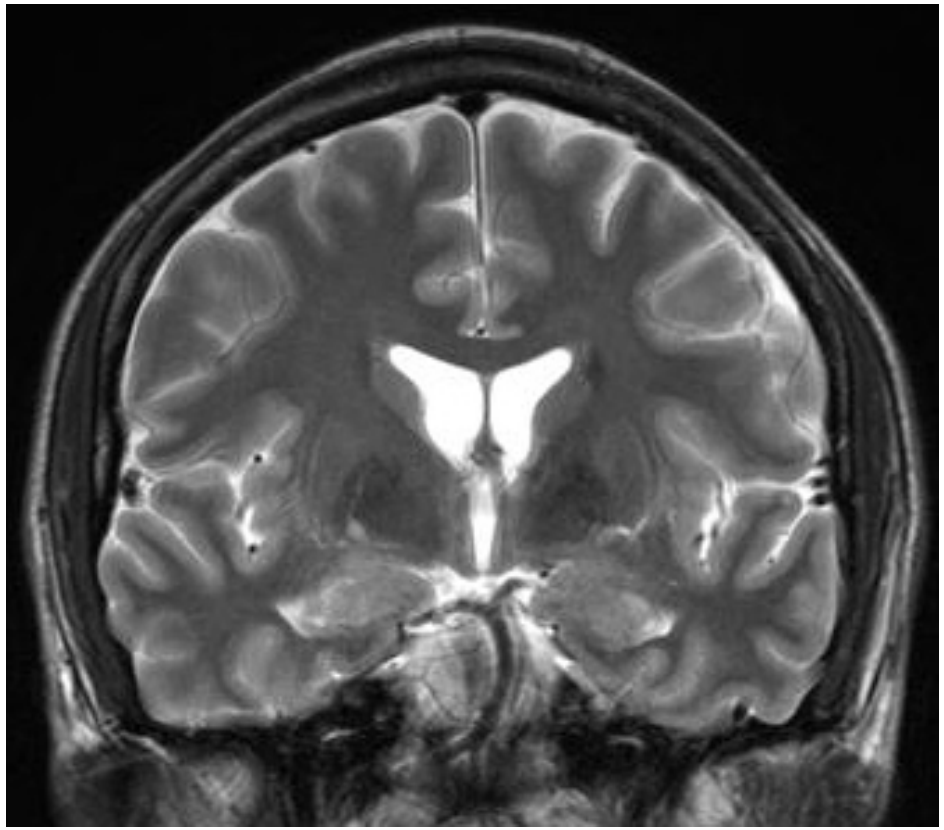

Test your knowledge

1 - Through which foramina do the lateral ventricles communicate with the third ventricle?

- Answer: Through the Monro foramina

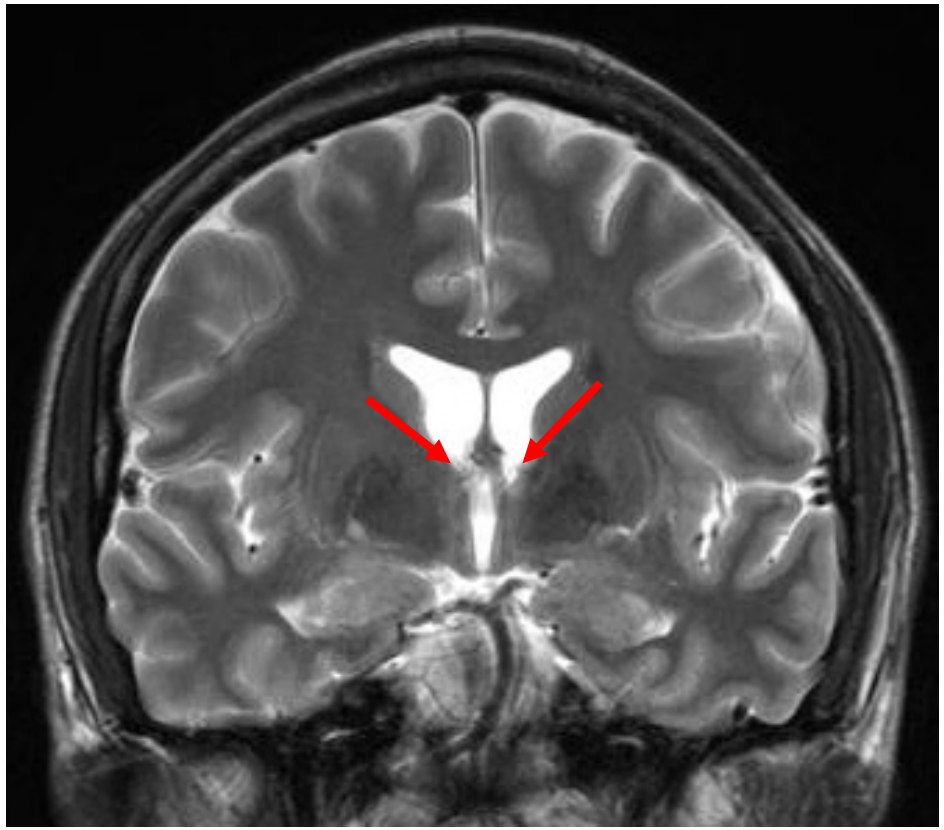

Test your knowledge

2 - What sulcus is the red arrow pointing to and what sulcus is the blue arrow pointing to?

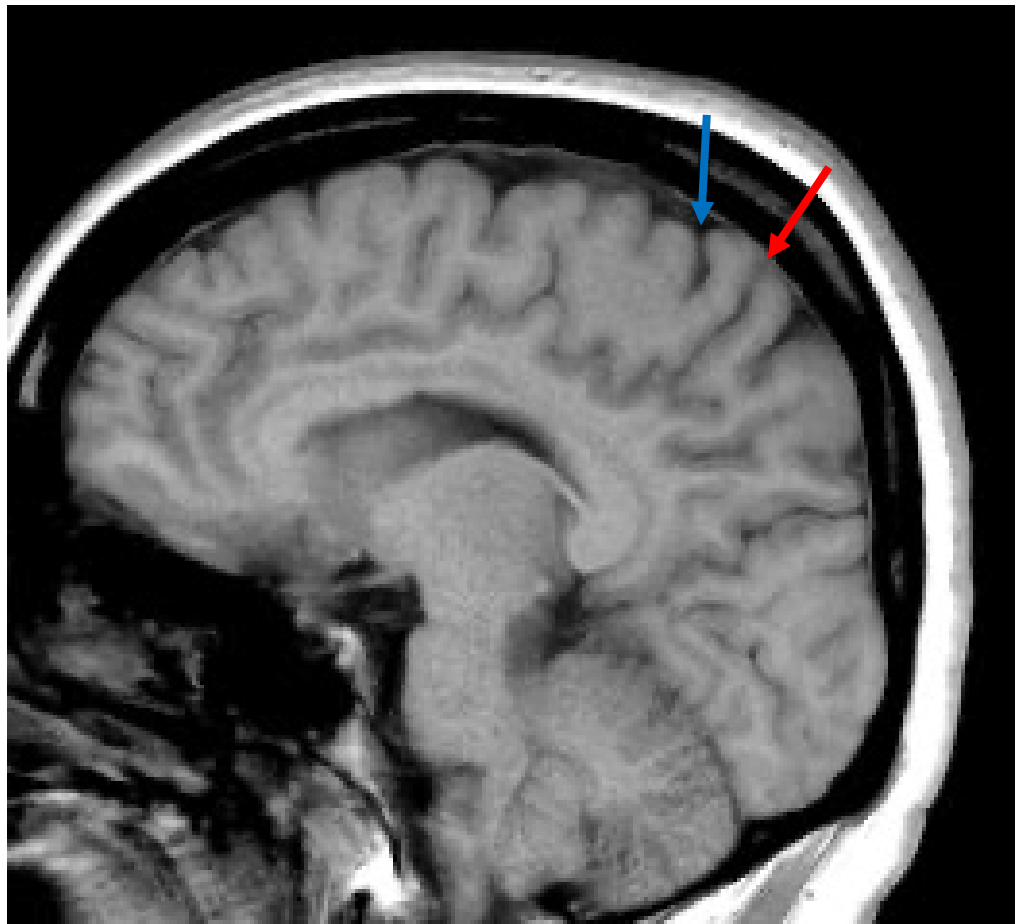

Test your knowledge

2 - What sulcus is the red arrow pointing to and what sulcus is the blue arrow pointing to??

- Answer: The red arrow points out the **marginal sulcus** running within the parietal lobe and the blue arrow points at the **central sulcus** (the central sulcus separates the frontal lobe from the parietal lobe)

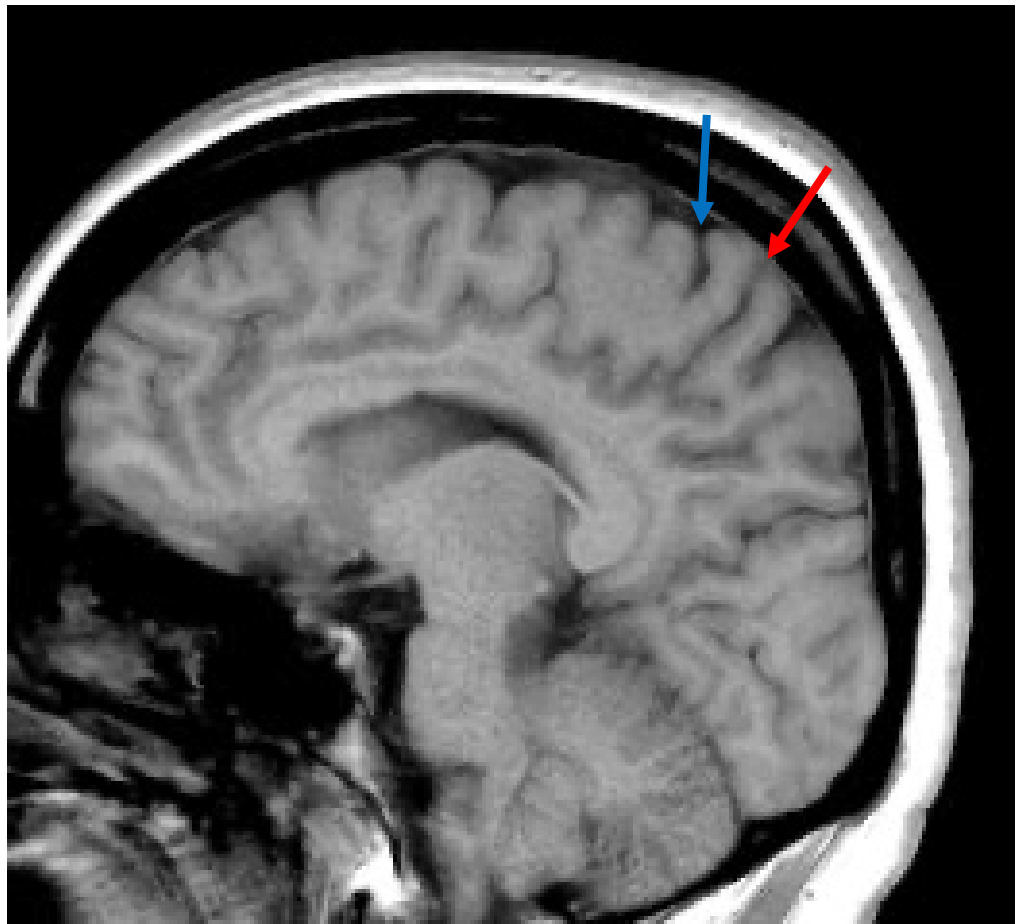

Chapter Outline

Test your knowledge

3 - 55-year-old male patient with right hemiparesis. What is the diagnosis?

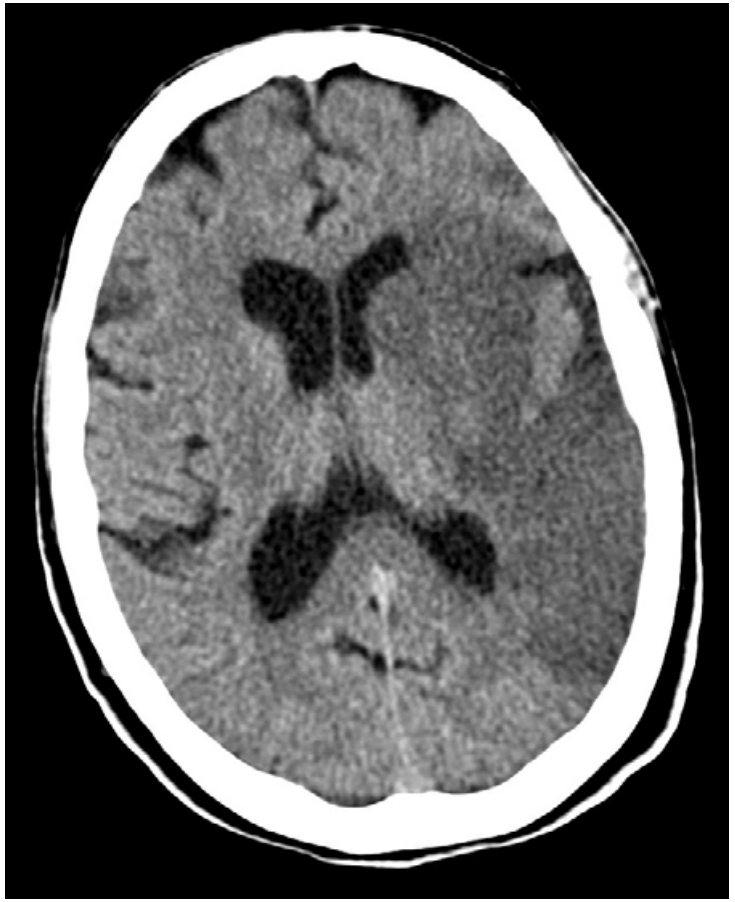

Test your knowledge

3 - 55-year-old male patient with right hemiparesis. What is the diagnosis?

- Answer:
  - Acute left infarct in the left middle cerebral artery vascular territory
  - Hypoattenuating brain tissue in the left hemisphere (arrows)
  - Gray and white matter involvement
  - Blurred basal ganglia (asterisk)
  - Insular Ribbon sign, hypodensity of the insular cortex (in)
  - Good differentiation between normal and affected tissue
  - Mass effect

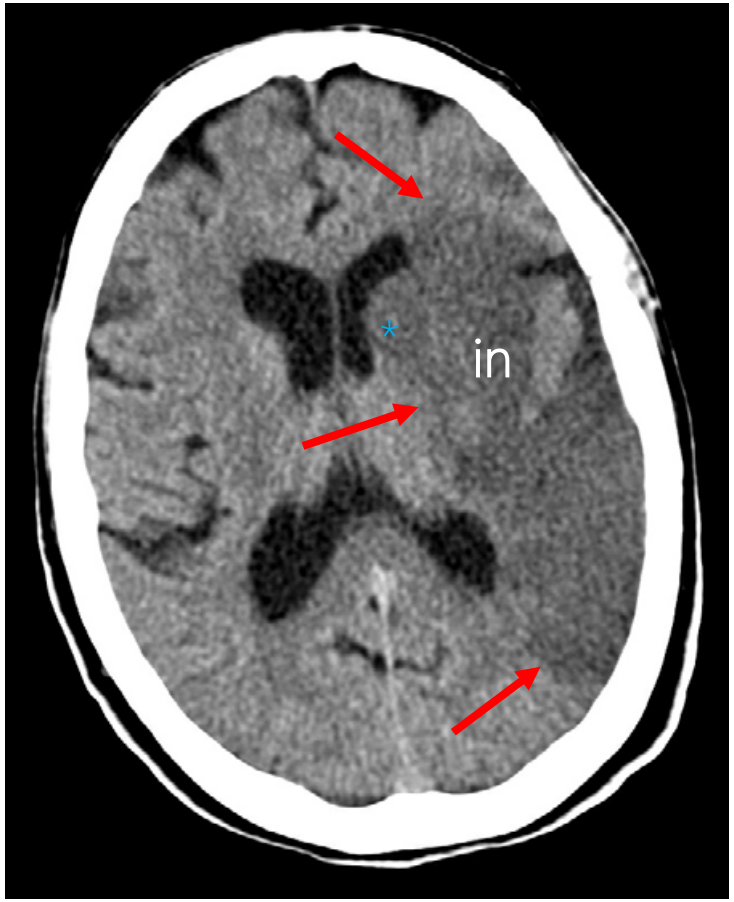

Chapter Outline

Test your knowledge

4 - 63-year-old male with right sciatica.
What is the diagnosis?

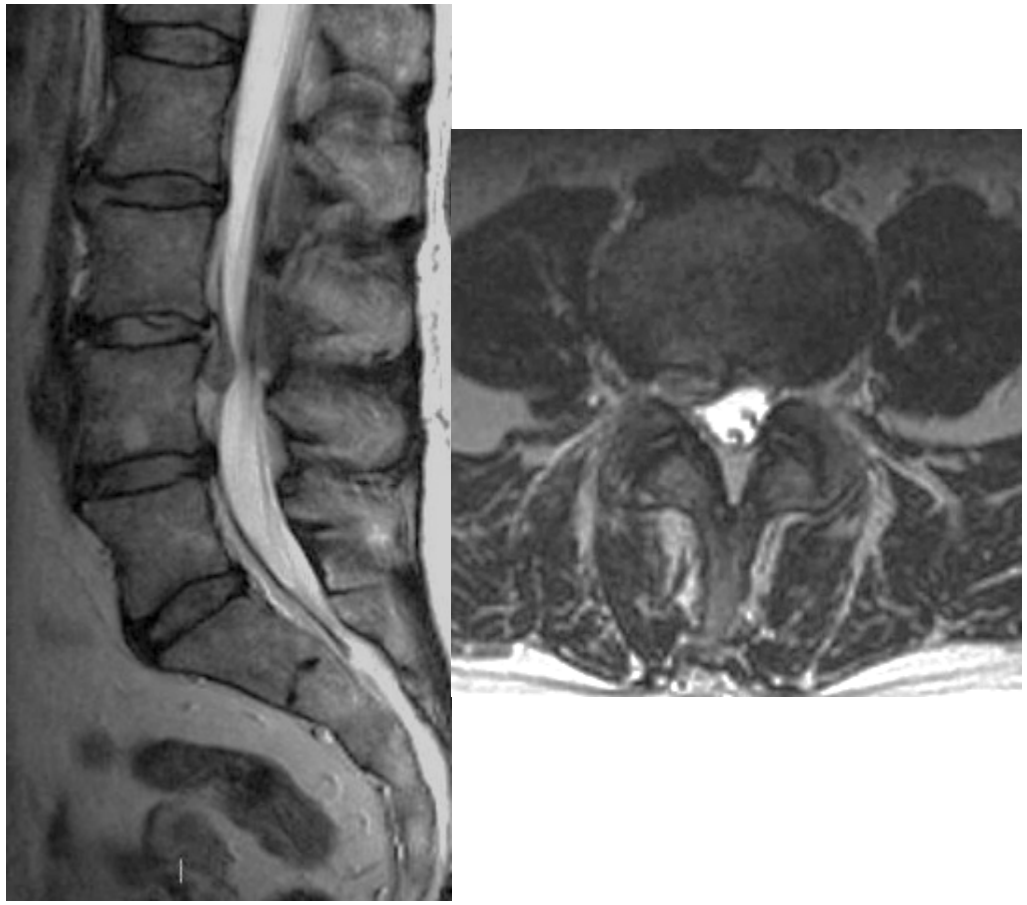

Test your knowledge

4 - 63-year-old male with right sciatica. What is the diagnosis?

- Answer:
  - L3-L4 right subarticular disc herniation (arrow).
  - Extrusion of the disc outside the annulus fibrosus, deforming the thecal sac on the right and compressing the right L4 nerve root.

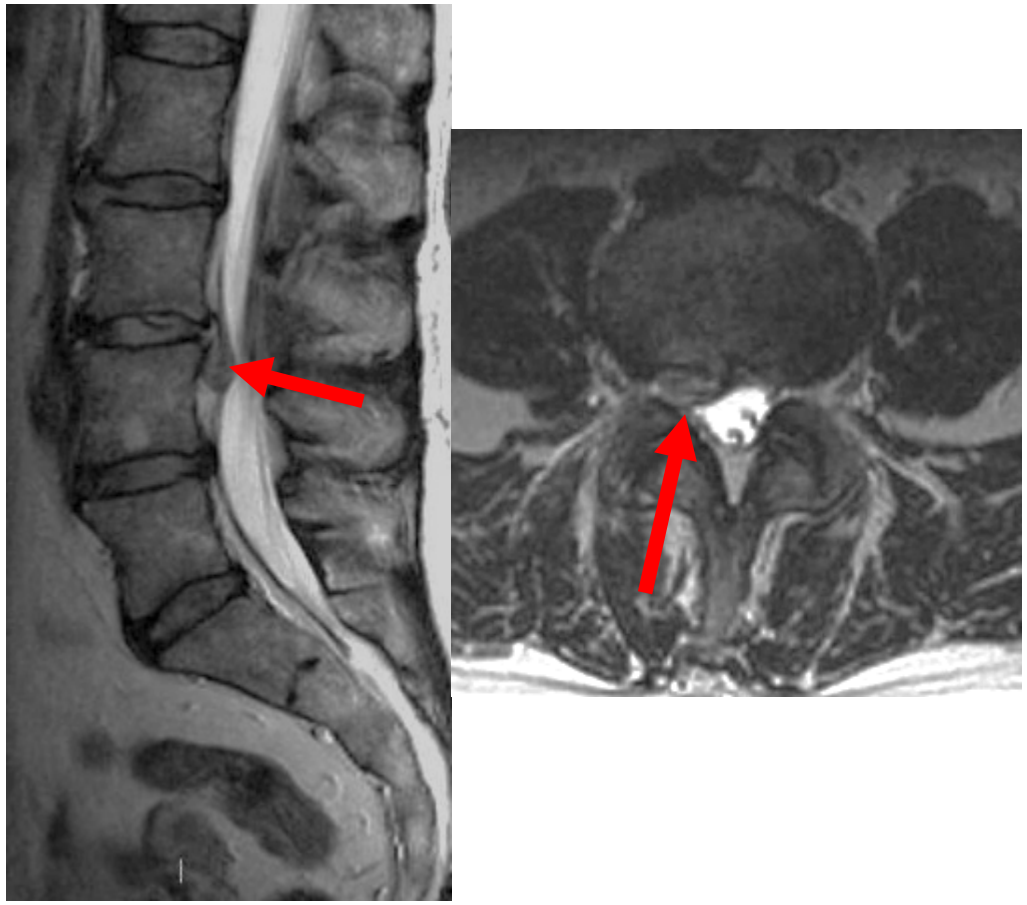

Test your knowledge

5 - 31-year-old female with a long history of recurrent episodes of numbness and tingling in her arms and legs, vision loss and fatigue

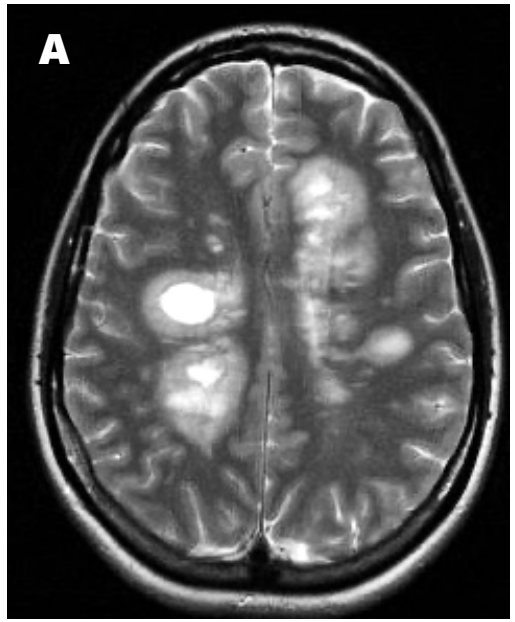

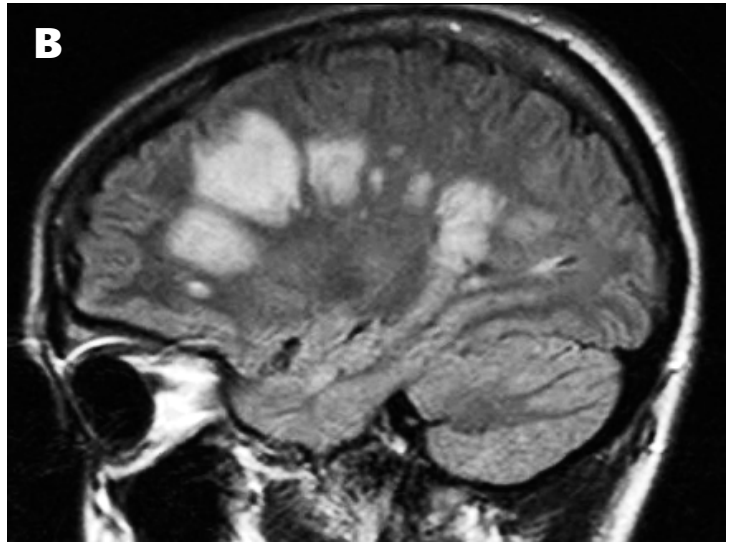

Chapter Outline

Test your knowledge

5 - 31-year-old female with a long history of recurrent episodes of numbness and tingling in her arms and legs, vision loss and fatigue

- Answer:
  - Multiple sclerosis
  - Multiple lesions wite matter lesions adjacent to the ventricles. Ovoid lesions perpendicular to the ventricles called Dawson fingers.

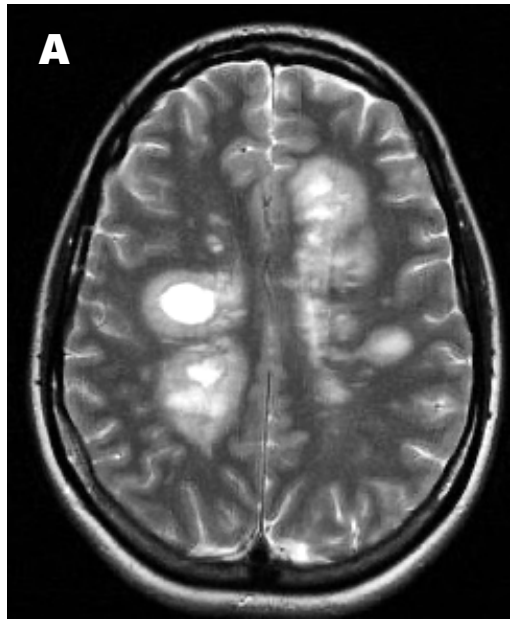

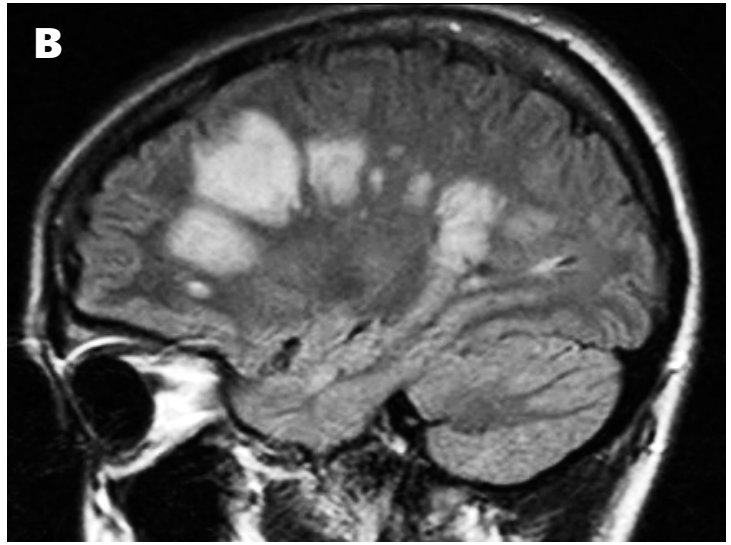

Chapter Outline

Test your knowledge

6 - 45-year-old male with acute onset of severe headache

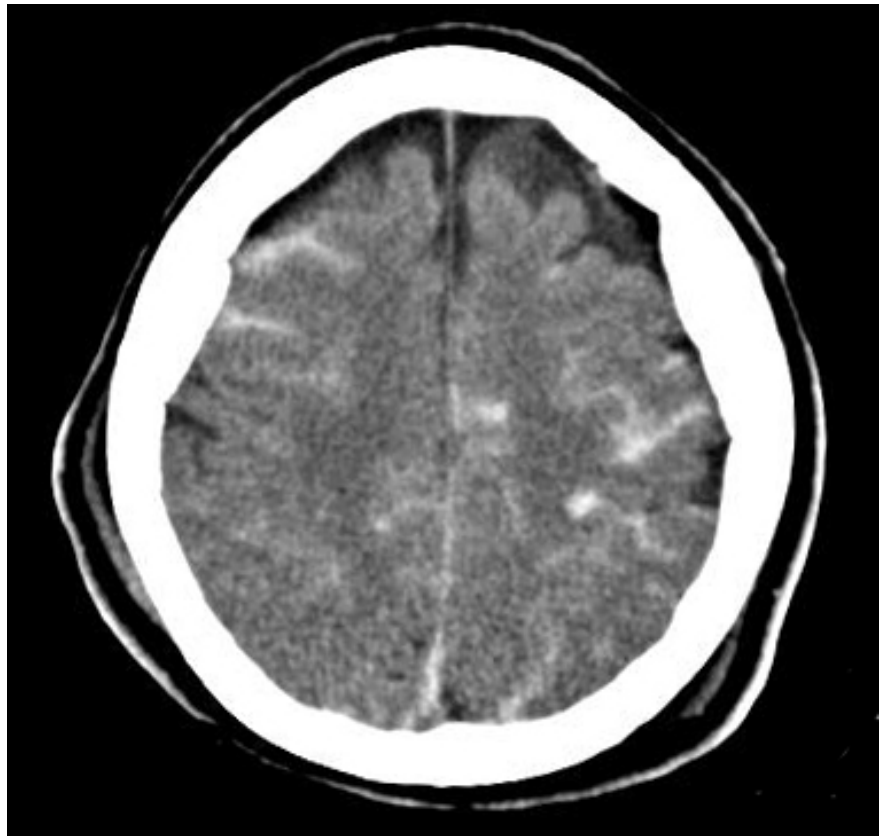

Chapter Outline

Test your knowledge

6 - 45-year-old male with acute onset of severe headache

- Answer:
  - Subarachnoid haemorrhage
  - High attenuation value fluid filling the sulci of the convexity

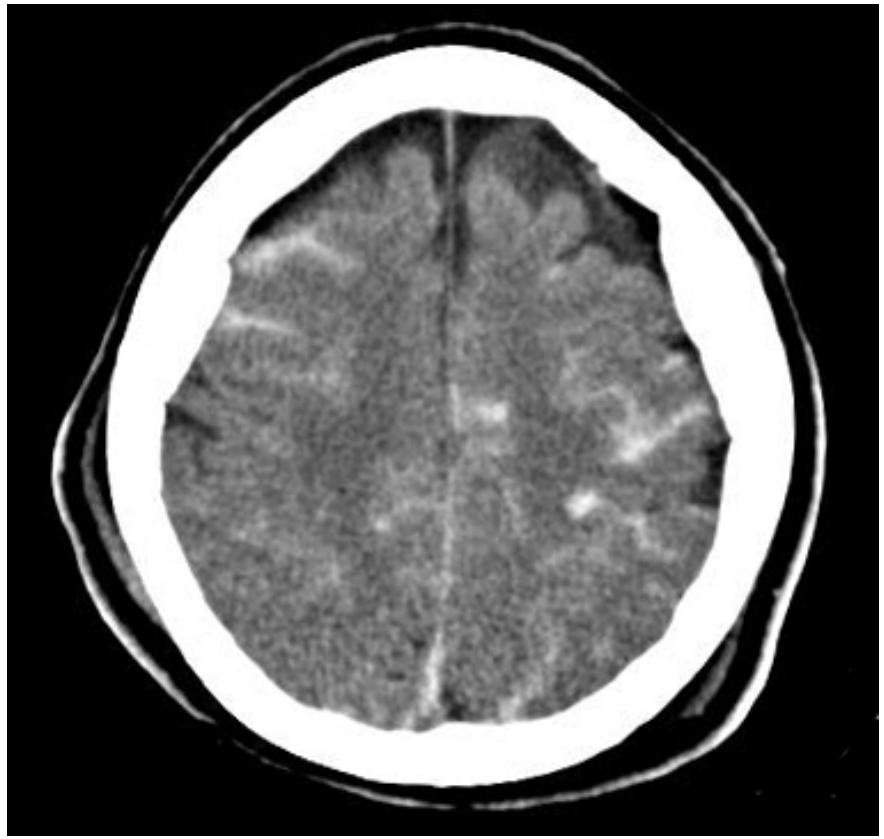

Test your knowledge

7 - 67-year-old male presents with seizures. Where is the lesion located?

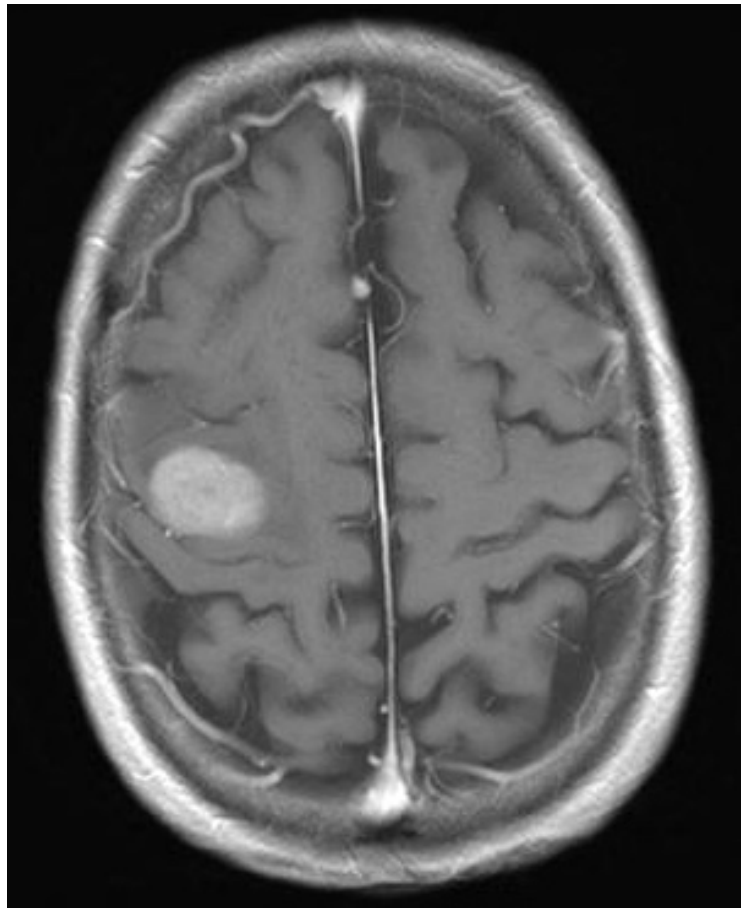

Test your knowledge

7 - 67-year-old male presents with seizures. Where is the lesion located?

- Answer: In the right central gyrus, immediately anterior to the central sulcus

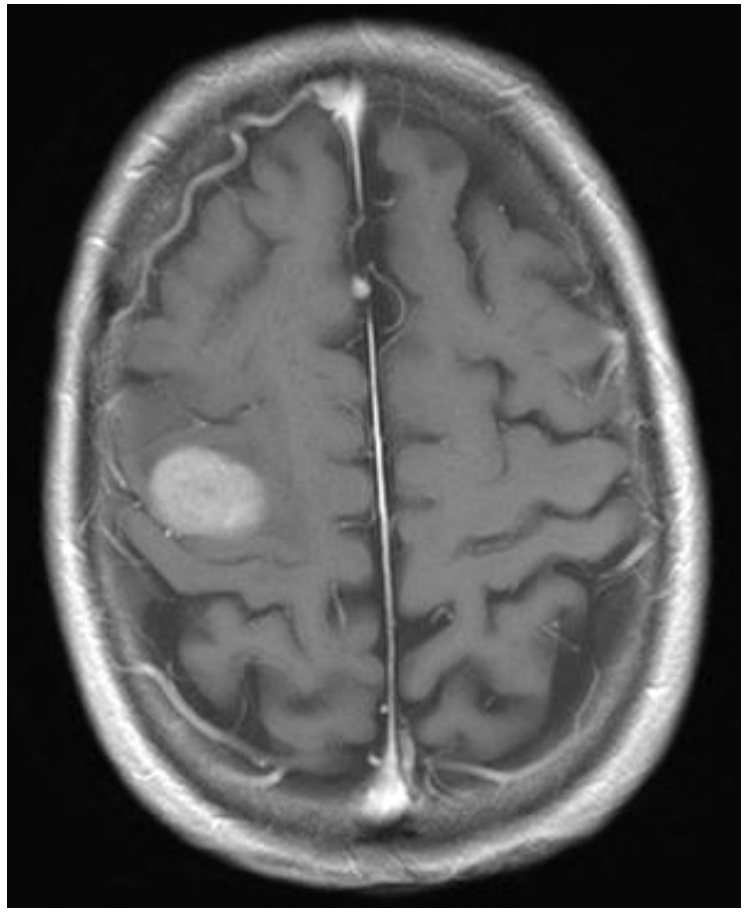

Test your knowledge

8 - 18-year-old female with sudden paraplegia. Reported a respiratory viral process the week before. What is the most likely diagnosis?

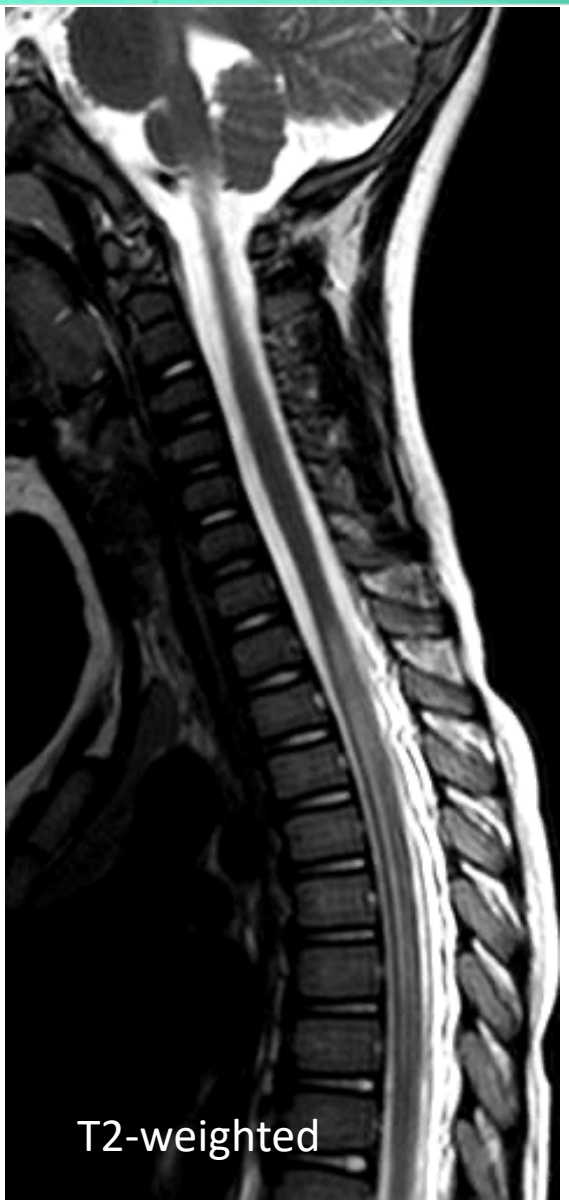

Test your knowledge

8 - 18-year-old female with sudden paraplegia. Reported a respiratory viral process the week before. What is the most likely diagnosis?

- Answer: Myelitis. Long segment of the spinal cord (over three segments) depicting high signal intensity on this T2-weighted MR image.

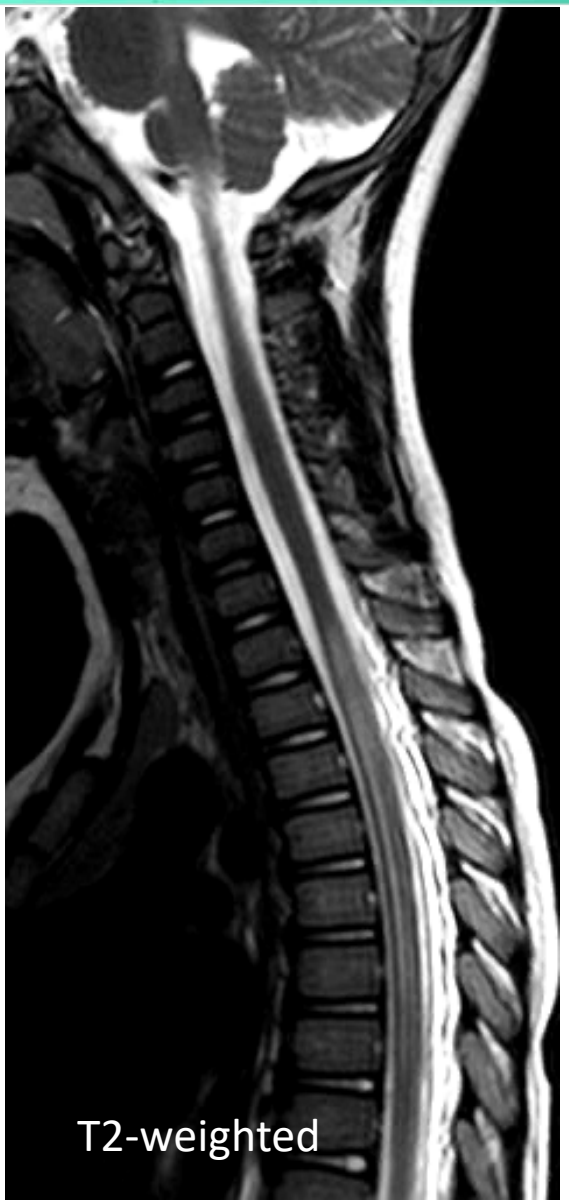

Chapter Outline

Test your knowledge

9 - In which compartment is this tumour located? What is the most likely diagnosis?

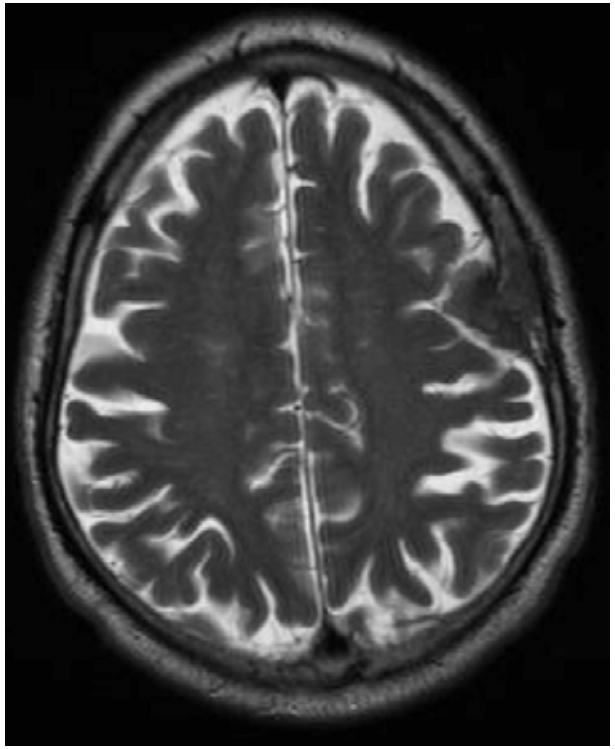

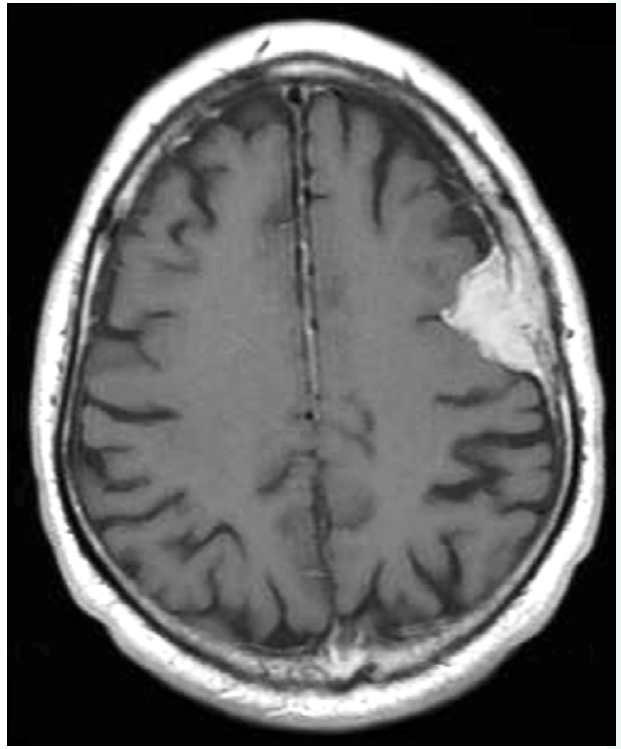

Test your knowledge

9 - In which compartment is this tumour located? What is the most likely diagnosis?

- Answer: It is an extra-axial tumour, displaces medially the CSF and the cortex. It enhances homogeneously and presents a dural tail. The most likely diagnosis is meningioma.

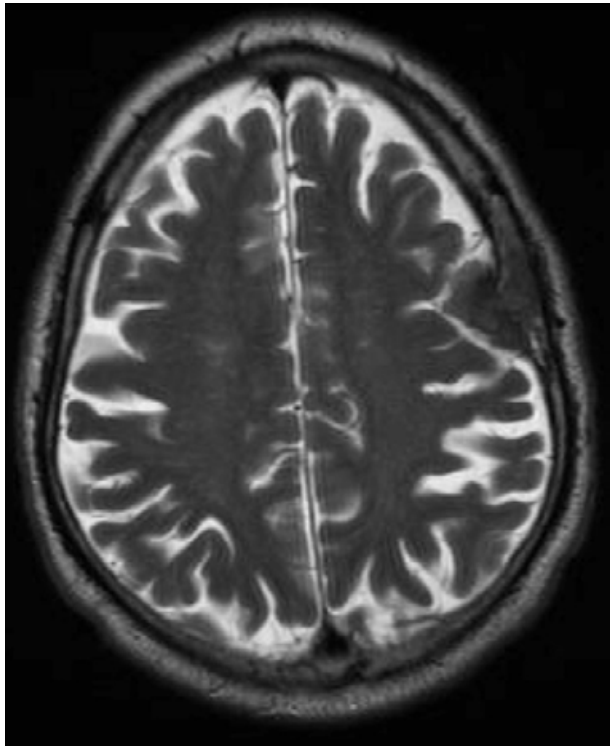

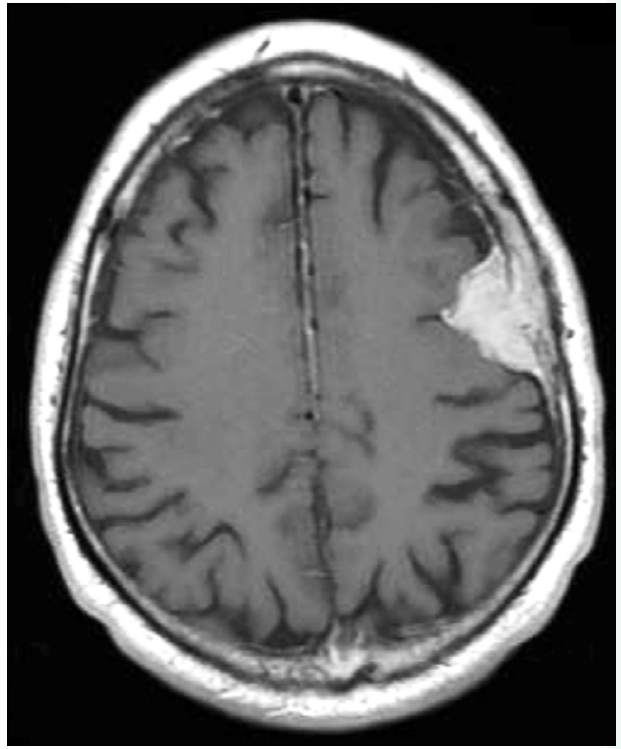

Test your knowledge

10 - What anatomical structure is the red asterisk indicating?

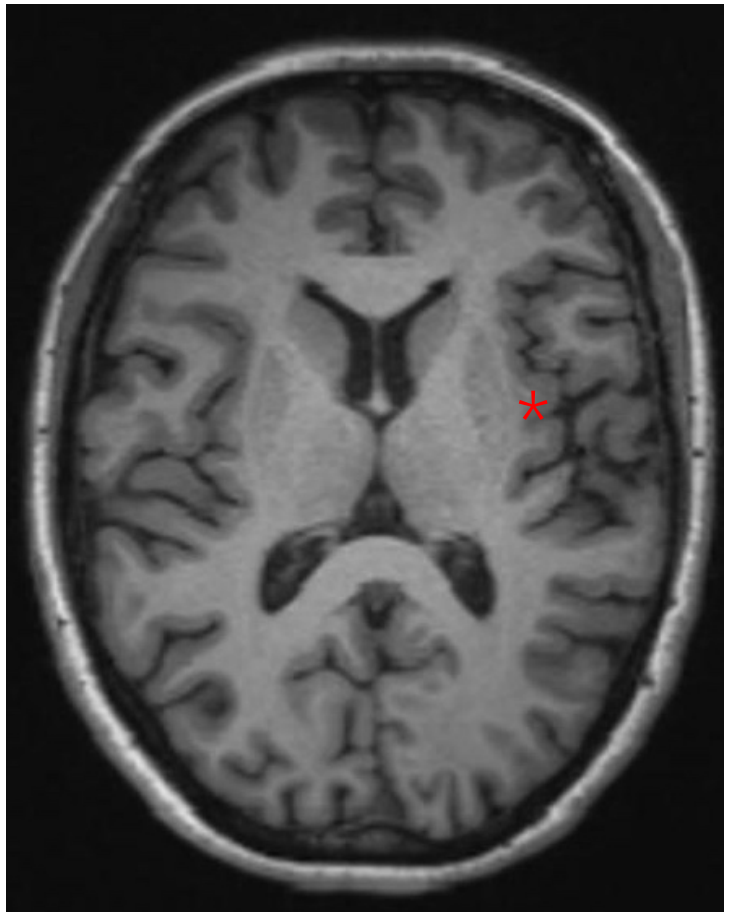

Test your knowledge

10 - What anatomical structure is the red asterisk indicating?

- Answer: The insula. It is located in depth to the Sylvian fissure.

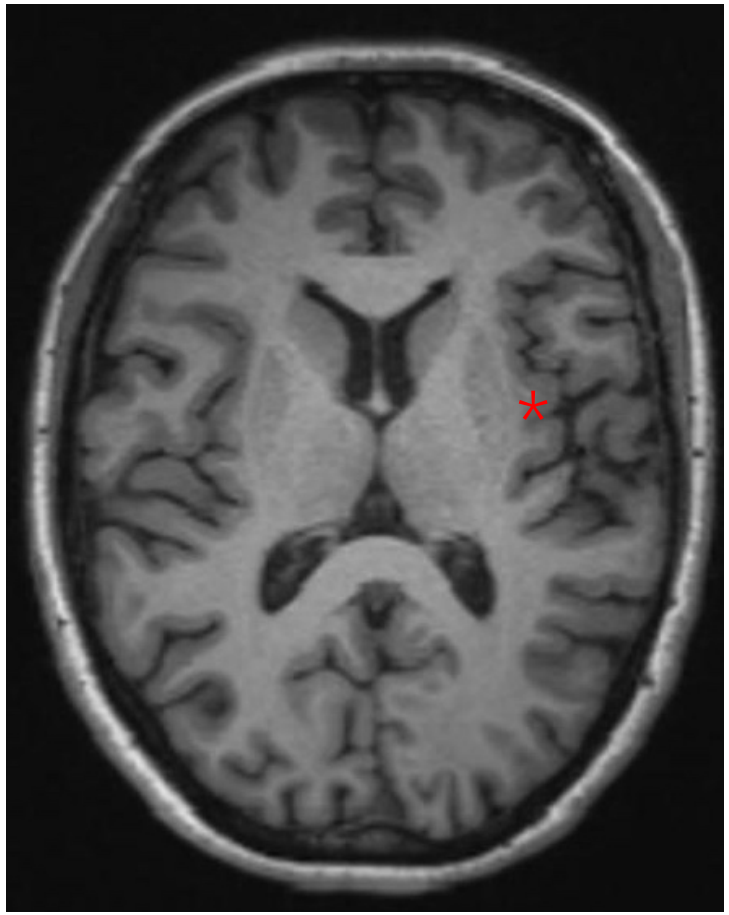

Chapter Outline